

# Historical soil erosion in the West Usambara Mountains, Tanzania

*A study based on hillslope deposits*

**MSc thesis**



# Historical soil erosion in the West Usambara Mountains, Tanzania

*A study based on hillslope deposits*

**MSc thesis**

MSc Thesis Physical Geography

P.S.J. Minderhoud

*Faculty of Geosciences*

*Department of Physical Geography*

*Utrecht University*

Under supervision of

Dr. G. Sterk

Dr. W.Z. Hoek

30<sup>th</sup> of June 2011



**Universiteit Utrecht**

## **Abstract**

Modern soil erosion triggered by anthropogenic forcing is a well studied phenomenon, but few studies focus on erosion on a longer timescale, forced by climatic changes. A better understanding of the way these long term climatic forcings act on soil erosion is needed to prepare ourselves for the future. Colluvial deposits form valuable archives of the past erosion on a hillslope. The West Usambara Mountains in Tanzania form an ideal location for research on the past erosion, since they are subjected to severe erosion, of which the present day part is well studied and documented. In this study, colluvial stratigraphies are interpreted and dated by OSL in order to reconstruct the geomorphic response of the landscape to past environmental changes, caused by both natural and anthropogenic forcings. The colluvial records, showing unstable periods with erosion alternated with stable periods of pedogenesis, can be linked successfully to the past climatic and anthropogenic history of the area. A reconstruction of the erosion history from the last three centuries is created, based on the information found in the colluvial deposits. This research proves that colluvium stratigraphies have a high potential for holding valuable sedimentary archives of the past erosion and environmental history. When interpreted and dated correctly, colluvial deposits can be used successfully to reconstruct the erosional history of an area.

## Contents

Contents .....	1
1. Introduction .....	3
2. Study area .....	6
2.1. Erosion history .....	9
2.2. Palaeoclimate and landscape response .....	9
2.3. Vegetation .....	13
3. Methods and approach .....	14
3.1 Field survey and site selection .....	14
3.2 Site description and sampling .....	14
3.3 Dating methods .....	14
3.3.1 Optical stimulated luminescence dating .....	14
3.3.2 Radiocarbon dating .....	15
3.3.3 Dating erosion using exposed tree roots .....	16
4. Results .....	17
4.1. Field survey .....	17
4.2. Selected sites and sampling .....	19
4.3. Mzungu site .....	20
4.4. Mshizii area .....	23
4.5 Dating results .....	25
5. The erosion history as recorded in the colluvial deposits .....	27
5.1 Mzungu area .....	27
5.2 Mshizii area .....	29
6. Discussion .....	32
6.1 Historical soil erosion .....	32
6.2 Mzungu area .....	33
6.3 Mshizii area .....	33

6.3.1 The origin of the charcoal rich soil layers .....	33
6.3.2 Colluvial deposits in the valley floor and the origin of the stream .....	33
6.4 Dating of colluvial deposits .....	34
6.5 Measuring erosion using exposed tree roots .....	35
6.6 Palaeo-erosion rates .....	35
6.7 Climatic forcing versus anthropogenic forcing .....	36
6.8 The use of colluvial records to reconstruct the soil erosion history .....	37
7. Conclusions.....	39
References .....	41
Appendices .....	44

## 1. Introduction

Soil erosion in Tanzania has been documented since the first arrival of European explorers in the 19<sup>th</sup> century (e.g. Burton, 1860; Speke 1865). In the East African Highlands, like the West Usambara Mountains, severe soil erosion poses a significant threat for the food security (Sanchez, 1994). Modern erosion in these areas is well documented (e.g. Kimaro et al., 2008; Lundgren, 1980) and all sorts of sustainable land management (SLM) measures, in order to limit the soil erosion, have been implemented in the past, some with more success than others (e.g. Tenge 2005, Vigiak, 2005). However, many studies focus on actual, anthropogenic erosion only and much less research has been done on past soil erosion and the erosional forcings that are active on a longer timescale (Eriksson & Christiansson, 1997).

Soil erosion is a natural geomorphological process that incorporates many causative factors. Two main triggers for soil erosion are widely recognized: 1) natural triggers, e.g. climatic change (altering the hydrological and vegetational conditions), tectonical uplift and tilting; 2) anthropogenic triggers, such as deforestation and overgrazing, resulting from introduction and/or intensification of agriculture and livestock keeping (e.g. Thomas, 1994). Few soil erosion studies incorporate the large scale erosional forcings, both spatial and temporal, such as geomorphologic unstable regions and longer scale climatic fluctuations. However, they can significantly influence soil erosion and should be taken into account when planning sustainable land management (SLM) measures for erosion reduction. Incorporating knowledge of the climatic impact on modern day erosion will strengthen its overall understanding. Especially with the rapid climatic changes that are witnessed at present, increased insight in the temporary scale and impact of climatic forcings on soil erosion is needed to prepare ourselves for the future.

The erosion behavior of a single hillslope over time is imbedded in the concept of the 'K-cycle', developed by Butler (1959). The K-cycle can be defined as, 'the interval of time covering the formation by erosion and/or deposition, of a new landscape surface, the period of development of soils on that surface, and ending with the renewal of erosion and/or deposition of that surface'. In general, the principle describes the cyclic behavior of periods of landscape instability and hillslope erosion and periods of stability with pedogenesis (soil formation). This phenomenon is witnessed by several studies in sub-Saharan Africa (e.g. Clarke et al., 2003; Eriksson et al., 2000; Temme et al., 2008). Deposition of previously eroded sediment on the same hillslope is called colluviation and the deposits are called colluvium.

The long-term processes that play a role in the temporal en spatial distribution of erosion and colluviation are not very well understood (Lang, 2003) and several erosion-deposition

cycles can create complex slope stratigraphies. Figure 1.1 shows the geomorphologic development of a hillslope during several arid-humid climatic cycles. When colluviation is largely reduced or even stopped during a longer time period, pedogenesis can take place.

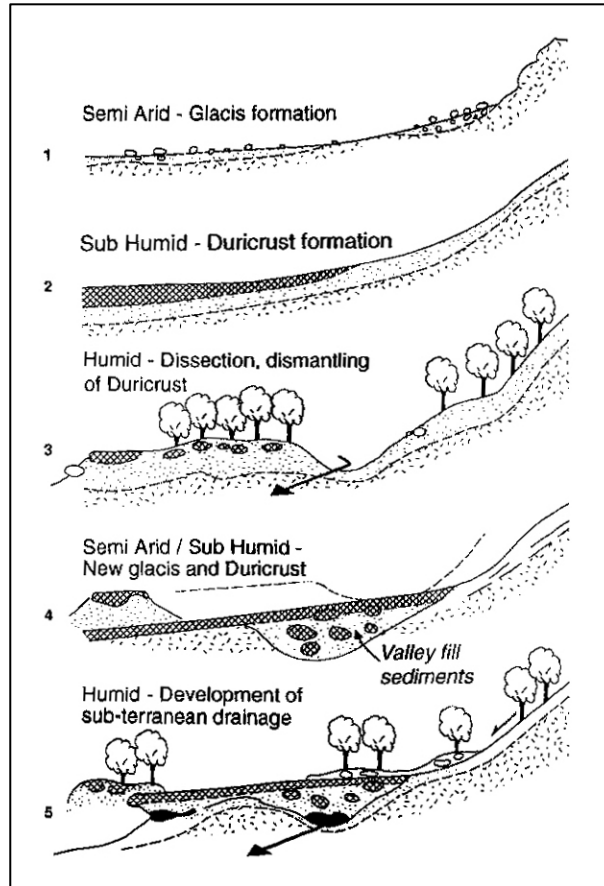


**FIG. 1.1** Reconstruction of Quaternary hillslope development in response to climatic changes. Glacis formation is the deposition of sediments on a gentle hillslope, transported downhill by water erosion during arid conditions. It is a form of colluviation. Duricrust is a hard layer at the soil surface formed by accumulation of minerals. Duricrust formation is a form of pedogenesis (Thomas, 1994).

The eroded and re-deposited hillslope material, like colluvial and alluvial deposits, can form valuable archives of the soil erosion history (Fuchs & Lang, 2009). Thomas & Thorp (1995) stressed the importance of these records to be dated and interpreted, in order to understand the geomorphic response of the landscape to past environmental changes, caused by both natural and anthropogenic forces. Palaeosols found within colluvial deposits can be used to identify such stable periods on a hillslope (e.g. Eriksson et al., 2000) or for past vegetation reconstruction (Zech, 2006). If several buried palaeosols are found in a colluvial sequence, these palaeosols can be used to investigate the K-cycles of sedimentation, distinguishing periods of stable hillslope conditions with intermediate periods of instability and colluviation (e.g. Botha & Fedoroff, 1995; Wintle et al., 1995). This will create a timeframe for the witnessed phenomena in the colluvial deposits. Subsequently, it

can be used for reconstructing the long-term soil erosion history and will increase the understanding of the timing and causes of landscape degradation (Fuchs et al. 2010).

The Usambara Mountains in Tanzania faced severe erosion in the recent past and present (Vigiak, 2005). However, little is known on the erosion on a longer timescale from before the end of the 19<sup>th</sup> century. The aim of this research was to determine the soil erosion history and the main causative factors in the West Usambara Mountains, NE Tanzania. The research was conducted by achieving the following objectives:

- Analyzing the sedimentary archives in colluvial deposits in the area and collecting samples of datable material for age control.
- Defining whether there were past periods with higher or lower water erosion and, therefore, colluvial sedimentation. And if so, resolving the driving forces behind these different erosional phases and linking them to past climatic events.
- Determining the impact of past climatic changes before human interference on hillslope stability and what can be expected with future climate changes.
- Unraveling the contribution to soil erosion of both the natural and anthropogenic erosional forcings during the period of human activity.
- Deriving past erosion rates using colluvial deposits and relating them to the present day erosion.

## 2. Study area

The study area is located in Lushoto district, situated in the West Usambara Mountains of northeastern Tanzania, within latitudes 4° 05' to 5° 00' and longitudes 38° 05' to 38° 40' (figure 2.1). The West Usambara Mountains, ranging from 600 meters to 2300 meters above sea level, are part of the East Arc Mountains in Tanzania, which belong to the East African Highlands. These mountains are tectonically uplifted with the formation of the East African Rift during the Tertiary (Shackleton, 1993). The highlands have a considerable relief with steep slopes and the drainage patterns follow fault-controlled troughs (Lundgren, 1980). The valleys are originally V-shaped, however often they are filled in with sediments, resulting in a flat valley floor. The main rock types consist of Precambrian metamorphic rocks such as pyroxene garnet-granulites and hornblende gneisses and schists, which form the substrates of the soils in Lushoto (Mutakytahwa et al., 2003). The major soil types in the Lushoto district are reddish-brown soils such as Humic, Haplic and Chromic Acrisols, Luvisols and Lixisols in the mountainous uplands and Fluvisols and Gleysols in the valley bottoms (Meliyo et al., 2002).

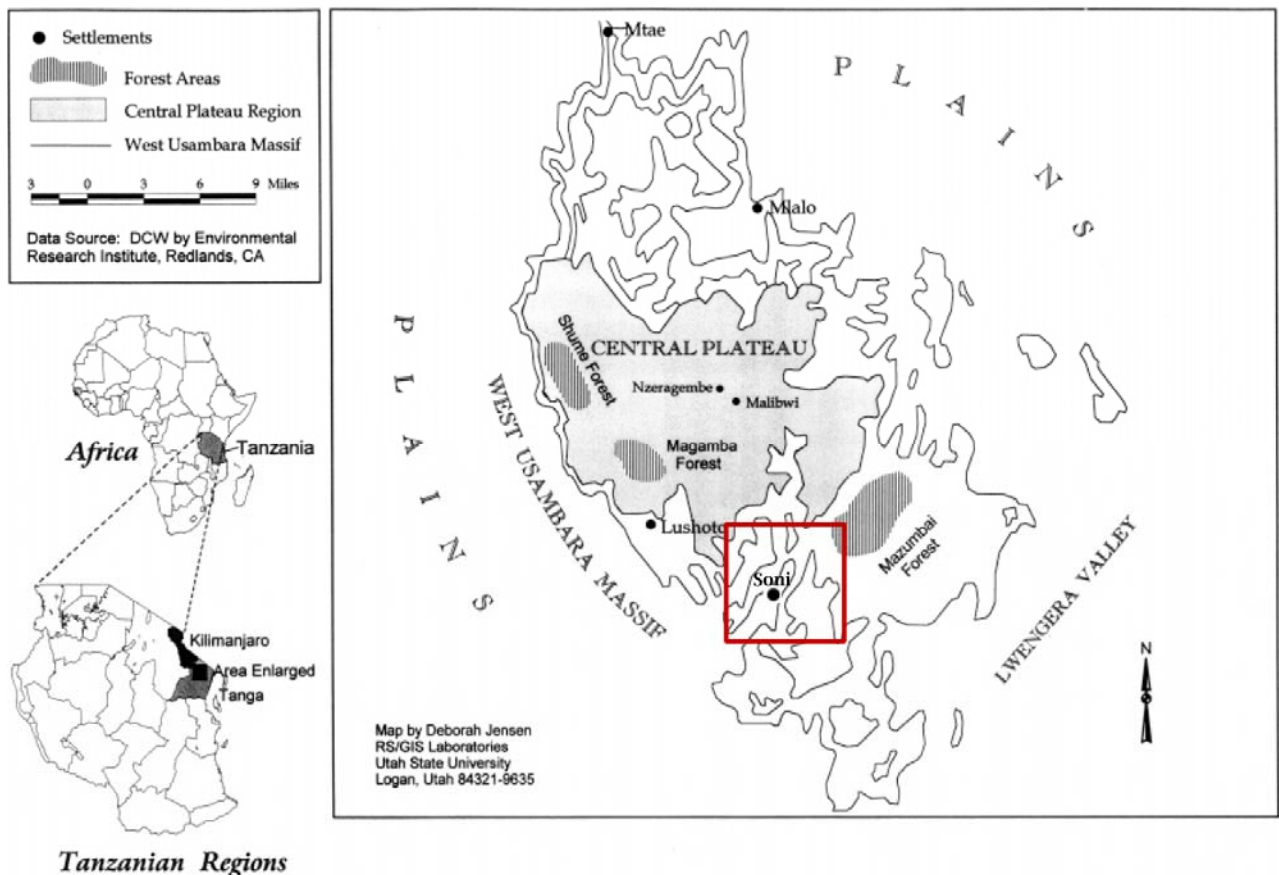


**FIG 2.1** Map of the West Usambara Mountains (Conte, 1999). The study area (10 by 10 km) around Soni is marked with the red square.

The climate has pronounced dry and wet seasons and precipitation is bimodal, varying between 800 and 1400 mm/yr, with larger extremes in both directions. The total annual precipitation experiences a decreasing trend since the start of the last century (figure 2.2).

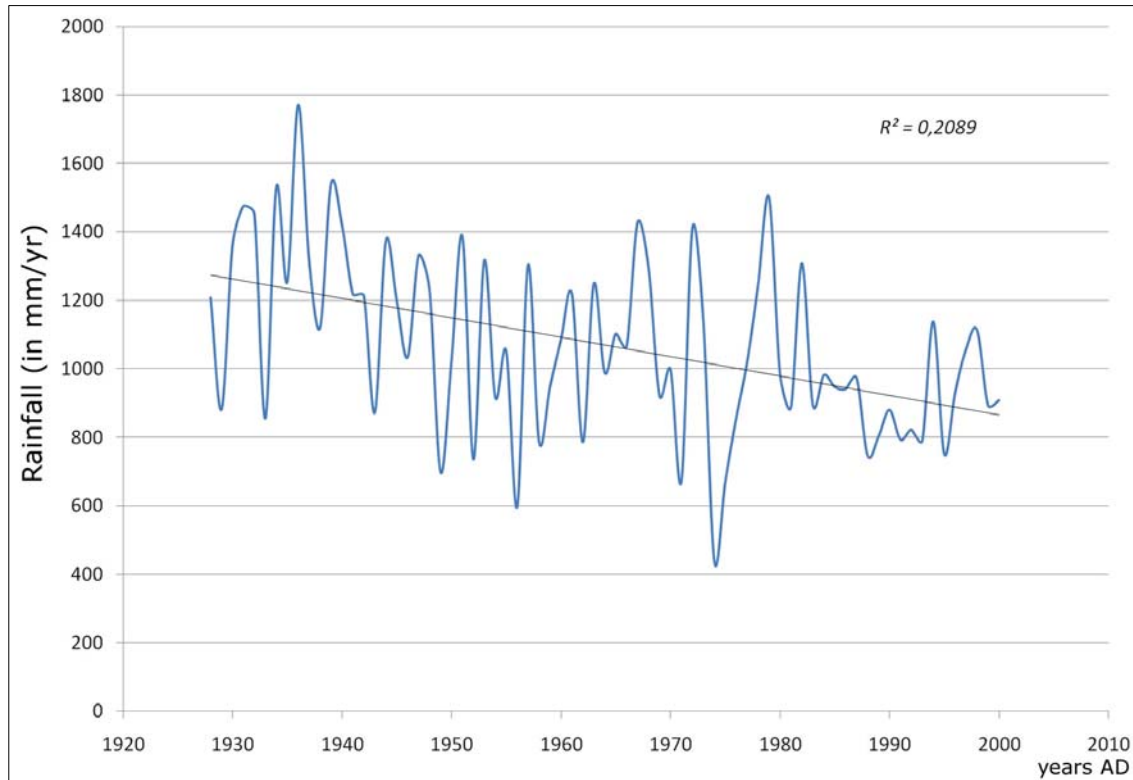


**FIG 2.2** Total annual rainfall amounts of the Usambara Mountains during the last century, measured in the study area at the Sakarani Mission. A linear trend line shows the decrease in total annual rainfall amounts.

The Usambara Mountains have been inhabited for at least 2000 years (Conte, 1999), unofficial sources even claim human habitation going back to 1.5 Ma yrs BP (Mambo, 2009). Until the 19<sup>th</sup> century the Usambara Mountains were mainly covered with mountain rain forest (Kaoneka et al., 2000). The small population of inhabitants practiced shifting cultivation and cleared plots of forest could regenerate again after agriculture shifted elsewhere. In the late 19<sup>th</sup> century, the Usambara Mountains fell under the German colonial administration. Land management changed dramatically and the traditional shifting cultivation was replaced by the establishment of large plantations of coffee and tea. At the same time the population density increased very fast and available land decreased rapidly, until around the 1930's all arable land was under cultivation (Conte, 1999). At present, the West Usambara Mountains are densely populated (200-400 persons/km<sup>2</sup>) because of their favorable conditions such as water abundance, reliable rainy seasons, good soils for agriculture, dense vegetation cover (Vigiak, 2005) and reduced occurrence of malaria (Balls

et al. 2004). The intensification of agricultural practices, since the late 19<sup>th</sup> century, led to acceleration of soil erosion, which ultimately led to severe degradation of the land in some areas (Vigiak, 2005).

A research area of 10 km x 10 km has been selected around the village of Soni (4° 48' S, 38° 20' E; 4° 53' S, 38° 25' E)(figure 2.1). Beside some small patches of protected forest, the area is largely deforested and agriculture is practiced everywhere. The area is expected to have had a turbulent and distinct erosion history, represented by large incised valleys visible in the Digital Elevation Model (figure 2.3). This, in combination with a low level of SLM measures adoption, possibly means a largely undisturbed colluvial record, making the Soni area a preferred study area.

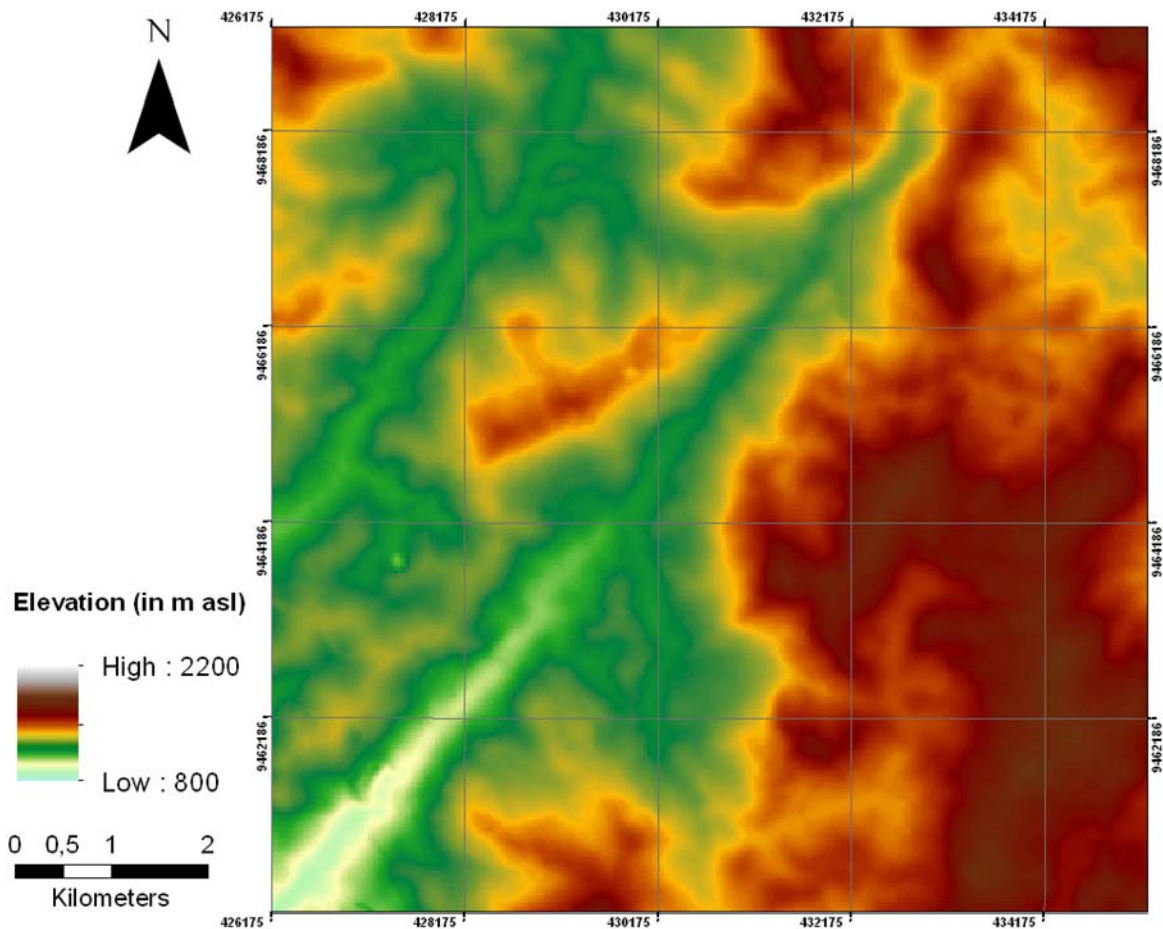


**FIG 2.3** The digital elevation model of the Soni study area, based on an Aster satellite image with 30 meter resolution. Elevation is shown in meters above mean sea level. The NE orientated drainage pattern is clearly visible. The study area has over a thousand meters of elevation difference.

## **2.1. Erosion history**

Two main periods in the erosional history of the area can be distinguished. The first period covers the long-term erosional history when climate change is believed to be the sole force behind hillslope erosion by altering the hydrologic conditions and the vegetation cover. During this period, the impact of the hunter-gatherer lifestyle of the human population on the landscape is considered to be very low or even absent. It is not expected to have altered the landscape in such a way that erosion was enhanced. The period lasted up until ca. 2000 yrs BP (Mumbi et al., 2008). A sedimentary archive from this period can yield valuable insights in the impact of long-term climatic variations on hillslope stability.

The second period, acting on century scale, covers the short-term erosional history coinciding with the period of increased anthropogenic activity in the study area, expected to range from ca. 2000 yrs BP up to the present. The anthropogenic impact on the hillslope stability gradually increased, and climate was no longer the only erosional forcing. Within this period, two distinct phases of soil erosion can be distinguished. The first phase covers the time when the population density was still low and shifting cultivation was practiced. During this phase little to moderate hillslope erosion is expected, covering the last millennia until the late 19<sup>th</sup> century. The second phase covers the recent period of severe enhancement of hillslope erosion, as a result of deforestation and implementation of large plantations and a rapid population growth under the German colonial administration (Conte, 1999). This phase began at the start of the 20<sup>th</sup> century until present and hillslope erosion is believed to be largely caused by this anthropogenic impact on the landscape (Vigiak, 2005).

## **2.2. Palaeoclimate and landscape response**

Climatic systems are a main forcing behind hillslope erosion and corresponding colluviation. They operate on various timescales, from several decades up to 10,000-100,000 years (Temme, 2008). Over the last 100 ka an increase in colluvial accretion was witnessed during arid periods. Periods with stable hillslope conditions, during which soils could develop in the colluvial deposits, coincided with higher annual precipitation rates. The increase in vegetation cover, due to the more humid conditions, is assumed to be the main cause for these stable periods. This makes precipitation a leading factor behind hillslope erosion. Temperature, on the other hand, does not seem to influence the landscape development much (Clarke et al, 2003).

The past climatic changes and their effect on the landscape development are described for the Usambara Mountains region to gain a better understanding of large scale climatic forcing on past hillslope erosion. Climatic changes from before the Late Glacial Maximum (LGM) are not considered to have significantly influenced the present day morphology, so the overview captures the period from the LGM till the present. Figure 2.4 shows the

general trends of the climate, and the effects it had on the environment and land surface processes from the LGM until present for the humid tropics (Thomas & Thorp, 1995).

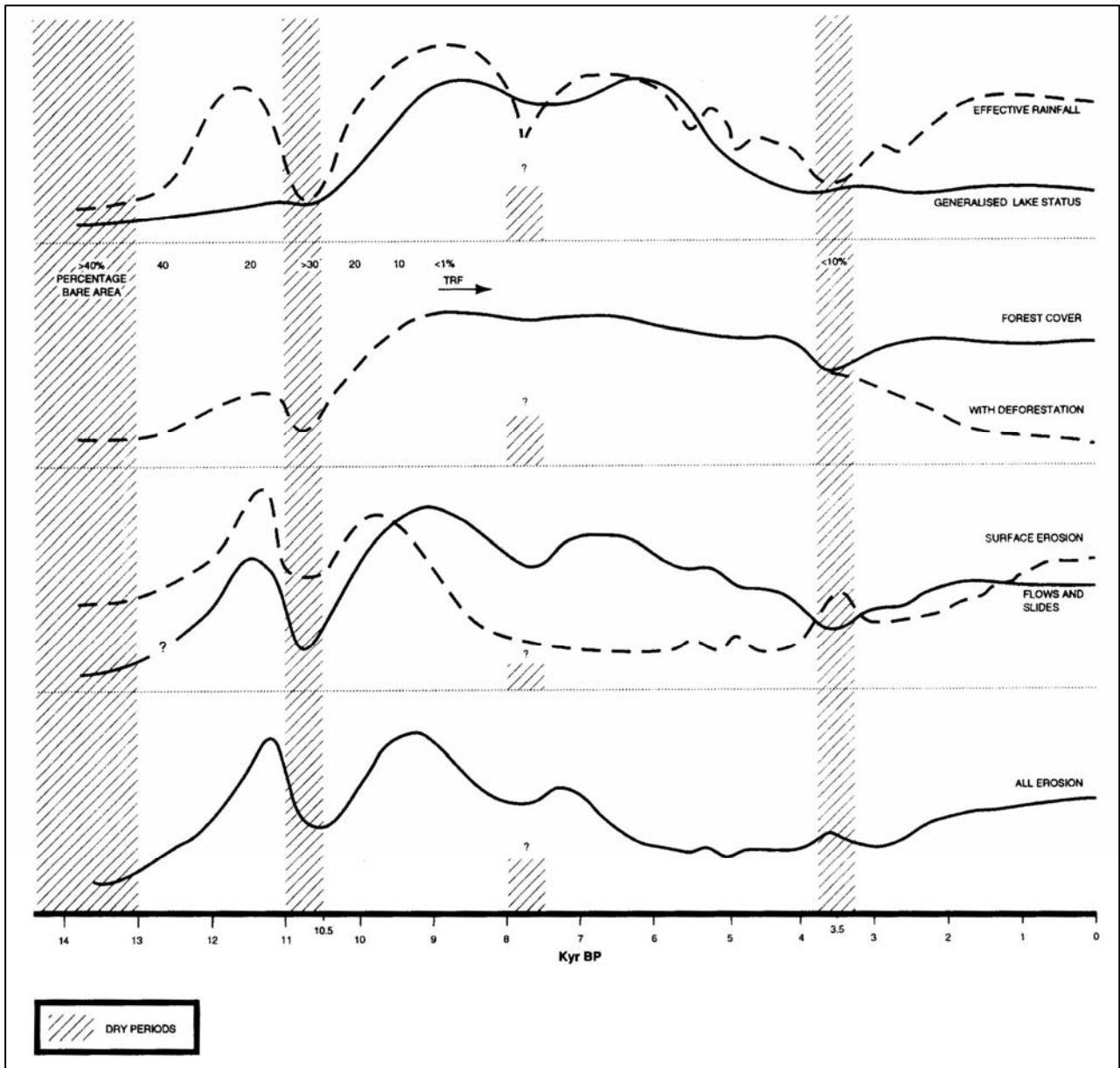


**FIG. 2.4** An overview of climate variability and the environmental response for the humid Tropics during the last 14 ka. Colluviation is not depicted on its own but is included in surface erosion, shown by the dashed line in the third graph from the top. During some arid periods the total erosion amount decreased, but colluviation increased (Thomas & Thorp, 1995).

During the LGM (23-18 ka BP) the climate of equatorial Africa was cooler and, due to reduced summer precipitation, arid. Around ca. 17-16 ka BP the first warming and wetting phase of the glacial-interglacial climate change started, a bit earlier than elsewhere in the world. It was followed by a very dry period ca. 15 ka BP, which was caused by the weakening of the monsoon and the strengthening of the NE Trades. Together with the decrease in latitudinal expansion of the Intertropical Convergence Zone (ITCZ), it reduced the precipitation strongly (Gasse, 2000). This caused in turn a decrease in vegetation cover. Without this protectional cover, even with decreased rainfall amounts, hillslope erosion and corresponding colluviation took place on the lower slopes (Thomas & Thorp, 1995).

During the Late glacial (13,000-10,000  $^{14}\text{C}$  yr BP), the climate became warmer and with the strengthening of the African Monsoon, more humid. The recovering of the vegetation cover lagged behind the increasing annual precipitation, leaving the soil vulnerable for water erosion. Hillslope erosion increased strongly and large colluvial deposits were formed (Thomas & Thorp, 1995). During the Younger Dryas, the African Monsoon weakened again (Garcin et al., 2007) and the climate in East Africa returned to drier conditions which persisted during the early Holocene (Gasse et al., 2008). This halted the spread of forests and largely decreased fluvial activity, but hillslope erosion still went on, though in reduced rates (Thomas & Thorp, 1995).

From the period between the LGM and the Younger Dryas, several palaeosols were found in colluvial deposits in South Africa, which point to smaller scale climatic fluctuations (Clarke et al., 2003). Such century-millennial scale dry-wet cycles within the larger scale changes are witnessed for sub-Saharan East Africa in several other studies as well (Barker et al., 2007; Gasse et al., 2008; Thompson et al., 2002; Zech, 2006).

After the Younger Dryas, there was an abrupt resumption of the African monsoon activity and the latitudinal migration of the ITCZ increased (Garcin et al., 2007). Lake levels and fluvial activity in East Africa increased by the increasing rainfall and due to a lag in vegetation recovery, hillslope erosion increased as well. However, after a couple of centuries, the vegetation cover had reached its stable state corresponding to the more humid climate, and hillslopes stabilized, resulting in a decrease of surface erosion (Thomas & Thorp, 1995).

This increasingly, humid climate was the onset of the so called 'African Humid Period', (ca. 9 ka BP till ca. 6 ka BP) when large parts of the Sahara and the rest of Africa were covered with green vegetation (deMenocal et al., 2000; Ritchie et al., 1985). Although the Holocene climate is commonly thought to have been fairly stable, for Africa this is all but true (Gasse, 2000). Ice core records from the Kilimanjaro show at least three large climatic events (Thompson et al., 2002). The first dry event recorded in the Kilimanjaro ice core records

happened around 8.2 ka BP. It coincided with a drop in temperature (Powers et al., 2005) and precipitation, which resulted in a fast and strong drop in lake levels in the region (Gasse, 2000). An abrupt and large change in the hydrological situation in the tropics, and particularly in Africa, is assumed to be causing this dry period (Thompson et al., 2002). Responses of hillslopes to this major dry period are not documented (Thomas & Thorp, 1995). After this dry period, a very humid period was recorded in the ice cores from 6.5 - 4.5 ka BP (Thompson et al., 2002), together with a temperature rise that peaked around 5 ka BP (Powers et al., 2005). Effects of this increase in humidity and precipitation on hillslope stability are not documented by Thomas & Thorp (1995). However, buried palaeosols found on the slopes of the Kilimanjaro by Zech (2006) were dated at 7.6 ka BP. This suggests stable hillslope conditions until 7.6 ka BP, followed by hillslope erosion and colluviation. But since the palaeosols were found on highly elevated slopes, the response from these slopes could differ from that of lower elevated places.

The final large event recorded in the ice cores, is the drought that occurred 4.2 – 4 ka BP, which coincided with the so called “First Dark Age”, the period of the greatest historical drought in Africa (Thompson et al., 2002). This period of severe dryness had a devastating effect on the vegetation cover, leaving the soil vulnerable to erosion during the rare rainstorms that occurred. Erosion of hillslope deposits increased, together with the colluviation (Thomas & Thorp, 1995). After this very dry period, the climate stayed dry until 3.3 ka BP, after which it slowly became wetter. The climate reached its wettest period around 1.7 ka BP, which lasted until 1.4 ka BP.

The climate over the period from ca. 1.4 ka BP on during the Medieval Warm period had an overall wetting trend. The Nile flood discharge record, which is a proxy for precipitation, shows two drier periods, from 1.1 ka BP till 0.9 ka BP and from 0.8 till 0.65 ka BP. For the intermediate period, from 0.9 till 0.8 ka BP, and the transition to the Little Ice Age, ca 0.65 till 0.55 ka BP, it shows higher precipitations (Hassan, 2011). The first part of the Little Ice Age (0.55 – 0.35 ka BP) was a dry period (Stager et al., 2009; Hassan, 2011). However, during the second part of the Little Ice Age (0.35 till 0.2 ka BP) a strong increase in lake levels in East Africa was witnessed (e.g. Lake Victoria and Lake Naivasha), indicating a regional wetting of the climate (Brown & Johnson, 2005; Stager et al., 2005).

Over the last two centuries, rainfall and lake level measurements show a dry climate at the first half of the 19<sup>th</sup> century. It was subsequently followed by a ‘normal’ wet climate that lasted until the beginning of the 20<sup>th</sup> century when the climate became more arid again (Nicholson, 2001). This is consistent with the decreasing trend in annual precipitation for the Usambara Mountains over the 20<sup>th</sup> century (Sakarani Mission data).

On long timescales a dry climate means increased hillslope erosion, compared to a wet climate, since well developed vegetation cover will protect the soil. However on a shorter timescales, during transitional periods, it is the other way around, an increase in precipitation will increase erosion while a decrease of precipitation will result in decreased erosion. This is because of the time it takes for the vegetation to adjust to the changed climatic conditions. Vegetation cover and its response to climatic changes are, hence of great importance when investigating climatic influence on hillslope erosion.

### **2.3. Vegetation**

The vegetation record from the East Arc Mountains in Tanzania shows a relatively stable ecosystem with a variety of taxa from 10,000 yr BP onward. Though small variations are present, which could have been caused by the above described climatic changes. From roughly 3000 yr BP onward, a significant decrease in some taxa started, which identifies targeted forest degradation due to ongoing climatic warming and human impact (Mumbi et al., 2008). For the last millennia, the effect of climatic events on hillslope stability started to mix with anthropogenic impact. Determining the weight of contribution of these two main triggers to hillslope erosion over this period is a challenge (Fuchs, 2007; Huang et al., 2006).

## **3. Methods and approach**

### ***3.1 Field survey and site selection***

In order to investigate the past erosion, colluvial and alluvial sedimentary records in the study area were studied. An extensive field survey was carried out to investigate the soils in the study area and the presence of colluvial and alluvial deposits in the landscape. The main focus was on deposits at the foot of hillslopes and in the valley bottoms, since these locations have the highest potential for valuable, sedimentary records. These areas were investigated using exposures in the landscape, both natural and anthropogenic, and corings, made with a hand corer.

### ***3.2 Site description and sampling***

Interesting sites, discovered during the field survey, holding thick colluvial or alluvial records, preferably containing one or more buried palaeosols, were mapped and stratigraphically and pedogenetically described. The descriptions contain soil texture, color (according to the Universal Soil Color Chart) and content (e.g. charcoal). For age control on these sedimentary records, soil samples were collected in light-closed pvc-tubes and, when present, charcoals samples were collected in plastic bags. The sampling strategy for datable material focused on buried palaeosols when present in the stratigraphy. For deposits without palaeosols, the samples were taken with fixed intervals to monitor changes in deposition rate (Fuchs et al., 2010).

### ***3.3 Dating methods***

Dating of the sediments is important in order to create a timeframe for the events captured in the colluvial and alluvial stratigraphies and palaeosols. Two dating methods were used: Optically Stimulated Luminescence (OSL) dating for quartz grains and radiocarbon ( $^{14}\text{C}$ ) dating for pieces of charcoal. Additionally, a method based on exposed tree roots to determine past erosion rates is explored.

#### ***3.3.1 Optical stimulated luminescence dating***

Optical Stimulated Luminescence (OSL) dating (Aitken, 1998; Huntley et al, 1985; Wallinga, 2002) is a technique that uses the ability of natural crystalline materials, like quartz, to store energy over a long period of time. Sunlight releases electrons from light-sensitive traps within the crystal lattice. This release of energy, if stimulated by light, is called optical stimulated luminescence. In a natural situation, when quartz or feldspar grains are exposed to sunlight, all the energy is released and the OSL signal is set to zero, so called 'bleaching'. When the grains become buried and remain unexposed to sunlight, they will slowly absorb energy by trapping electrons in their crystal lattice due to the flux of ionizing radiation from surrounding natural radioactivity and cosmic rays. The amount of energy storage within the

lattice will be a function of time since last exposure to light. By measuring the total energy absorbed within the quartz or feldspar grains and dividing it by the measured radiation dose of the surrounding sediments, the age of last sunlight exposure, and thus age of deposition, can be determined (Madsen & Murray, 2009; Murray & Roberts, 1997).

Several studies have successfully used OSL dating to date colluvial and alluvial sediments (e.g. Clarke et al., 2003; Eriksson et al., 2000; Fuchs & Wagner, 2005; Fuchs et al., 2010; Lang & Hönscheidt, 2003) and palaeosols (e.g. Bush & Feathers, 2003). The prerequisite for successfully applying OSL for dating sediments requires a reset of the 'clock', full bleaching, before burial. When dating palaeosols with OSL, samples should preferably be taken from A-horizons. Maximal bleaching is assured by exposure to daylight of the quartz grains through bioturbation and mechanical processes (Bush & Feathers, 2003; Fuchs & Lang, 2009). This immediately points out difficulties implied when dating colluvial material that is not located at the top of a palaeosol. Due to the short transport distance of sediments in colluvial systems (Stokes, 1999) and small scale processes that might block sunlight (Fuchs & Lang, 2009), the sediment might not become fully bleached during transport. This leaves colluvial sediments to be prone to insufficient bleaching, resulting in an overestimation of the deposition age when dated (Fuchs & Wagner, 2003). Fortunately, by using adjusted measurement techniques and statistical analyses the OSL dating of poorly bleached sediments can still be done (e.g. Fuchs & Lang, 2001; Galbraith et al., 1999). OSL dating has an advantage over other dating methods when dating the age of deposition of colluvial and alluvial sediments compared to other dating methods. OSL directly dates the sediments themselves, instead of using a proxy for sediment deposition (Lian & Roberts, 2006). This reduces the error sensitivity, making OSL dating a preferred method for dating colluvial deposits.

The dating of the OSL samples used in this study were carried out at the Netherlands Centre for Luminescence dating (NCL), which is part of the Reactor Institute Delft (Faculty of Applied Sciences, TU Delft, The Netherlands). A detailed description of this process can be found in appendix III.

### **3.3.2 Radiocarbon dating**

Radiocarbon ( $^{14}\text{C}$ ) dating is a radiometric dating method that is based on the unstable isotope  $^{14}\text{C}$ . By measuring the amount of the natural occurring radiocarbon isotope in organic matter and comparing it to well known atmospheric concentrations in the past, an age can be established. Radiocarbon dating can be used to date organic material and palaeosols in colluvial and alluvial deposits.

Organic matter in palaeosols (e.g. Botha & Fedoroff, 1995; Clarke et al. 2003; Wintle et al. 1995) and pieces of charcoal (e.g. Zech, 2006) can be used to date the time of burial of A-

horizons. In this study, the preferred material for radiocarbon dating is charcoal, because after formation (burning) it does not deteriorate further, which could be the case for other organic carbon remains. When using charcoal to date colluvial deposits and palaeosols, there is a possibility of age overestimation due to incorporation of older charcoal (Lang & Hönscheidt, 2003). Charcoal which is not re-deposited after formation and still in situ, e.g. charcoal layers, as remnants of past wild fires or controlled forest clearing, can be used to date the surfacing of the horizon.

### 3.3.3 Dating erosion using exposed tree roots

There is a gap of at least several decadal between the present day soil erosion and the erosion record stored in the sedimentary archives of colluvial and alluvial deposits. A method developed by Gärtner (2007) could bridge this gap. The method uses exposed roots of living trees to determine the erosion rate since the year of exposure of the root. Roots start to develop differences in their annual rings when they become exposed at the surface. By determining the age of exposure and some simple mathematics concerning soil depth and root thickness (figure 3.1), the past erosion rate can be determined. By applying this method at several locations, an estimate of the total soil loss on a hillslope can be made. The roots should be of living trees of shrubs and the dating method is therefore useful to quantify the net erosion loss from the present up to several decennia or even longer depending on the age of the tree. Gärtner (2007) state that this method can be applied on all sorts of trees, both coniferous and deciduous, and can be conducted in all parts of the world where trees form annual rings.

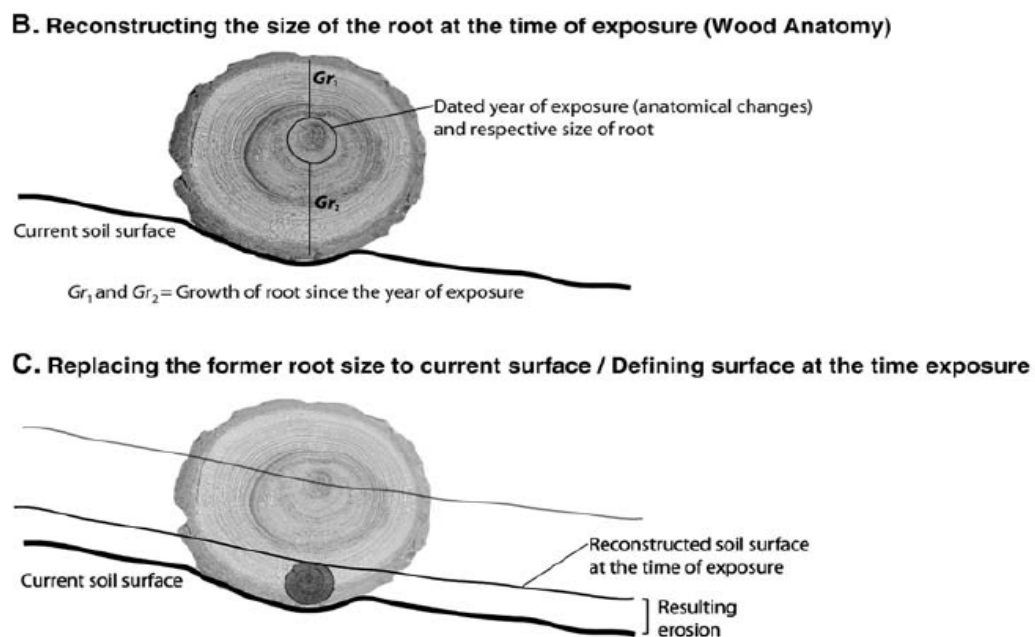


**FIG. 3.1** Visualization of the method by Gärtner (2007) to quantify the erosion since the exposure of the root.

## 4. Results

### 4.1. Field survey

During the field survey several locations with notable features were observed. These sites have been logged and mapped. Figure 4.1 shows a Worldview-2 satellite image of the study area with the logged locations. An extensive description of these sites can be found in appendix I. In the following a concise description of the soil and colluvial features found in the study area is given.

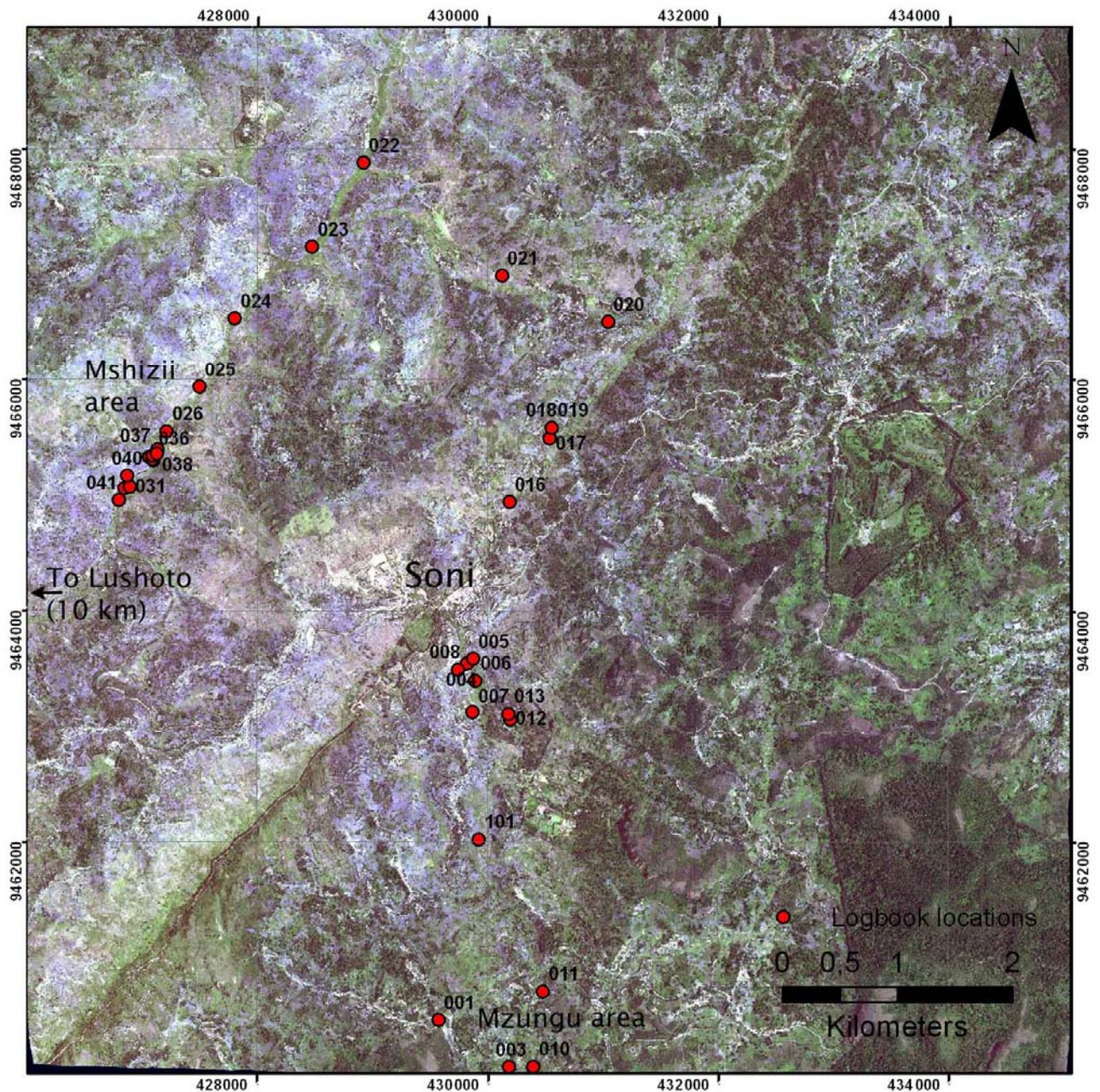


**FIG. 4.1** Worldview-2 satellite image (30-01-2010) of the study area showing the locations of notable features in the landscape.

The soils on the hillslopes of the Usambara Mountains are shallow and weathered bedrock is rarely found deeper than 1.5 m. By far most places have a single soil profile of the present day surface on top of the weathered bedrock (figure 4.2).



**Fig. 4.2** A typical example of a single soil profile found in the Usambara Mountains, with the dark, brown A-horizon at the top, followed by the reddish subsoil. The slightly darker layer in the middle is a result of clay accumulation, leached from higher horizons. The weathered bedrock starts where the white spots are visible (Photo from location 014).

In some areas, mainly downslope of agricultural fields, this single soil profile is buried by colluvial material, as can be seen in figure 4.3. Apart from areas situated downslope of agricultural fields, places where colluvial deposits have buried soil profiles are rare. But the valley floors in the study area often hold thicker sediment deposits and several meters of unconsolidated material can be found before bedrock is reached.



**Fig. 4.3** A single soil profile on a hillslope buried by colluvial material. The profile is situated downslope of a small agricultural field (Photo from location 015).

## 4.2. Selected sites and sampling

With the insights gained by the field survey, a number of sites were selected for more thorough analysis and sampling of datable material. The locations of these promising colluvial archives, most of them contain buried palaeosols, are shown in figure 4.4. The digital terrain model is shown on top of the worldview image to provide a better view of the geomorphology. The stratigraphy of the sites has been described and where possible, samples of datable material have been collected. For a full overview of the site descriptions and the samples collected see appendix II. The OSL samples of two sites were subsequently dated and these two sites have been used for reconstruction of the erosional history. The sites are named after the neighbouring villages, respectively Mzungu (waypoint 002) and Mshizii (waypoint 031).

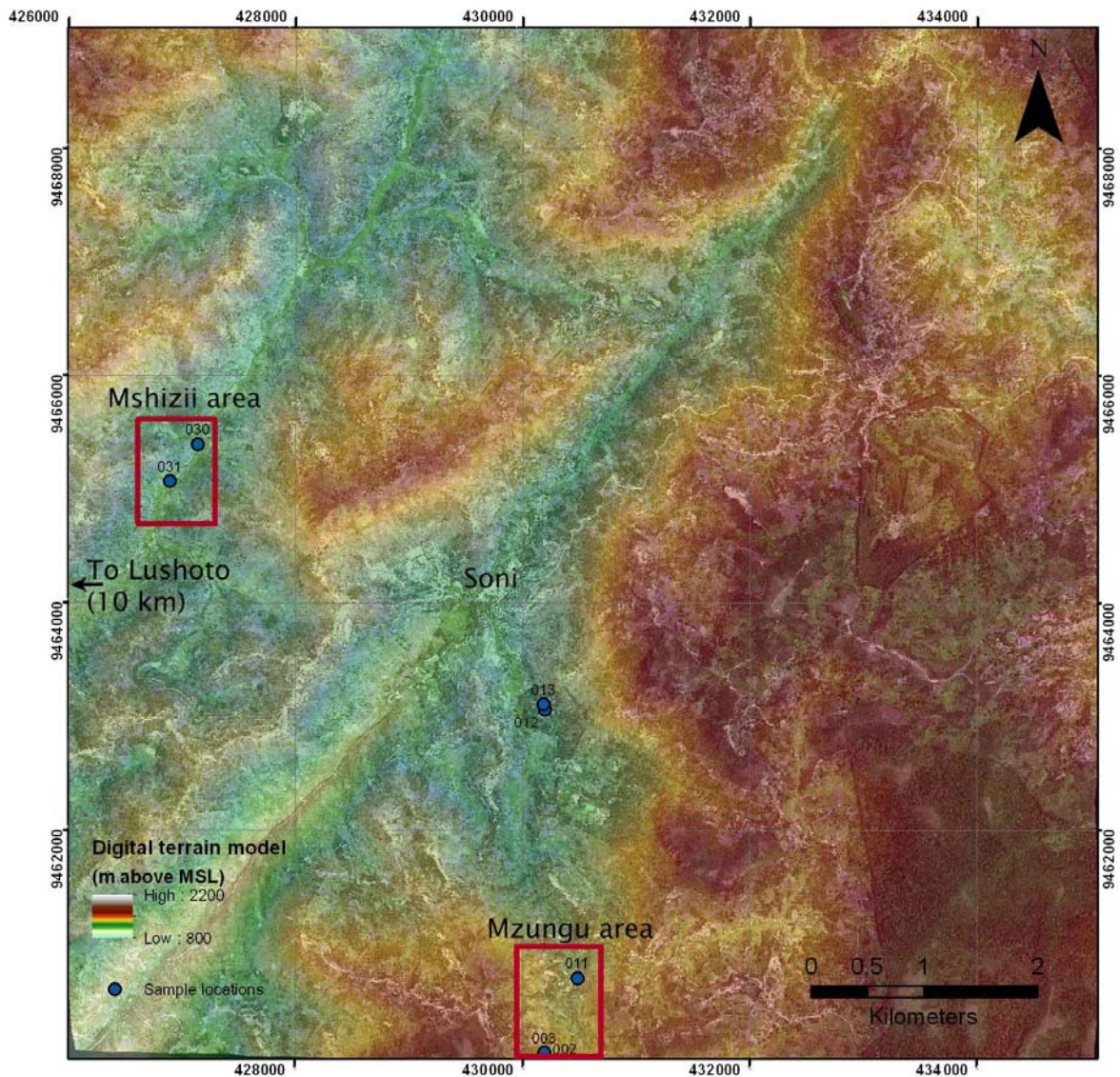


**FIG. 4.4** Sample locations for datable material from promising colluvial stratigraphies, described in detail in appendix II. The digital elevation model is shown on top of the Worldview-2 satellite image. The red box shows the location of the geomorphological map of the Mshizii area.

### 4.3. Mzungu site

The Mzungu site is situated on a hillslope at the beginning of a small valley. Further down the valley, it joins other valleys into a broader valley that runs all the way down to Soni. The area is situated 1400-1500 meter a.s.l., overlooking the lower areas in its surroundings. The landscape is covered by agricultural fields and small patches of shrubs and trees. The area is populated by small scale farmers who live in houses on the ridges, cultivating their crops on the steep, adjacent hillslopes.

Figure 4.5 shows an exposure by a road of the soil profile of the upslope agricultural field. A dark, blackish soil layer is buried by 60 cm colluvium. The spatial occurrence of this buried soil layer on the hillslope was studied using corings and exposures on the hillslope. The result of this investigation is shown in the hillslope profile given in figure 4.6.



**FIG. 4.5** The Mzungu site shows a soil profile buried by colluvium. Note that the color of the colluvial material is a mix of the dark soil horizon and the orange subsoil.

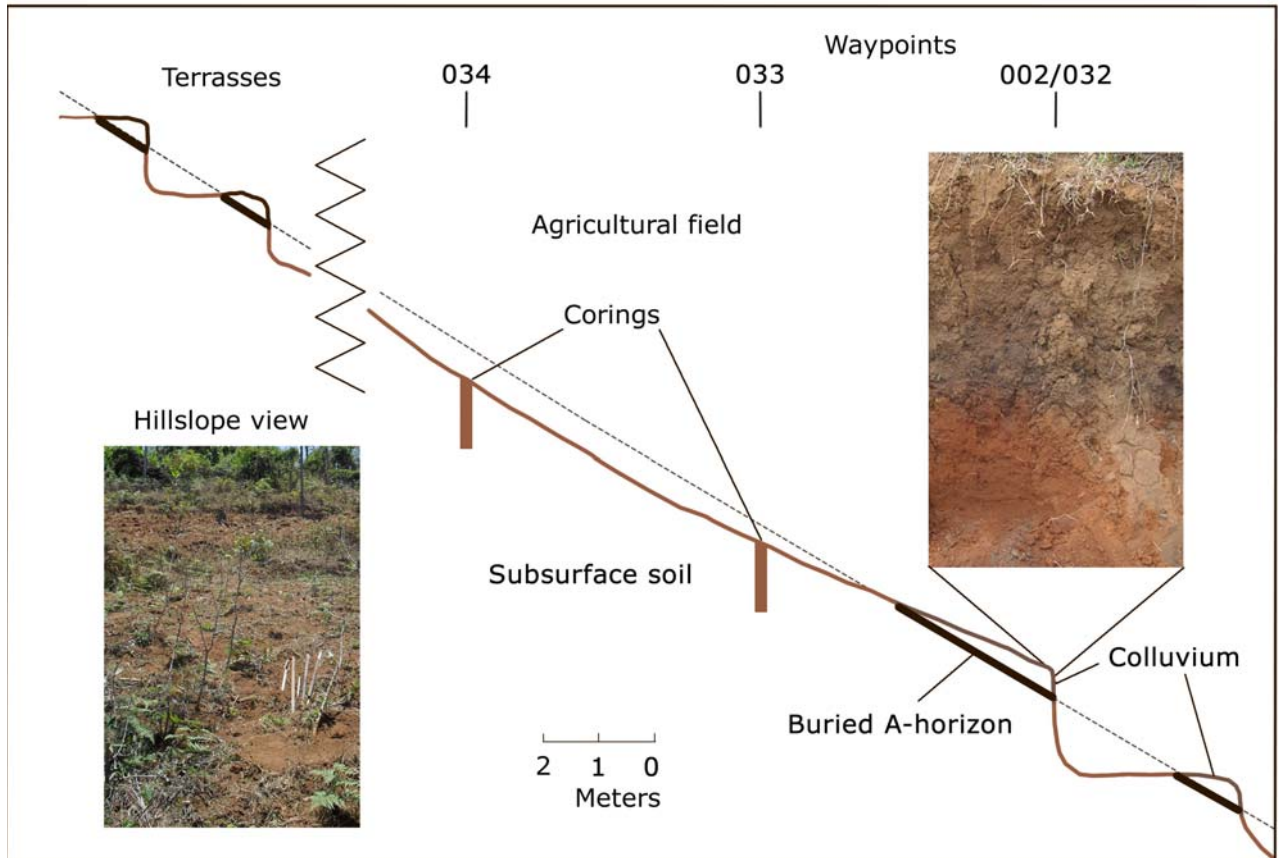


**FIG. 4.6** Schematic representation of the spatial distribution of the dark soil layer buried by colluvium for the Mzungu site. The dashed line represents the expected palaeosol surface during its formation.

The two corings, 5 and 10 meter uphill from the road exposure, did not show the dark black layer buried by colluvial material. Only orange brown subsoil was found. At the surface on field level, conglomerates of dark, blackish color are mixed with the topsoil material. The distinct black layer, buried by colluvial material, was found at the side of terraces, footpaths and at the boundaries between different fields. The colluvial material that buries the dark horizon consists of a mixture of dark material and subsurface soil, probably eroded from the uphill agricultural field.

The original soil surface, when the horizon developed and before erosion started to dissect the hillslope, is shown by the dashed line in figure 4.6. This dark layer is assumed to be the A-horizon of this palaeosol. One OSL sample (Mzungu-I, sample code: TZ02-60) has been taken from the top of the buried palaeosol, see appendix II for details.

An aerial photograph from 1955 (figure 4.7) shows the Mzungu area. The photo shows large, deforested areas and a large number of roads that cross the area. Some of the houses present in the area today can already be distinguished in the photograph. The land use can be divided into three groups, namely forest (dark trees), agricultural areas (light patches with no pattern) and areas that have been deforested covered by shrub vegetation. These areas could both be agricultural plots with full grown crops on it or shrub vegetation as can also be found at present. The aerial photograph shows that the uphill area of the Mzungu site was already deforested in 1955.



**FIG. 4.7** Aerial photograph from 1955 showing the largely deforested Mzungu area. The red arrow points in uphill direction to the road where the Mzungu site is located.

#### 4.4. Mshizii area

The Mshizii area is a medium size valley located at an altitude around 1100 m. The valley is V-shaped and has steep slopes between 30 and 55% that gradually become gentler close to the valley floor. The valley floor is incised by a small stream, exposing fresh colluvial deposits on its outer bends. The Mshizii site is located in such a place, where 230 cm of colluvium is exposed by the incising stream (figure 4.8a). The colluvium is located at the end of a long hillslope that is vegetated by grasses with some trees. The colluvium deposits in the exposure contain several dark horizons together with distinct layers of charcoal (figure 4.8b).

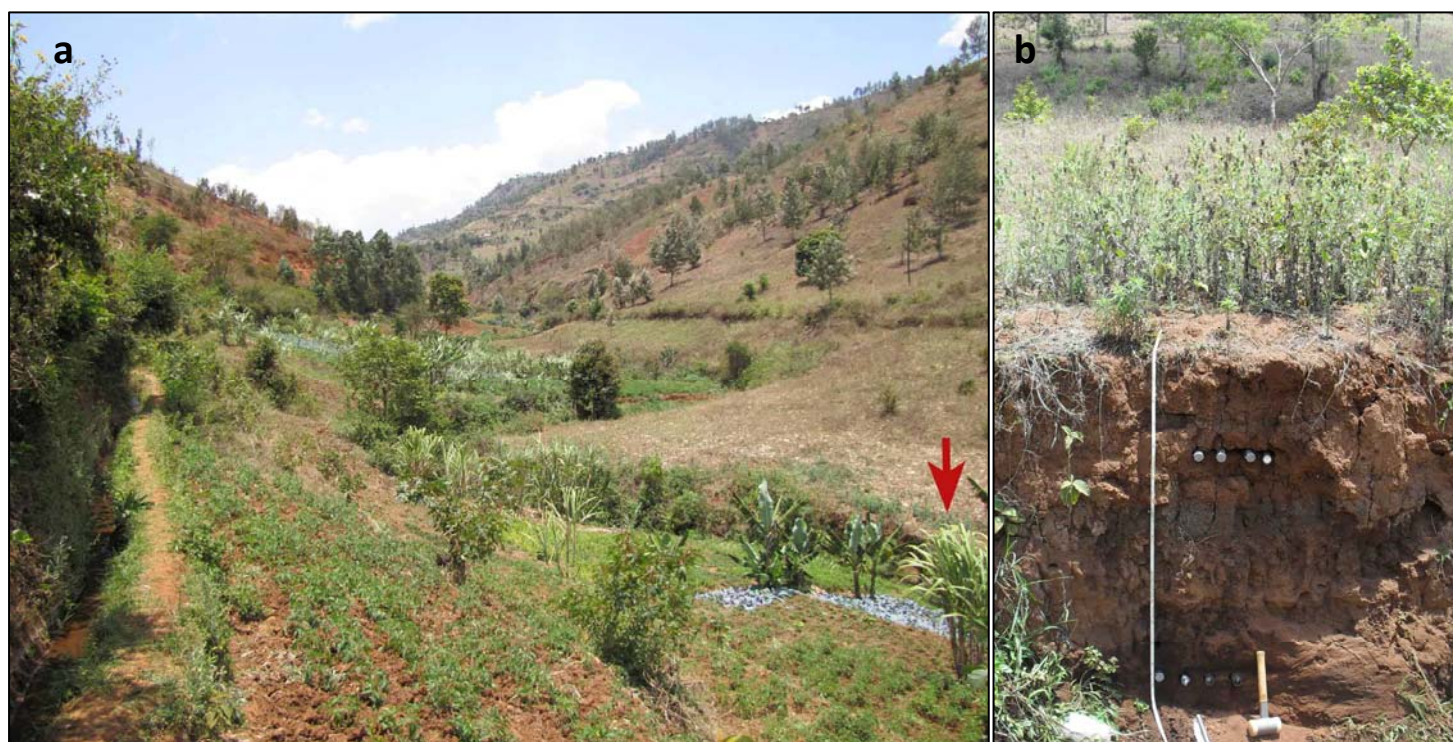


**FIG. 4.8 a)** Mshizii valley in NE direction showing the meandering stream incised in the V-shaped valley bottom. The red arrow indicates the location of the exposed colluvium of Mshizii site. **b)** The colluvial sediments exposed by the incising stream of the Mshizii site. The exposure shows several dark soil horizons. The pvc-tubes were inserted for collecting OSL samples.

The stratigraphy of the exposed colluvium was described and the geomorphology of the surrounding area was mapped. Figure 4.9 shows the geomorphological map of the Mshizii area together with a cross-section of the valley (figure 4.10). The location of the colluvium at the end of a long and steep hillslope is clearly visible. The exposure was sampled extensively for charcoal pieces and at two depths OSL samples were taken (Mshizii-I, sample code: TZ31A-55; Mshizii-II, sample code: TZ31A-155). The other layers in the exposure were physically too hard to be sampled for OSL. For a detailed overview of the exposure description and the samples collected see appendix II.

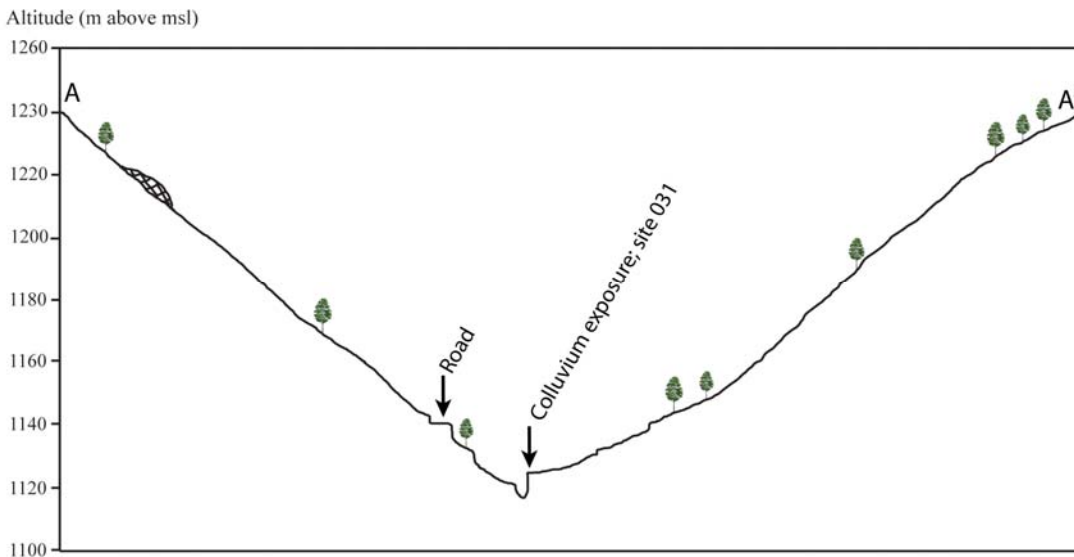
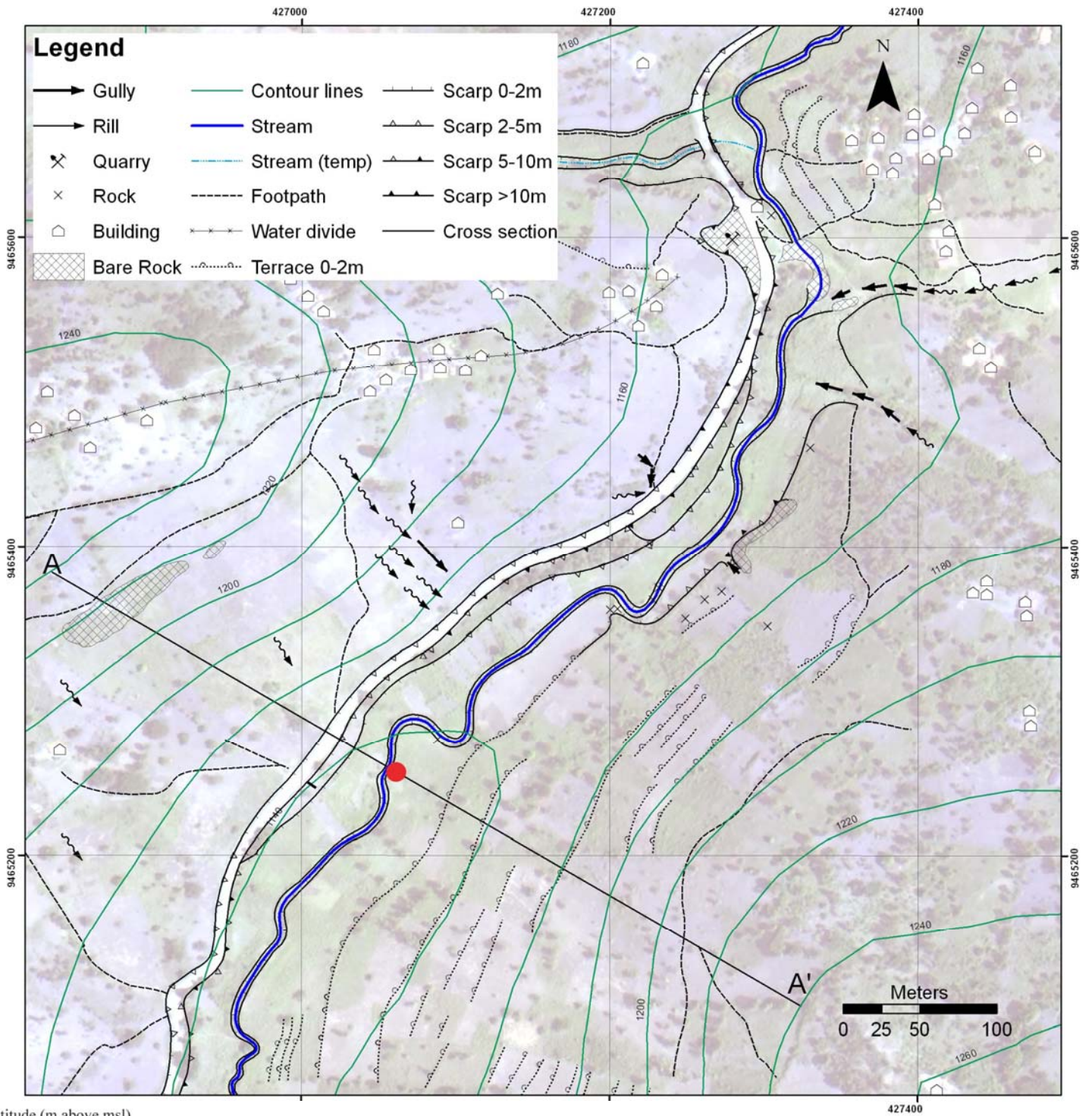


**FIG. 4.9** Geomorphological map of the Mshizii area, projected on the Worldview-2 image. The colluvium exposure of the Mshizii site is indicated with the red dot.

**FIG. 4.10** Cross section of the Mshizii valley in NE direction. The horizontal scale is similar to that of the geomorphological map.

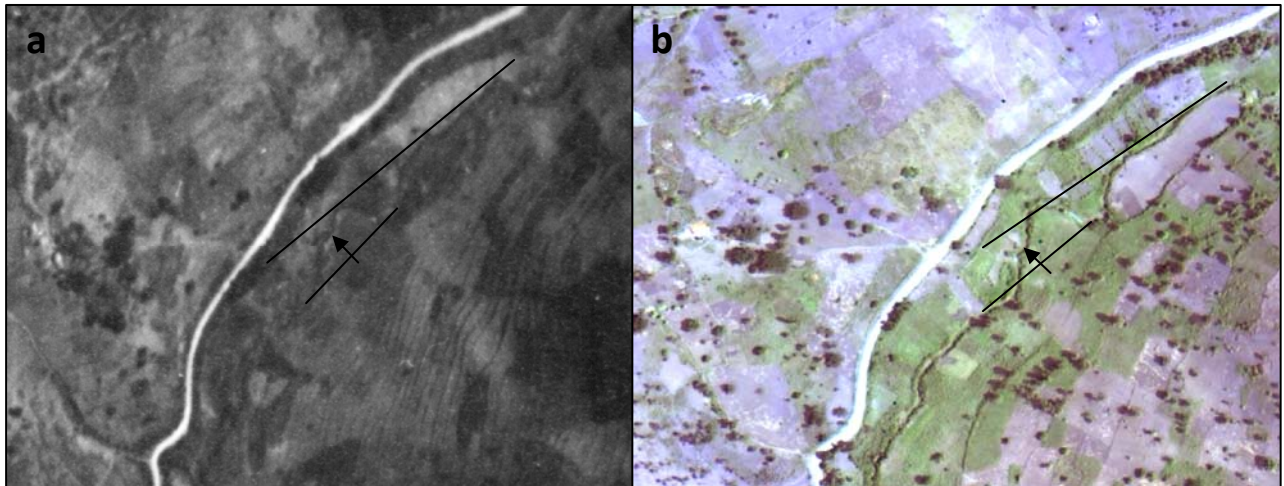


**FIG. 4.11 a)** Aerial photograph (1955) and **b)** Worldview-2 satellite image (2010) of the Mshizii valley. The location of the stream near the Mshizii site is marked with the black arrow. Over the course of 55 years, the position of the stream changed only little.

The colluvial stratigraphy of the Mshizii site does not show signs of fluvial reworking and the valley is V-shaped, with no distinctively flat alluvial bed. An aerial photograph of 1955 and the Worldview-2 image of the Mshizii valley are shown in figure 4.11. Comparison of the two learns that the location of the stream, incising the valley floor, has only moved a couple meters over a period of 55 years. This confirms the field observation that the exposure of the Mshizii site is fresh and that the colluvial sediments have not been recently reworked by fluvial meandering.

The aerial photograph shows a large number of terraces on the east side of the valley, indicating large scale agricultural practices on the hillslope. At present, this hillslope is much less intensively cultivated, also visible in the Worldview-2 image. This is likely a result of the poor soil condition of the hillslope at present, due to severe soil erosion.

#### **4.5 Dating results**

The samples collected at the Mzungu and Mshizii sites for OSL dating have been taken to the Netherlands Centre for Luminescence dating (NCL) at TU Delft for analysis. OSL measurements were done in both the conventional way, on sets of ca. 200 quartz grains, and on individual grain level. The single grain measurements in combination with the minimum age model (Galbraith et al., 1999) provided the best minimum age estimate, which represents the age when the sampled soil layer got buried by colluvial material.

Following the recommendations of Cunningham and Wallinga (2011), the age outcomes are represented as a probability density functions (PDF) rather than fixed values (figure 4.12). In order to be able to use the ages on a calendar timescale, the PDF's were converted to a mean value with error terms (table 4.1). For a detailed description of the dating methods and discussion on the ages of the samples, see appendix III for the full OSL dating report.

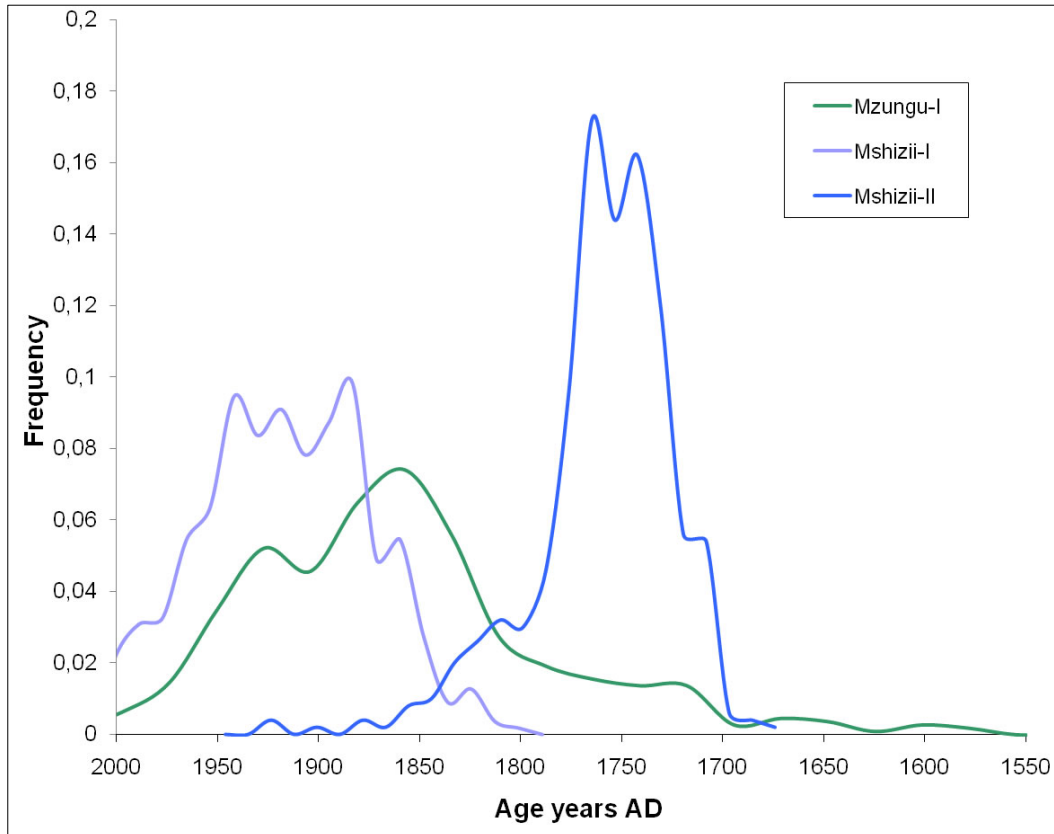


**FIG. 4.12** Probability density functions (PDF's) of the minimum age of the three OSL samples. The broadness of the PDF for sample Mzungu-I is caused by large errors in the underlying dataset.

Error		OSL age		
	Sample name	Mzungu-I	Mshizii-I	Mshizii-II
	Field code	TZ02-60	TZ31A-55	TZ31B-155
	Lab code	(NCL-4211015)	(NCL-4211016)	(NCL-4211017)
1 sigma (68% certainty)		154 ± 70 OSL yrs BP	92 ± 45 OSL yrs BP	253 ± 28 OSL yrs BP
		<i>1856 ± 70 yrs AD</i>	<i>1918 ± 45 yrs AD</i>	<i>1757 ± 28 yrs AD</i>
2 sigma (95% certainty)		154 ± 125 OSL yrs BP	92 ± 85 OSL yrs BP	253 ± 88 OSL yrs BP
		<i>1856 ± 125 yrs AD</i>	<i>1918 ± 85 yrs AD</i>	<i>1757 ± 88 yrs AD</i>

**Table 4.1** Probability density functions of the three OSL minimum age outcomes described numerically, using the mean and the sigma 1 and 2 quantiles, respectively 68% and 95% certainty, as error terms. Ages in OSL yrs BP, are years before 2010.

At the time of writing, the radiocarbon dating results from the charcoals samples have not been obtained yet. The outcomes of the OSL dates form, therefore, the only age control on the sedimentary records.

## 5. The erosion history as recorded in the colluvial deposits

### 5.1 Mzungu area

The distinct, dark A-horizon present in the exposure of the Mzungu site is not present in areas where human activities altered the landscape, such as agricultural fields, terraces and roads. It can still be found in places on the hillslope, where material was deposited instead of eroded (figure 4.6). This strong connection to land use practice makes it very likely that the erosion and subsequent colluviation on top of the palaeosol was caused by anthropogenic impact. This suggests that the palaeosol was indeed the soil surface before the onset of deforestation and agricultural practice.

The OSL age of the time of burial of the palaeosol is  $154 \pm 70$  OSL yrs BP ( $1856 \pm 70$  yrs AD with 68% certainty; Mzungu-I) (figure 5.1). The dating is not very precise; however it acknowledges that the palaeosol has been buried at least several decades up to two centuries ago. The most probable burial age is somewhere in the second half of the nineteenth century. This coincides with the period of strong increase in human activity in the study area, following the German colonial rule (Conte, 1999). It strengthens the expectation that the palaeosol represents the soil surface from before deforestation and the onset of agricultural practice in the area.

The age of burial of the palaeosol, together with the strong link of its presence to anthropogenic land use, indicate that the erosion and, subsequent, colluviation, was probably caused by anthropogenic influence on the landscape. On this short timescale, climate is not expected to have had a significant influence on enhancing erosion compared to the anthropogenic impact.

The above suggests that the Mzungu area was fully vegetated and had clear soil profiles. Somewhere, probably during the 19<sup>th</sup> century, the situation changed and the hillslope was deforested and subsequently used for agricultural practice. This made the original soil surface vulnerable to water erosion and mechanical erosion due to cultivation of the land. Gradually, the original soil surface on the hillslope became dissected by erosion. The top soil eroded away from poorly protected, agricultural fields and colluvial deposits formed in sediment sinks elsewhere on the hillslope, such as at the exposure of the Mzungu site. The stratigraphy of the soil exposure does not show signs of a sudden event, like a mass movement, that caused the palaeosol to be buried. The well mixed characteristics of the colluvial material in both texture and color indicate a gradual burial history.

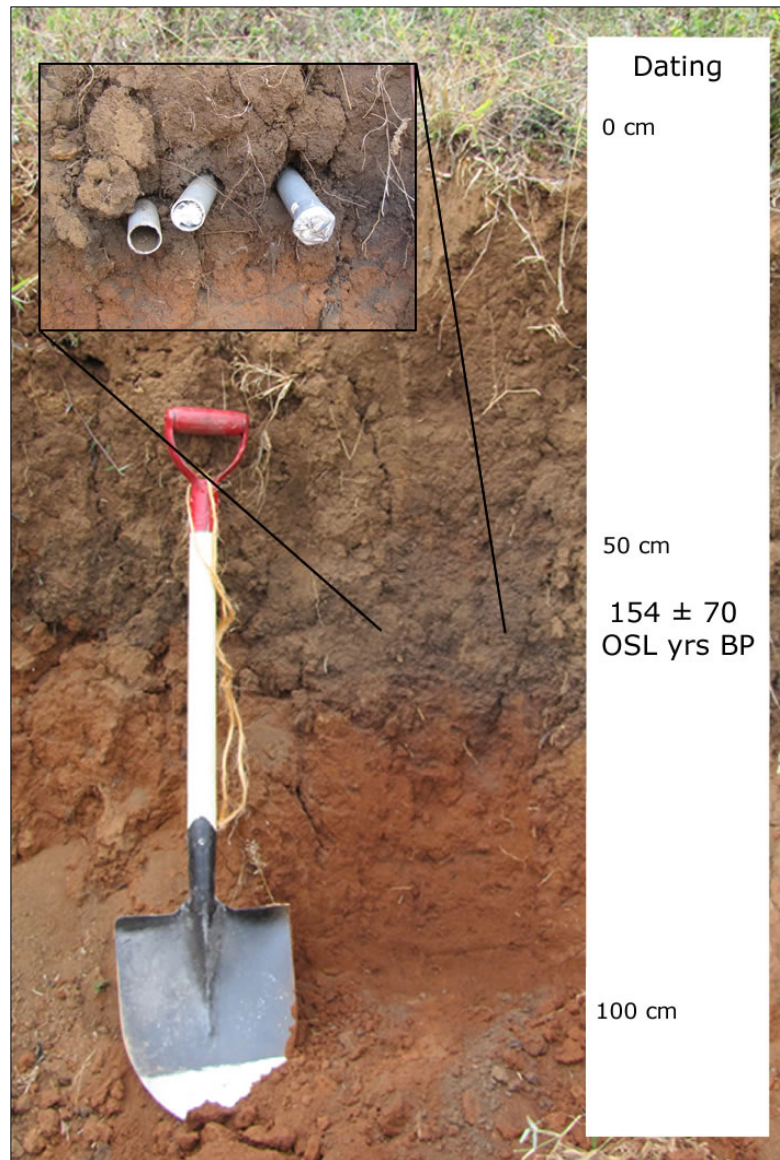


**FIG 5.1** Exposure of the buried palaeosol by colluvial deposits at the Mzungu site. The OSL samples are collected at 60 cm depth, as is shown in the insertion. The OSL burial age of the palaeosol is given on the right (with 68% certainty).

A single soil profile buried by colluvium, like at the Mzungu site, is a widespread phenomenon witnessed in the whole study area. It is often present in areas downslope of agricultural fields. Those areas are expected to have had similar erosion histories as described for the Mzungu area, with the start of colluviation after the removal of the natural vegetation and the onset of agricultural practice uphill. The wide distribution of this phenomenon coincides with the dramatic changes in land management following the German colonial administration at the end of the 19<sup>th</sup> century (e.g. Conte, 1999). The strong link to these anthropogenic activities suggests that the area was in most places rather stable before the onset of large scale deforestation, with well developed soil profiles.

## 5.2 Mshizii area

The exposure in the valley bottom of the Mshizii area is one of the rare places where more than one dark soil horizon was found in one sequence. These horizons are assumed to have formed at the surface, before they became buried by younger colluvial deposits. The horizons probably indicate quiet periods during which palaeosols could develop. Figure 5.2 shows the position of the two palaeosols in the profile. Their presence suggests at least two stable periods during which these soil profiles could develop in the colluvial deposits. Beside these palaeosols, the colluvial stratigraphy shows three distinct layers that deviate from the other deposits in texture and contain a large amount of charcoal (figure 5.2, at depths of 35, 65 and 100 cm). They might indicate poorly developed soil profiles and suggest a palaeo-process that altered the colluvial deposits.

The two OSL samples collected from the exposure date the time of burial. The layer at 55 cm depth (Mshizii-I) was dated at  $92 \pm 45$  OSL yrs BP ( $1918 \pm 45$  yrs AD with 68% certainty) and the layer at 155 cm depth (Mshizii-II) at  $253 \pm 28$  OSL yrs BP ( $1757 \pm 28$  yrs AD with 68% certainty) at 155 cm depth (figure 5.2). For the interpretation of these ages, the following effect should be taken into account. The soil type of the colluvial deposits is a luvisol. These soils are known for their clay leaching from higher layers and subsequent accumulation in lower layers (Thomas, 1994). Clay leaching means subsequent leaching of radio nuclides, which in turn influences the OSL measurements. This might have resulted in an age overestimation of the sample at 55 cm depth and an age underestimation of the sample at 155 cm depth. See appendix III for more details.

The deposits in which palaeosol II was developed, at a depth of 130 cm, are homogeneous, sandy deposits. They contain much less clay than the deposits overlying them. The layer contains no further palaeosols or any sort of deviating horizon and it is at least a meter thick till the end of the exposure (230 cm). These deposits suggest a prolonged period with unstable hillslope condition, during which erosion and colluviation continued uninterrupted. The dating at the upper part of the layer coincides with the end of the Little Ice Age (0.35 – 0.2 ka BP). For the Usambara Mountains, this was an increasingly wet period (Brown & Johnson, 2005), after two dry centuries (0.55 – 0.35 ka BP) (Stager et al., 2009). This increase in precipitation, succeeding a dry period that probably reduced the vegetation condition on the hillslope, could have caused an increase in erosion on the hillslope and subsequently colluviation at its base. This corresponds with the deposits in the exposure.

The formation of palaeosol II in the colluvial deposits indicate a period with increased hillslope stability and subsequently ceased erosion. This is probably caused by the gradual recovery of the vegetation cover after a while, as an effect of the increasing precipitation

rates. Palaeosol II is thought to have formed during this period, at the ending of the Little Ice Age.

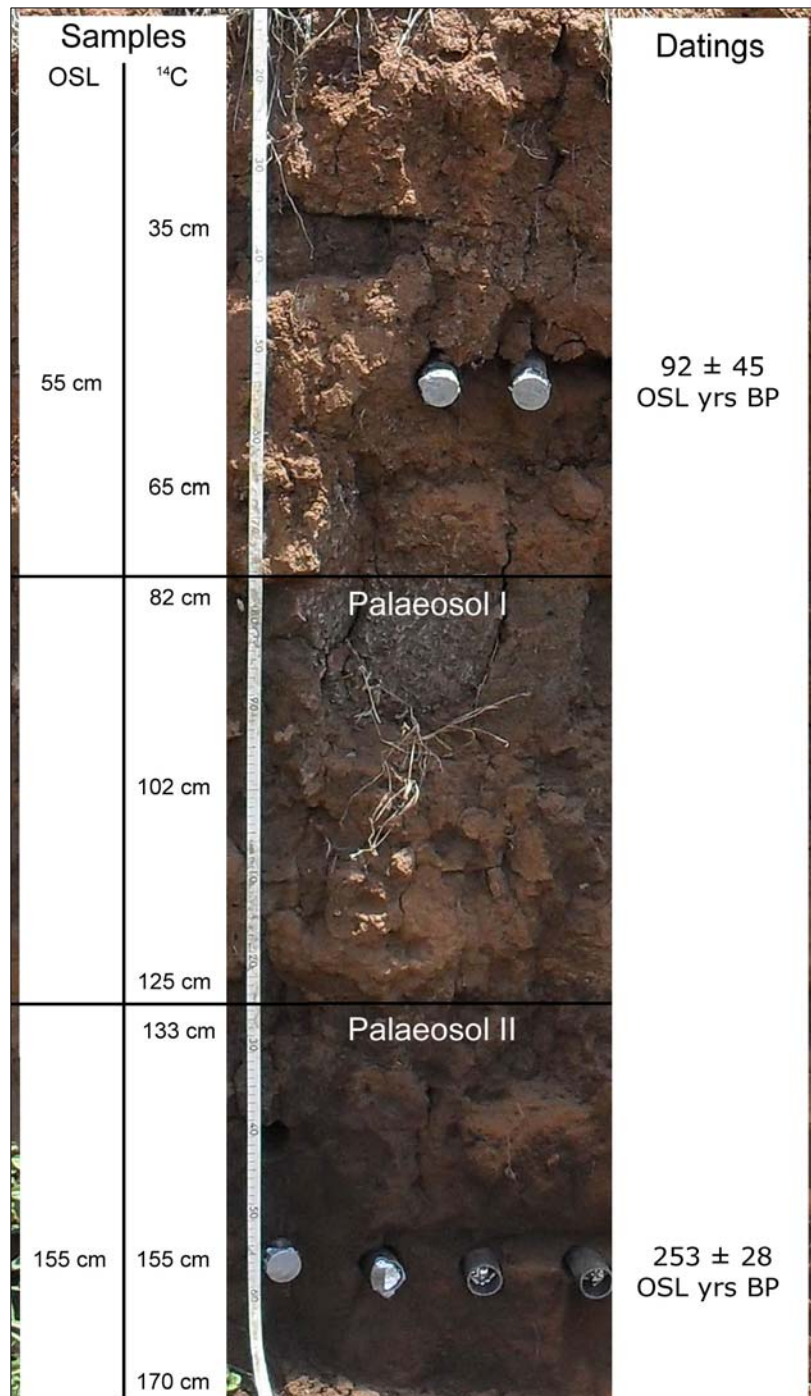


**FIG 5.2** Exposure of the colluvial deposits of the Mshizii site. The palaeosol horizons are indicated, together with locations of the <sup>14</sup>C and the OSL samples. On the right the OSL burial ages of the corresponding layers are given (with 68% certainty). A detailed description of the soil layers is presented in appendix II.

The colluvial deposits that buried palaeosol II point at another period of unstable hillslope conditions and erosion. In the climatic record, the wet end phase of the Little Ice Age was

followed by a drier period at the start of the 19<sup>th</sup> century (Nicholson, 2001). This drier period could be the cause for the renewal of the hillslope erosion by affecting the protective vegetation cover, subsequently causing the burial of palaeosol II. These events all together represent one 'K-cycle' of the adjacent hillslope (Butler, 1959), which starts with the period of erosion and deposition during the Little Ice Age, followed by pedogenesis and ended by renewed erosion and deposition.

Palaeosol I was formed in the colluvial deposits that bury palaeosol II, indicating another stable period on the hillslope. This formation probably coincided with the change to a 'normal' wet climate, which occurred subsequently during the second half of the 19<sup>th</sup> century (Nicholson, 2001).

A second 'K-cycle' ends when palaeosol I becomes buried by new colluvium. The OSL date of these overlying, colluvial deposits, halfway between palaeosol I and the present day surface, yields a burial age somewhere in the first part of the 20<sup>th</sup> century. This corresponds with the erosional phase triggered by large scale deforestation and agricultural practice in the Usambara Mountains at the end of the 19<sup>th</sup> century. This suggests that palaeosol I was the soil surface from the time before the German colonial rule, just like the buried palaeosol of the Mzungu site. The colluvial deposits that bury the palaeosol, are believed to be the result of the increased anthropogenic impact on the landscape.

Over a period of ~200 years a colluvium layer with a thickness of 100 cm has been deposited. This means an annual deposition of at least 5 mm of colluvial material. When this value is used to estimate the corresponding erosion rates on the adjacent hillslope, it yields much higher values than, for example, are measured for steep, forested hillslopes (Lundgren, 1980). This suggests that the vegetation cover on the hillslope was not in a full state throughout the period of deposition. This is in line with the expected effects of the climatic changes of the past centuries on the vegetation. Furthermore, the presence of two palaeosols in this colluvial record shows the high speed in which soil profiles can develop in the Usambara Mountains.

The pedostratigraphy and the OSL datings from the exposure of the colluvium in the Mshizii site are in line with the climatic and agricultural history. The unstable periods in the past, together with the two stable periods on the hillslope, can be explained by the past climatic changes and are confirmed by the OSL datings. The colluviation and pedogenesis of the palaeosols are therefore considered to be a consequence of climatic forcing on the hillslope stability. Although the colluvial and the climatic record go hand in hand, it is not possible to fully exclude anthropogenic impact on the hillslope stability during this period. The last and at present ongoing erosional phase, that buried palaeosol I, can be ascribed to anthropogenic influence following the German colonial rule, similar to the Mzungu site.

## 6. Discussion

In the following discussion the results are summarized and hypotheses are given that explain the results. Furthermore, the implications and usefulness of the research methods are discussed. Due to the absence of literature on this topic, the results on the erosion history can not be compared in depth to other studies. Therefore, the involved implications and uncertainties in the results will be pointed out and discussed.

### 6.1 Historical soil erosion

The soil erosion history as derived from in the Mzungu and Mshizii colluvial archives is shown graphically in figure 6.1. Periods of colluviation and pedogenesis, as a result of a dry or wet climate, are in line with the results of studies elsewhere (e.g. Clarke et al., 2003; Thomas & Thorp, 1995; Wintle et al., 1995). The dramatic changes in the landscape after the arrival of the German settlers correspond to historical observations in the area (Conte, 1999; Vigiak, 2005). The boundaries between the stable and unstable conditions are an interpretation, since no exact age control is available at present.

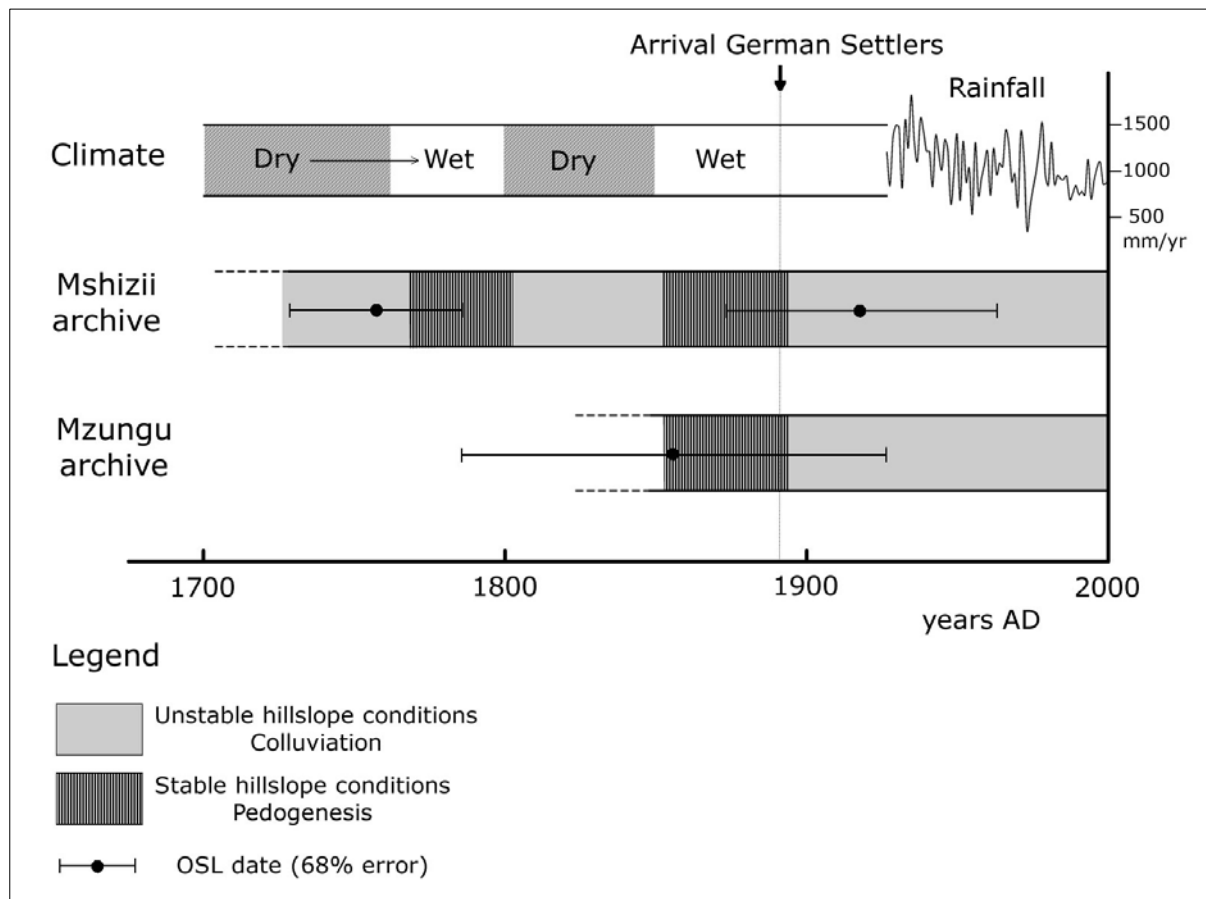


**Fig. 6.1** Soil erosion history of the Usambara Mountains based on the hillslope deposits of the Mshizii and the Mzungu site. The wetness of the climate is based on literature (Brown & Johnson, 2005; Hassan, 2011; Nicholson, 2001; Stager et al., 2005).

## **6.2 Mzungu area**

The buried palaeosol of the Mzungu site is situated right on top of the reddish subsoil. It does not show a complete soil profile like in other sites and looks more like an A-horizon on top of a degraded soil. This might indicate that the period during which the palaeosol had formed was preceded by a phase of severe erosion that removed the original soil surface, leaving the reddish subsoil at the surface. It would explain why the palaeosol is situated directly on top of the subsoil with no intermediate soil profile, as witnessed for other sites. Evidence on a possible, earlier erosional phase is not found in the Mzungu area, but it might be present in sedimentary archives further down in the valley, similar to deposits of the Mshizii area.

## **6.3 Mshizii area**

### **6.3.1 The origin of the charcoal rich soil layers**

The exposure of the Mshizii site contains three soil layers that differ in texture from the other deposits. At first they were marked as possible palaeosols. However they are by far not as distinct and as well developed as the two clear palaeosols in the exposure. The three soil layers share the same coarse texture, porosity and hardness and they all contain a large amount of charcoal. This stood at the base of the hypothesis that the layers are not palaeosols, formed during a longer time of hillslope stability, but that they are artifacts of past (wild)fires. These fires would have burned the vegetation, which would explain the presence of the charcoals layers. Secondly, the high temperature could have altered the soil properties, which would explain the deviating texture and the hardness of the layers. The layer at 100 cm depth has 1 cm layer of pure sand deposited on top of it. A recent study by Stoof (2011) found an increase in runoff and erosion shortly after a fire due to increased water repellency of the soil. This would explain the deposition of sand, due to increased runoff. The absence of clays in this layer strengthens the hypothesis the clays at the surface were 'baked' and hardened in conglomerates by the heat of the fire, leaving only sand to be transported by water. It would also explain the extraordinary texture and hardness of the layers. However, there is no hard evidence to validate this hypothesis.

### **6.3.2 Colluvial deposits in the valley floor and the origin of the stream**

The exposure of the Mshizii site was created by an incising stream and is located in the valley floor. This raises the question whether the deposits are of colluvial or alluvial (fluvial deposition) in nature. The characteristics of the stream, together with the undisturbed nature of the sedimentary stratigraphy in the exposure, suggest a colluvial, rather than alluvial origin. The sediments are believed to be deposited solely by hillslope processes and fluvial contribution to the sedimentation process is believed to be insignificant.

The comparison of the 1955 aerial photographs with the recent Worldview-II image learned that the stream has a very slow meandering speed. The little amount of water carried by the stream and the very cohesive stream banks probably account for this slow meandering of the stream. However, even a slowly meandering stream, when given enough time, would eventually have reworked a small valley floor like in the Mshizii area. The fact that the colluvial deposits are not reworked, at least since the end of the Little Ice Age, and the valley floor still has a clear V-shape, could mean that the stream is of relatively, young age. It might have started to incise when the hydrological regime in the area severely changed due to large scale deforestation and agricultural practice. With equal precipitation amounts, deforestation, in general, means less evapotranspiration (Zhang et al., 2001), leaving more water available to reach the valley bottoms, by both overland and subsurface flow. This could, subsequently, have resulted in the formation of an incising stream, as is apparent at present. This would also explain why the colluvial deposits of Mshizii site have not been eroded away earlier.

#### **6.4 Dating of colluvial deposits**

In this study two dating methods were used, to determine the age of colluvial deposits. As mentioned before, OSL dating is the favorable method over radiocarbon dating, since it dates the sediments directly, instead of using carbon as a proxy (Lian and Roberts, 2006). The three OSL datings presented in this study are all of very young age and the samples all suffered from poor bleaching. The use of single grain dating, in combination with the minimum age model (Galbraith et al, 1999) and the PDF presentation of the age (Cunningham & Wallinga, 2011), made the dating of the sediment possible. Processes like clay and subsequently radionuclides leaching, altering the dose rate over time, or the incorporation of younger sediments from higher layers, form additional uncertainties, which are difficult to quantify. For an extensive discussion on uncertainties concerning the OSL datings and methods used, see the OSL dating report in appendix III. The ages of the OSL samples are in line with the information present in the colluvial records and temporarily consistent with the erosion history of the area. This validates the conclusion that OSL dating forms a valid method for dating colluvial deposits (e.g. Eriksson et al., 2000; Fuchs & Lang., 2009)

At the time of writing, the radiocarbon results are not yet available. This makes a discussion on the accuracy of  $^{14}\text{C}$  dating of colluvial deposits not possible. It is believed that  $^{14}\text{C}$  datings of charcoal pieces, originating from distinct layers, likely relics of past wildfires, can be used as a valid proxy for dating a soil layer. The ages of the charcoal samples that have been submitted for dating can improve the understanding of the processes captured in the colluvial records and may create a better temporal link with the climatic record.

## **6.5 Measuring erosion using exposed tree roots**

The application of the erosion measurement method using exposed tree roots by Gärtner (2007) appeared to be impossible, after some field pilots and studies of the local vegetation, for the following reasons:

- Trees in the Usambara Mountains form their rings according to the irregular bimodal raining season. This creates an irregular production of tree rings on annual basis, which results in large uncertainties when counting years from tree rings.
- Agricultural fields mostly lack large trees and the agricultural activities on the plot have disturbed the situation too much.
- In patches of natural forest this disturbance is not present, but here another problem occurs. The forest floor has a thick litter cover. This strongly reduces any possible erosion and could alter the reaction of the tree root to exposure, which would give unclear results.
- The growth rate of some native species is extremely high. For example, a tree with a stem size of approximately 50 cm, took only 7 years to grow. Trees with a growth speed this high are not suitable for this method since their age is too young to yield significant information on a decennial timescale.

The above described reasons resulted in the conclusion that this method is not suitable for the type of region and vegetation cover of the Usambara Mountains in Tanzania. Hence, the statement of the author that the method is applicable in all parts of the world where trees form annual rings is proven to be incorrect.

## **6.6 Palaeo-erosion rates**

In order to investigate past erosion rates, colluvial deposits can be used, preferably without interrelated palaeosols, because their presence indicates hiatuses. When colluvial deposits are dated with fixed intervals, the deposition rate and possible changes over time can be studied. In the Mshizii area, a 4 meter thick colluvium layer is exposed by a road (site 030). This colluvium was sampled for OSL dating by using fixed intervals of one meter, as is shown in figure 6.2a. However an error was made by measuring the distance between the samples in a vertical direction. Since the exposure is not exactly vertical itself, the intervals were not equally distributed in the direction of the sediment deposition. This is set out graphically in figure 6.2b. Since the angle of deposition is unknown, OSL samples taken at site 030 can not be used for determining past erosion rates. Determining the angle of deposition for such deposits can be very challenging and might prove to be impossible.

However, knowing the angle of deposition is crucial when samples are not super positioned exactly in a vertical profile.

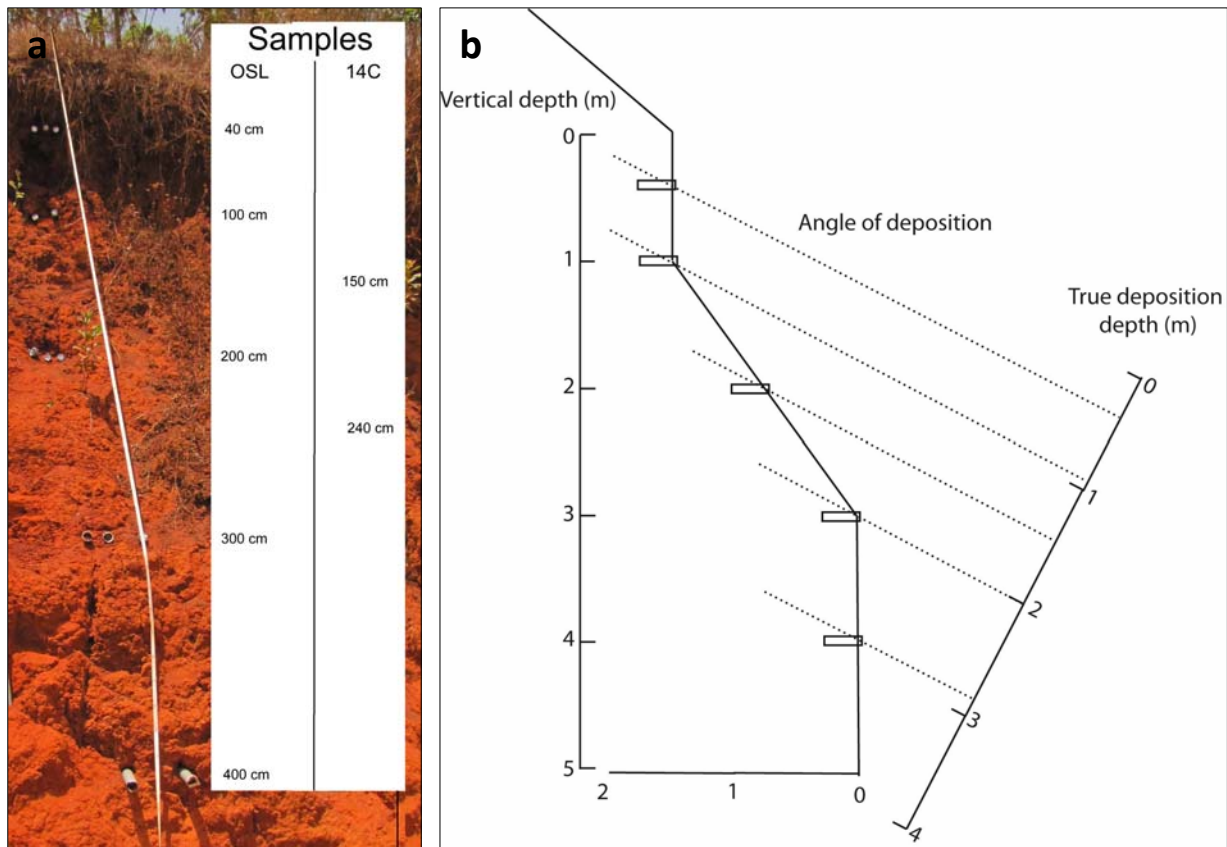


**FIG 6.2 a)** The colluvium exposed at site 030 in the Mshizii area. The position of the OSL and <sup>14</sup>C samples is indicated. **b)** Schematic representation of the OSL samples collected for site 030, with their 'true' depositional depth dependant on the (unknown) angle of deposition.

The two OSL datings of the Mshizii site can only be used to give a rough indication of the past erosion rate, since, as mentioned before, its intermediate palaeosols indicate hiatuses. When trying to compare the present day erosion rates to the past erosion rates as recorded in colluvial deposits, another problem is faced. The thickness of a layer in an exposure does not give a straight forward estimate of the total amount of eroded sediment. In order to calculate the total volume, the spatial distribution of the sediment cover should be known. It also requires a closed sedimentary system, with no sediments leaving the catchment, in order to get a valid outcome. For the Usambara Mountains such a study will be very challenging, since it is very difficult to find and to determine suitable deposits in closed systems.

### **6.7 Climatic forcing versus anthropogenic forcing**

The determination of the main forcing behind a certain erosional phase as captured in a colluvial archive can be a difficult task. It is a challenge to separate climatic forced erosion from anthropogenic, especially since the latter can, most of the time, not be excluded with

certainty. For the Mshizii site, the two 'K-cycles' to which the two palaeosol belong, are dated before the major landscape changes following the German colonial rule. The historical information on hillslope stability captured in the sedimentary archive, can be correlated positively to the climatic record of the 18<sup>th</sup> and 19<sup>th</sup> century. Therefore, it is very likely that climate was indeed a main forcing factor on the hillslope stability during that time. But anthropogenic impact cannot be excluded with certainty.

The severe erosion event, captured in the exposure of the Mzungu area, is strongly linked to anthropogenic deforestation and cultivation of the land. When anthropogenic influence on erosion is so prominently present, the role of climate change on erosion is not expected to be significant compared to the anthropogenic forcing. This is mainly because the vegetation cover is no longer influenced by climatic changes, but artificially by human activity. However, increasing wetness will enhance erosion further, when the vegetation cover is damaged by human activity.

This is interesting because in a natural situation an increase in precipitation will eventually lead to a decrease in hillslope erosion due to the growth of a protective vegetation cover, instead of an increase (Thomas & Thorp, 1995). In an artificial situation, when vegetation cover is no longer a result of the water availability but of human activity, an increase in precipitation may lead to more erosion. So there is a reverse in the effect of climatic change on hillslope stability when humans affect the vegetation cover.

### ***6.8 The use of colluvial records to reconstruct the soil erosion history***

The results from this study show that it is possible to reconstruct the soil erosion history by using the sedimentary records from colluvial deposits. However, a main problem with this method is the availability of useful colluvial archives. Using corings to investigate a colluvial depository is possible, as is shown for site 013 (appendix II), but a lot of information on the soil stratigraphy is lost due to the mixing of the sediments when using the corer. In order to investigate a colluvium stratigraphy thoroughly, exposures in the landscape, created both naturally, like river incisions (Mshizii site) and artificially, like roads (Mzungu site), are required. This dependency made it difficult to find good-quality exposures of colluvial deposits. When dealing with exposures created by natural causes, one should be careful since the process that created the exposure, could also have eroded the colluvial record at an earlier time. This could have created a hiatus in the sedimentary record. As argued before, for the Mshizii site, this is probably not the case.

The potential for colluvial deposits to hold a valuable record of the erosion history over a certain time is depending on the location in the landscape. In general, the potential to capture a longer time in the colluvium increases with decreasing altitude in the landscape,

as long as fluvial activity is limited. Figure 6.3 shows this concept schematically. It shows that the deposits closer to and in the valley bottom have the highest potential for holding large colluvial archives of historic information. This is proven to be valid when the Mzungu and Mshizii sites are compared, and it is expected to be true on both single hillslope and on full catchment scale.

A second advantage of sites in a valley bottom, is that they could act as a magnifier, since even a small amount of erosion on the adjacent hillslope will accumulate in significant deposits. This makes it possible to distinguish small erosion events because of this effect. A prerequisite for this is that the sediment has to reach the valley floor. The disadvantage of these sites in a valley bottom is mentioned before, namely the possibility of fluvial erosion and reworking of the record.

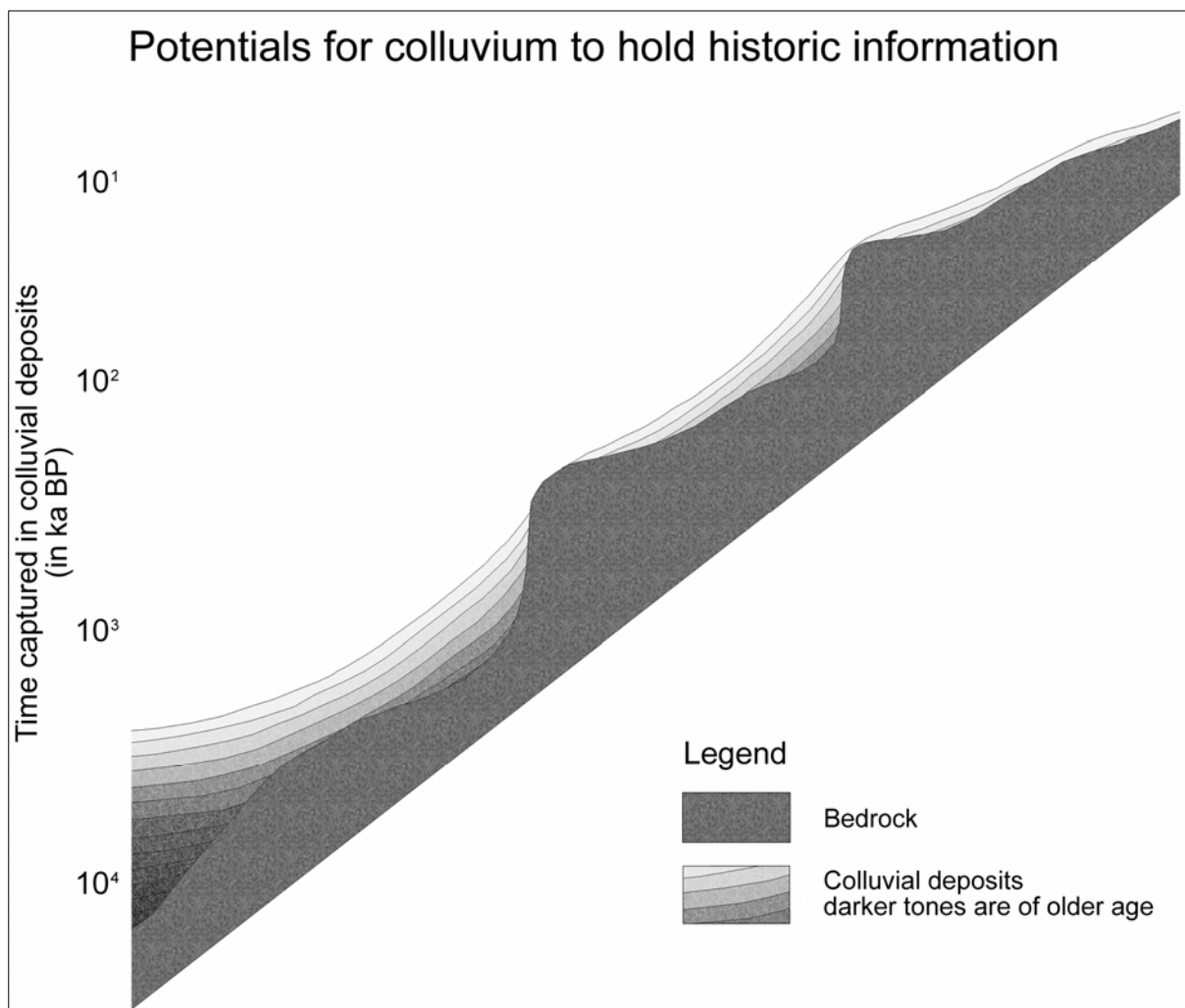


**FIG 6.3** A schematic representation of the site-specific potentials of colluvial deposits to hold a certain temporal record. The age on the left axis show the increase in potential time-depth for colluvial records with decreasing altitude in the landscape.

## 7. Conclusions

This study showed that colluvial sedimentary records can be used successfully to investigate the soil erosion history of the hillslopes in the West Usambara Mountains, Tanzania. The colluvial archives from two key sites, Mzungu and Mshizii, recorded fluctuations in the past hillslope stability over the past three centuries. Periods with water erosion on the hillslope, and corresponding colluviation, are witnessed together with stable periods with no erosion during which palaeosols could develop on the surface of the colluvium. Geomorphologic, stratigraphic and pedogenetic investigation of the sites, together with OSL datings for age control, suggests two different erosional phases.

The first phase, ranging from the start of the 18<sup>th</sup> century till the end of the 19<sup>th</sup>, is recorded in the Mshizii site by two 'K-cycles' of hillslope erosion. These deposits are dated by OSL ages and their stratigraphy can be explained by the response of the hillslope stability to the past climatic changes. Climatic forcing is considered to be the main controlling factor of the hillslope stability during this phase. However, anthropogenic forcing on the hillslope stability cannot be excluded with certainty.

The second phase of hillslope erosion, as registered in both the Mshizii and the Mzungu site, started at the end of the 19<sup>th</sup> century. It concerns a period of severe, widespread hillslope erosion. Hillslope geomorphology show a strong link to the anthropogenic erosional forcing and OSL dating coincides with the dramatic land management changes following the German colonial administration. This erosional phase, that is still ongoing at present, is considered be the result of anthropogenic activities like deforestation and subsequent agricultural practice on the hillslopes. Since the vegetational cover is artificially controlled by human practice, and annual precipitation amounts show a decreasing trend, climatic change is not believed to be significant driving force behind hillslope erosion during this period.

Vegetation plays a major role for the hillslope stability. The triggering of erosion on a hillslope by both natural and anthropogenic forcings, is based on the decrease of the protective vegetational cover. On short timescales, climatic variation and its influence on the vegetation cover is overshadowed by the severe impact of deforestation and agricultural practice. However, variations in the precipitation will still influence the amount of water erosion on a hillslope. Unraveling the contribution of the two main erosional forcings to the actual erosion, is not possible based on hillslope deposits only.

The use of colluvial archives to reconstruct the past erosion history is limited to the time captured in the colluvial deposits in the landscape. It is also depending on the presence of palaeosols and datable material. Dating of these colluvial archives forms the backbone for age control and linkage to the climatic and anthropogenic historical records. Attempts to

derive the past erosion rate from the colluvial deposits were obstructed by the difficulty to determine the angle of deposition and to quantify the total sediment accumulation in colluvial deposits. The results from the radiocarbon datings are expected to improve the age control further and underpin the conclusions. Overall, colluvial deposits prove to be valuable sedimentary archives for studying the erosion history of an area.

## References

- Aitken, M.J., 1998. *An Introduction to Optical Dating*. Oxford University Press, Oxford.
- Balls, M.J., Bodker, R., Thomas, C.J., Kisinza, W., Msangeni, H.A., Lindsay, S.W., 2004. Effect of topography on the risk of malaria infection in the Usambara Mountains, Tanzania. *Transactions of the Royal Society of Tropical Medicine and Hygiene* 98, 400-408.
- Barker, P.A., Leng, M.J., Gasse, F., Huang, Y., 2007. Century-to-millennial scale climatic variability in Lake Malawi revealed by isotope records. *Earth and Planetary Science Letters* 261, 93-103.
- Botha, G.A., Fedoroff, N., 1995. Palaeosols in Late Quaternary colluvium, northern KwaZulu-Natal, South Africa. *Journal of African Earth Sciences* 21, 291-311.
- Brown, E.T., Johnson, T.C., 2005. Coherence between tropical East African and South American records of the Little Ice Age. *Geochemistry, Geophysics, Geosystems* 6, no 12.
- Burton, R., 1860. *The Lake Regions of Central Africa*. Longmans Green, London.
- Bush, D.A., Feathers, J.K., 2003. Application of OSL single-aliquot and single-grain dating to quartz from anthropogenic soil profiles in the SE United States. *Quaternary Science Reviews* 22, 1153-1159.
- Butler, B.E., 1959. *Periodic Phenomena in Landscapes as a basis for Soil Studies*. CSIRO Australia, Soil Publication 14.
- Clarke, M.L., Vogel, J.C., Botha, G.A., Wintle, A.G., 2003. Late Quaternary hillslope evolution recorded in eastern South African colluvial badlands. *Palaeogeography, Palaeoclimatology, Palaeoecology* 197, 199-212.
- Conte, C. A. (1999). The forest becomes desert: forest use and environmental change in Tanzania's West Usambara mountains. *Land Degradation & Development*, 10: 291-309.
- Cunningham, A.C., Wallinga, J., submitted. Realizing the potential of fluvial archives using robust OSL chronologies. Submitted to *Quaternary Geochronology*.
- deMenocal, P., Ortiz, J., Guilderson, T., Adkins, J., Sarnthein, M., Baker, L., Yarusinsky, M., 2000. Abrupt onset and termination of the African humid period: rapid climate responses to gradual insolation forcing. *Quaternary Science Reviews* 19, 347-361.
- Eriksson, M.G., Christiansson, C., 1997. Accelerated soil erosion in central Tanzania during the last few hundred years. *Physics and Chemistry of the Earth* 22, 315-320.
- Eriksson, M.G., Olley, J.M., Payton, R.W., 2000. Soil erosion history in central Tanzania based on OSL dating of colluvial and alluvial hillslope deposits. *Geomorphology* 36, 107-128.
- Faniran, A., Jeje, L.K., 1983. *Humid Tropical Geomorphology*. Longman Inc., New York.
- Fuchs, M., 2007. An assessment of human versus climatic impacts on Holocene soil erosion in NE Peloponnese, Greece. *Quaternary research* 67, 349-356.
- Fuchs, M., Lang, A., 2001. OSL dating of coarse-grain fluvial quartz using single-aliquot protocols on sediments from NE Peloponnese, Greece. *Quaternary Science Reviews* 20, 783-787.
- Fuchs, M., Wagner, G.A., 2003. Optical dating of sediments: recognition of insufficient bleaching by small aliquots of quartz for reconstructing soil erosion in Greece. *Quaternary Science Reviews* 22, 1161-1167.
- Fuchs, M., Wagner, G.A., 2005. Chronostratigraphy and geoarchaeological significance of an alluvial geoarchive: comparative OSL and AMS <sup>14</sup>C dating from Greece. *Archaeometry* 47, 849-860.
- Fuchs, M., Lang, A., 2009. Luminescence dating of hillslope deposits – A review. *Geomorphology* 109, 17-26.
- Fuchs, M., Fischer, M., Reverman, R., 2010. Colluvial and alluvial sediment archives temporally resolved by OSL dating: Implications for reconstructing soil erosion. *Quaternary Geochronology* 5, 269-273.
- Galbraith, R.F., Roberts, R.G., Laslett, G.M., Yoshida, H. & Olley, J.M., 1999. Optical dating of single and multiple grains of quartz from Jinmium rock shelter, northern Australia: Part I, experimental design and statistical models. *Archaeometry* 41: 339-364.
- Garcin, Y., Vincens, A., Williamson, D., Buchet, G., Guiot, J., 2007. Abrupt resumption of the African Monsoon at the Younger Dryas-Holocene climatic transition. *Quaternary Science Reviews* 26, 690-704.
- Gärtner, H., 2007. Tree roots. Methodological review and new development in dating and quantifying erosive processes. *Geomorphology* 86, 243-251.
- Gasse, F., 2000. Hydrological changes in the African tropics since the Last Glacial Maximum. *Quaternary Science Reviews* 19, 189-211.
- Gasse, F., Chalié, F., Vincens, A., Williams, M.A.J., Williamson, D., 2008. Climatic patterns in equatorial and southern Africa from 30,000 to 10,000 years ago reconstructed from terrestrial and near-shore proxy data. *Quaternary Science Reviews* 27, 2361-2340.
- Hassan, F.A., 2011. Nile flood discharge during the Medieval Climate Anomaly. *PAGES news* 19, no 1, 30-31.

- Huang, C.C., Jia, Y., Pang, J., Zha, X. and Su, H. 2006. Holocene colluviation and its implications for tracing human-induced soil erosion and redeposition on the piedmont loess lands of the Qinling Mountains, northern China. *Geoderma* 136, 838-851.
- Huntley, D.J., Godfrey-Smith, D.I., Thewalt, M.L.W., 1985. Optical dating of sediments. *Nature* 313, 105-107.
- Kaoneka, A.R.S., Ngaga, Y.M., Menla, G.C. 2000. Case study: forests of Usambara Mountains: historical perspectives and future prospects. *Forests in sustainable mountain development: a state of knowledge report for 2000*. CABI Publishing, 97-103.
- Kimaro, D.N., Poesen, J., Msanya, B.M. and Deckers, J.A., 2008. Magnitude of soil erosion on the northern slope of the Uluguru Mountains, Tanzania: Interrill and rill erosion. *Catena* 75, 38-44.
- Lang, A., Hönscheidt, S., 2003. Age and source of colluvial sediments at Vaihingen-Enz, Germany. *Catena* 38, 89-107.
- Lang, A., 2003. Phases of soil erosion-derived colluviation in loess hills of South Germany. *Catena* 51, 209-221
- Lian, O.B., Roberts, R.G., 2006. Dating the Quaternary: progress in luminescence dating of sediments. *Quaternary Science Reviews* 25, 2449-2468.
- Lundgren, J., 1980. Comparison of Surface Runoff and Soil Loss from Runoff Plots in Forest and Small-Scale Agriculture in the Usambara Mts., Tanzania. *Geografiska annaler. Ser. A, physical geography* 62, 133-148.
- Madsen, A. T., Murray, A. S., 2009. Optically stimulated luminescence dating of young sediments: A review. *Geomorphology* 109, 3-16.
- Mambo Footprints, 2009. Human footprints in sedimentary rocks of 1.5 Ma age. [www.mambafootprints.com](http://www.mambafootprints.com)
- Meliyo J, W., Kabushemera Tenge A. 2002. Characterization and mapping soils of Kwalei subcatchment, Lushoto district. Agricultural Research Institute Mlingano, Tanga.
- Mumbi, C.T., Marchant, R., Hooghiemstra, H. and Wooller, M.J. 2008. Late Quaternary vegetation reconstruction from the Eastern Arc Mountains, Tanzania. *Quaternary research* 69, 326-341.
- Murray, A.S., Roberts, R.G., 1997. Determining the burial time of single grains of quartz using optically stimulated luminescence. *Earth and Planetary Science Letters* 152, 163-180.
- Nicholson, E., 2001. Climatic and environmental change in Africa during the last two centuries. *Climate research Vol. 17*: 123-144.
- Powers, L.A., Johnson, T.C., Werne, J.P., Castañeda, I.S., Hopmans, E., Sinninghe Damsté, J.S. and Schouten, S., 2005. Large temperature variability in the southern African tropics since the Last Glacial Maximum. *Geophysical research letters* 32.
- Ritchie, J.C., Eyles, C.H., Haynes, C.V., 1985. Sediment and pollen evidence for an Early to Mid-Holocene humid period in the Eastern Sahara. *Nature* 314, 352-355.
- Sakarani mission rainfall data. Monthly rainfall data collected at the Sakarini Mission located in the study area. Record starts in 1928.
- Sanchez, P. 1994. Alternatives to slash and burn: a pragmatic approach for mitigating tropical deforestation. J.R. Anderson, *Agricultural Technology Policy Issues for the International Community*, CAD International, 451-480.
- Shackleton, R., 1993. Tectonics of the lower crust: a view from the Usambara Mountains, NE Tanzania. *Journal of Structural Geology* 15, 663-671.
- Stager, J.C., Cocquyt, C., Bonnefille, R., Weyhenmeyer, C. and Bowerman, N. 2009. A late Holocene paleoclimatic history of Lake Tanganyika, East Africa. *Quaternary research* 72, 47-56.
- Stokes, S., 1999. Luminescence dating applications in geomorphological research. *Geomorphology* 29, 153-171. Soil erosion history based on hillslope deposits in the Western Usambara Mountains of Tanzania 19.
- Stoof, C.R., 2011. Fire effects on soil and hydrology. Doctoral Thesis Wageningen University.
- Speke, J.H., 1865. *Upptäckten af Nilens källor*. E.T. Berggren, Stockholm.
- Temme, A.J.A.M., 2008. Understanding Landscape Dynamics over thousands of years: combining field and model work. With a case study in the Drakensberg Foothills, KwaZulu-Natal, South Africa. PhD Thesis, Wageningen Univ.
- Temme, A.J.A.M., Baartman, J.E.M., Botha, G.A., Veldkamp, A., Jongmans, A.G. and Wallinga, J. 2008. Climate controls on late Pleistocene landscape evolution of the Okhombe valley, KwaZulu-Natal, South Africa. *Geomorphology* 99, 280-295.
- Tenge, A.J.M., 2005. Participatory appraisal of farm-level soil and water conservation planning in West Usambara highlands, Tanzania. Doctoral Thesis Wageningen University. *Tropical Resource Management Papers* 63.
- Thomas, M. F., 1994. *Geomorphology in the tropics: a study of weathering and denudation in low latitudes*. Wiley.

- Thomas, M.F., Thorp, M.B., 1995. Geomorphic response to rapid climatic and hydrologic change during the late Pleistocene and early Holocene in the humid and sub-humid tropics. *Quaternary Science Reviews* 14, 193–207.
- Thompson, L.G., Mosley-Thompson, E., Davis, M.E., Henderson, K.A., Brecher, H.H., Zagorodnov, V.S., Mashiotta, T.A., Lin, P.N., Mikhalenko, V.N., Hardy, D.R., Beer, J., 2002. Kilimanjaro ice core records: evidence of Holocene climate change in tropical Africa. *Science* 298, 589–593.
- Vigiak, O., 2005. Modelling spatial patterns of erosion in the West Usambara Mountains of Tanzania. Doctoral Thesis Wageningen University. *Tropical Resource Management Papers* 64.
- Wallinga, J., 2002. Optically stimulated luminescence dating of fluvial deposits: a review. *Boreas* 31, 303–322.
- Wintle, A.G., Botha, G.A., Li, S.H., Vogel, J.C., 1995. A chronological framework for colluviation during the last 110 kyr in KwaZulu/Natal. *South African Journal of Science* 91, 134–139.
- Zhang, H., Henderson-Sellers, A., McGuffie, K., 2001. The compounding effects of tropical deforestation and greenhouse warming on climate. *Climatic change* 49, 309–338.
- Zech, M., 2006. Evidence of Late Pleistocene climate changes from buried soils on the southern slopes of Mt. Kilimanjaro, Tanzania. *Palaeogeography, Palaeoclimatology, Palaeoecology*. 242, 303–3112.

## Appendices

- I. Field logbook
- II. Site description and samples for dating
- III. Optical dating report

# Historical soil erosion in the West Usambara Mountains, Tanzania

*A study based on hillslope deposits*

## Appendices

MSc Thesis Physical Geography  
P.S.J. Minderhoud

*Faculty of Geosciences  
Department of Physical Geography  
Utrecht University*

Under supervision of  
Dr. G. Sterk  
Dr. W.Z. Hoek

30<sup>th</sup> of June 2011



**Universiteit Utrecht**

## Appendix I: Field logbook

This is the digital version of the field logbook notations made during the field survey. It provides an overview of all observations done. They are ordered by their waypoint number and correspond with the location given in figure 4.1. Color codes are according to the Universal Soil color Chart. A list of all waypoints is given at the end of this appendix.

Waypoint:      Observation/description:

101

Sashuhi village, location at the end of a slope in the valleyfloor, coring. Slope angle 34 degrees. Slope length: 100m. Coring ends in weathered bedrock.  
 0 cm Sandy clay, Br, unconsolidated, dry.  
 20 cm Sandy clay, DBrBI (7.5YR3/2). quartz grains.  
 50 cm Sandy clay, DBrR (5YR3/4). transition with above layer 10 cm, large quartz grains. Pieces of charcoal. 80-100 cm more reddish (5YR3/6).  
 150 cm Sandy clay, DBrBI (7.5YR3/2). Yellow pieces.  
 200 cm Sandy clay, YeBr (10YR4/3), mz/gz ps.  
 250 cm Sandy clay, Br (7.5YR4/3), fz/mz. Decrease in sand content. Strongly compacted. Yellow spots.  
 280 cm Sandy clay, Br (7.5YR4/4). Strong increase coarse quartz grains. Fast oxidation.  
 300 cm Sandy clay, BrYe (7.5YR5/6). Increase yellow colour and pieces of weathered bedrock with depth. Coring in weathered bedrock.  
 360 cm END

001

Mzungu village area  
 Field with terraces with a distinct dark layer, possible A horizon. Dark horizon right on the bed rock. Layer buried under 30 cm of colluvium. Probably a very young buried palaeosol.

002

Mzungu village area  
 Roadcut with dark (grey/black) horizon buried with Br material.

003

Mzungu village area. Small valley floor in a horseshoe shaped valley.  
 Two buried, dark horizons. First possible palaeosol, at 100 cm, expected to be the onset of agriculture. Charcoal sample taken. Second possible palaeosol, at 230 depth, could represent an older phase, OSL sample taken. *Uncertain whether second dark horizon represents old buried A-horizon.*

0 cm Sandy clay, Br (10YR3/3), fz ps a2, quartz grains GGD:3 mm. Moderately clayey, high sand content. Rich of plant material and roots.  
 100 cm Sandy clay, DBrBI (7.5YR3/2), mz/gz vps, high sand content, charcoal, roots. Increase in clay content with depth. Sharp, 1-2 cm, transition with underlying horizon. *Possible buried horizon. Charcoal sampled at 110 cm. (TZ03-110-C14)*  
 120 cm Sandy clay, BrR (2.5YR3/3), mz, vps, roots.  
 150 cm Sandy clay, DRBr (5YR3/6), mz,vps, clay increase.  
*Charcoal sampled at 150 cm. (TZ03-150-C14)*  
 180 cm Sandy clay, RBr (5YR3/4), clay increase.  
 220 cm Sandy clay, DYeBr (7.5YR4/3), little sand. Black, dark spots. Gradual transition.

230 cm Sandy clay, BrBl (5YR3/2), mz, GGD 2 cm. Fe spots. Sharp transition with above layer (2cm). No charcoal. *Old palaeosol. OSL Sample taken, top at 230, bottom at 235. (TZ-03-230)*

245 cm Sandy clay, Br (5YR4/3).  
(start coring)

260 cm Sandy clay, OrBr (5YR5/8), little sand. Loamy. Pieces of weathered bedrock.

340 cm Weathered bedrock, END

OSL sample taken:

TZ-03-230 Mzungu village, Lushoto District, 02-11-2010, PVC pipe

C14-samples taken:

TZ03-110-C14 Mzungu village, Lushoto District, 02-11-2010. Various charcoal pieces from a 'layer' at this depth.

TZ03-150-C14 Mzungu village, Lushoto District, 02-11-2010. At the top of the DBrR layer.

004

Start interesting place in valley bottom.

005

Housecut East of Sashuhi colluvium, single soil profile.

006

Colluvium housecut close to valleyfloor. Quartz layer.

007

Quarry with strongly weathered bedrock. 5-6 m deep dug out with shovel. Very soft. *N.B. The bedrock becomes very soft and this could prove difficulties for distinguishing between soil and weathered bedrock.*

008

Soni Market cut, 5 m, single soil profile of 3-4m on weathered bedrock.

009

Roadcut Mzungu village, 1.5m. slope 15/20 degrees, 100-300m long. Roadcut half way on the hillslope. Agricultural field category 5/6 (very little adoption of SLM). Probably severe erosion with sufficient rain.

0 cm Sandy clay, Br (10YR4/3), fz/mz, ps, a1, high sand content. Organic material.

60 cm Sandy clay, BrBl (10YR2/2), fz/mz, ps, a1. *Possible buried palaeosol. Burial age expected to be at the onset of agricultural practice.*

80 cm Sandy clay, ROr (7.5YR4/4), fz/mz, ps, a2/a1, toucher material, higher clay content, roots. Charcoal.

120 cm Sandy clay, dBr (7.5YR4/3), mz, vps, a1, roots, charcoal.

140 cm Sandy clay, BrR (5YR4/4). Same structure

160 cm END

010

Valley near Mzungu village, dark, BrBl layer buried under 30 cm colluvium. Charcoal. On top of orange horizon, very touch, high clay content. Could be interesting spot for a coring.

011

Valleycut, start of the cut is 1,5 m down of the road, 7m above valley floor, at the end of a 300 m long slope. Natural colluvium. Very rocky, large stones up to 10 cm.

0 cm Sandy clay, RBr (5YR4/4), charcoal. At 55 cm piece of cloth, human deposited. *Possibly deposited with roadcontruction.*

60 cm Sandy clay, IRBr (5YR3/4), iron spots, OrR rocks. Some areas more clayey than others.

85 cm Sand, Or, mz (210-300), ps.

90 cm Sandy clay, IRBr (5YR3/4), charcoal (large).

100 cm Sand, gz (1000-1400), vps. Sharp transition with underlying horizon.

105 cm Sandy clay, dRBr (5YR3/3), charcoal layer. Covered with coarse sand. *Charcoal sample taken at 110 cm.*

115 cm Sandy clay, ROrBr (2.5YR4/6), very coarse pieces of weathered bedrock, GGD 2 cm.

125 cm Sandy clay, dRBr (5YR3/3), very tough. At 130 charcoal pieces, at 140 red layer, at 145 dark brown layer.

150 cm (start coring) Sandy, loamy clay. dRBr (5YR3/4) charcoal pieces.

180 cm Sandy, loamy clay. IRBr (5YR4/6)

190 cm Sandy, loamy clay. RBr (5YR4/4). Charcoal

210 cm Sandy, loamy clay. BrR (5YR4/8)

240 cm Weathered yellow bedrock. END

C14-samples taken:

TZ11-110-C14 Mzungu village, Lushoto District. 110 cm depth from layer with abundant charcoal.

012

Nice valley with steep slopes, little agriculture, many trees. Backwards eroding gullies. Probably good colluvium deposits. But many large rock at the surface.

013

Location: Maweni area, Magila village, Lushoto district.

Coring at 3 m distance downslope of a large boulder, best chance for nice hillslope deposition. Hopefully a thick deposition of colluvial material present. Conifer forest with fields used for agricultural practise of maize. Trees very abundant. gentle slopes.

Revisite 27-11-2010: The suspected palaeosol at around 150 cm depth is only slightly darker than the rest of the coring. Could mean a poorly developed palaeosol. Or the colour is given due to the black minerals that are spread out throughout the sample in lines due to coring. At least the palaeosol much less developed than present day soil profile. Charcoal found at 160 cm and 200 cm, samples taken. Charcoal not found in the rest of the coring except for top. The fact that it is present at 160 cm depth, strengthened the possible palaeosol. OSL sampling of possible palaeosol at 150 cm depth failed.

0 cm BBr (7.5YR3/2) charcoal present, probably from maize cultivation. Treeroot at 60 cm, 5 cm diameter.

70 cm Sandy, loamy clay. From BrBl (7.5YR4/3) changing to GrBr (10YR4/3). Fe, Mg accumulation and 'concreties'. Orange spots. Many different colour due to mineral accumulation. Very stiff and hard due to dryness.

110 cm Sandy, loamy clay. Br (10YR4/3). Fe spots. Quartz grains up to 1 cm diameter.

150 cm Clayey loam. BrBl (10YR3/2). *Possible palaeosol.*

160 cm Clayey loam. BrBl (10YR3/1) very loamy, very stiff. Quartz. Fe 'concreties'. *Charcoal sampled at 160 cm. Possible palaeosol.*

170 cm Sandy, loamy clay. dBrBl(10YR3/2). Increase in Fe. Weathered bedrock.

180 cm Sandy, loamy clay. GrBr (10YR4/2). Mix of many different colours and minerals.

190 cm Sandy, loamy clay. GeBr (10YR4/3). Purpleblack metal 'concreties'. Fe<sub>2</sub>  
 200 cm Sandy, loamy clay. GrBr (10YR4/1). Fe<sub>2</sub>. Mix with pieces of bedrock.  
 Charcoal sampled at 200 cm, small piece.  
 240 cm Bedrock, gray. END

C14-samples taken:

TZ13-160-C14 Maweni area, Magila Village, Lushoto District, 27-11-2010. 160  
 cm depth, in the possible palaeosol.  
 TZ13-200-C14 Maweni area, Magila Village, Lushoto District, 27-11-2010. 200  
 cm depth, very small samples, probably not large enough for dating.

014

Housecut in Kwalei, halfway the slope of a medium catchment. 100-150 m slope uphill.  
 1.5 m cut. Single profile. Bt (clay) very distinct. A Horizon 20/30 cm thick.

015

Housecut in Kwalei, close to the road and the mayor's office. 1.5m cut (no soil color  
 chart, see pictures for color). The buried A-horizon looks different at the left and right  
 side of the cut. Either topped or less developed on the right side, or two palaeosols on  
 the left side on top of each other. The clay accumulation at 40 cm depth might mean  
 that the soil has been buried for some time. At the left side the buried horizon is 20 cm  
 deeper. Maybe a later filled up depression, with 2 A-horizons on top of each other.

Description left side:

0 cm RBr top colluvium layer  
 40cm BrR, very clayey (accumulation) horizon. Tough.  
 50 cm Br horizon of a buried soil. Much less clay. Kwartz grains fz-gz vps. Very sharp  
 boundary /1. Charcoal. *Sample of charcoals from the top 3 cm of the  
 horizon. (TZ-C-15-50) charcoal not very abundant.*  
 80 cm BrBl horizon. Same texture. Charcoal very abundant in a line at the top of this  
 horizon. Large pieces of burned wood. *Sample taken. (TZ-C-15-80)*  
 90 cm RBr B/C horizon up to the END

Right side of the cut: the BrBl layer is not present and the Br horizon is only 20 cm  
 thick and less distinct and less dark.

0 cm RBr top colluvium layer  
 40cm BrR, very clayey (accumulation) horizon. Tough.  
 50 cm Br horizon of a buried soil. Much less clay. Kwartz grains fz-gz vps. Very sharp  
 boundary /1.  
 70 cm RBr B/C horizon up to the END

C14-samples:

TZ15-50-C14 Kwalei Village, Lushoto District, 08-10-2010. Charcoal from the top 3 cm  
 of the brown horizon, 50 cm depth. Waypoint 015.  
 TZ15-80-C14 Kwalei Village, Lushoto District, 08-10-2010. From the top of the black  
 layer at 80 cm depth. Charcoal (burned wood) very abundant. Waypoint  
 015.

016

Small settlement in valleyfloor north to Soni, Klance, on the way to Lwandai village.  
 East of the waypoint rock outcrop 50 m high. Possible colluvial deposits downslope.  
 Prehaps very difficult for drilling due to large buried boulders.

017

Very steep and long slope ending in a V-shape valley. Large colluvial deposits on the  
 side. Possible coring spot in the valleyfloor.

018/019

Gully on the side of the valley, at the end of a long slope. Big boulders, possible colluvial deposits like point 016, but gully shows very rocky subsoil with big boulders up to meter in diameter. Coring might prove very difficult at 016 as well. No clear colluvial deposits in the gully.

020

East of Lwandai village. Nice, flat and broad valleyfloor, E-W. 50-100 m broad. 50 m above from the main valley North of Soni N-S valley. Maybe nice deposits, however not expected very thick due to smaller catchment. Maybe at some 'stepping stones'. Roadcut on the south side has buried palaeosol under 60 cm coll.

021

West of Lwandai Village. Valley broadens up and dips other side to the west. Kwandai village is the water divide of the E-W orientated valley. Roadcut shows very dark A horizon on yellow-grey mothermaterial.

022

Large valleyfloor, flat bottom, very much agriculture. Maybe interesting deposits? Valley E-W joins with this larger N-S valley.

023

Large valleyfloor with fanya yu terraces on the west side.

024

Side valleyfloor, roadcut 1m soil profile on top of bedrock, single soil profile. 40 cm brown, than 20 cm black. 30 meter further, a large gully.

025

On Westside of the road, halfway hillslope, large rock outcrop, but very rocky terrain. Less steep than the outcrop at 016. Might be an option if 016 fails.

026

Flat valleyfloor, 50m broad. Natural cut by the stream, stream upwards of the 'waterfall'.

027

Cut in valleyfloor by incised river. Present soil + at least 1 buried palaeosol visible. 3e one might be present! Come back for description and investigation.

028

Roadcut 5m, thick colluvium all the way. At the side of deep, V-shape valley to the west, 30m deeper.

029

on steep slope, thick continuous colluvium deposits, no horizons, homogeneous colour, small A horizon at the top, good location for continuous sampling.

030

Sideview of the roadcut, so the roadcut is continuous record behind stepping stone, this is the reason why the pack is so thick.

030

OSL Samples of 4 meter thick colluvium deposits. 55% slope of the the uphill of the colluvium.

Middle part of the cut is 105%, see sketch in notebook.

0 cm clayey-sand. Fz, ps. dRBr (5YR3/6). *A poorly developed topsoil profile*

55 cm clayey-sand. Increase in clay content. dBrR (2.5YR3/6). Further down, colour gets more reddish.

OSL sampled at 40 cm TZ30A-40

OSL sampled at 100 cm TZ30B-100

OSL sampled at 200 cm TZ30C-200

OSL sampled at 300 cm TZ30D-300

OSL sampled at 400 cm TZ30E-400

(height is measured vertically)

C14 sampled at 150 cm TZ30-150-C14

C14 sampled at 240 cm TZ30-240-C14 (sample taken 1,5 m left of the OSL sample line. Some sand entered samplebag, could have caused contamination)

(N.B. Small chance samples have been switched, Bags both contained the same depth code, but different description of depth. Depth description is expected to be correct. However would explain future error in dating)

031

Mshizii village, Shangai area, Lushoto district

In small valleyfloor, 2m cut at the outerbank of small meandering stream. 2 clear possible palaeosol horizons, 2 less clear, vaquer, possible palaeosols horizons. Material is very touch due to drought. Very resistant, OSL sumping only possible at two depths. Maybe at the downpart where the soil is soft, due to wetting of the stream, however no horizon there. Two clear cuts are visible, 5 meter apart from one another. The north cut exists of 2m wide profile, and the south cut of 1 m wide profile. Description is made incorporation both cuts. Where large differences arise between the two, this is noted. C14 sampling of palaeosols might be possible due to presence of charcoal, at least very abundant in second, dark horizon.

0 cm Sandy clay, RBr (5YR4/4), fz vps, colluvial top layer

35 cm Sandy clay, dRBr (5YR3/4), increased clay. mz vps, ggd:20mm. Charcoal very abundant in a layer on the top at the boundary. A crack at this boundary. Charcoal sampled (TZ31N-35-C14). *Could have been the top at the onset of agriculture, and charcoal layer is relic of burning for cultivation.*

40 cm Sand, dRBr (5YR3/4), pure sand, very little clay. Gz 420-1000 vps GGD: 5cm. Very sharp transition to next layer, /1. Thickness of sandy layer varies between 5 cm and 20 cm thickness. OSL sampled at 55 cm.

65 cm Sandy clay, Br (7.5YR4/3), charcoal, porous, very tough, clay accumulation, little sand. Thickness varies between 5 cm (N-cut) and 10 cm (S-cut). Charcoal sampled (TZ31N-65-C14-I and II). *Possible palaeosol I, only little developed.*

75 cm Clayey sand, RBr (5YR4/4), mz-gz vps a1

80 cm Sandy clay, BrBI (7.5YR3/2), fz ps a1 ggd:10mm, very tough. Charcoal sampled at 82 cm, 2 cm below /1 boundary. *Possible palaeosol II, clear, well developed.*

90 cm Sandy clay, Br (7.5YR4/3), vps a1, touch, less clayey.

100 cm Sandy clay, BrBI(7.5YR3/2), charcoal, very touch. Layer is covered by 1 cm layer of sand (mz), Br (7.5YR4/4). Charcoal very abundant in a layer. Less distinct than layer at 80 cm. *Possible palaeosol III, less developed.*

110 cm Sandy clay, dBr (7.5YR4/3)

130 cm Sandy clay, BrBI (7.5YR3/2). Charcoal in the upper part. Layer is covered by 1 cm thick sand layer, OrBr(7.5YR4/4), mz ps a1. Contains fe coating. *Possible palaeosol IV, clear, well developed.*

155 cm Clayey sand, Br (7.5YR4/3), fz ps. Large piece of charcoal at 170 cm. GW 190

200 cm Clayey sand, BrGr (7.5YR4/1), mz ps a1. Black spots, might be plant remains/soft charcoal. Wet, makes the layer soft. And might also cause a colour change. *Charcoal sample taken.*

230 cm Level of the active stream. END

## OSL samples:

- TZ31A-55 Mshizii village, Lushoto District, 20-11-2010, PVC pipe  
 TZ31B-155 Mshizii village, Lushoto District, 20-11-2010, PVC pipe

## C14 samples:

- TZ31N-35-C14 Mshizii village, Shangai area, Lushoto District, 20-11-2010. Valleycut. Charcoal sample from layer at boundary at 35 cm, crack with above colluvium. *Possible pre-agricultural soil surface.*
- TZ31N-65-C14-I Mshizii village, Shangai area, Lushoto District, 30-10-2010. Valleycut. Charcoal sample of 65-70 cm, North-cut. Very clayey layer. *Possible palaeosol I*
- TZ31N-65-C14-II Mshizii village, Shangai area, Lushoto District, 20-11-2010. Valleycut. Charcoal sample from inside the horizon. *Possible palaeosol I*
- TZ31N-82-C14 Mshizii village, Shangai area, Lushoto District, 20-11-2010. Valleycut. Charcoal samples at 2 cm below boundary. *Possible palaeosol II*
- TZ31N-102-C14 Mshizii village, Shangai area, Lushoto District, 20-11-2010. Valleycut. Charcoal samples at 2 cm below boundary. *Possible palaeosol III*
- TZ31N-125-C14 Mshizii village, Shangai area, Lushoto District, 20-11-2010. Valleycut. Charcoal samples at 2 cm above boundary to *Possible palaeosol IV*
- TZ31N-130-C14 Mshizii village, Shangai area, Lushoto District, 30-10-2010. Valleycut. Charcoal sample of 130 cm, top of layer. North-cut/left. *Possible palaeosol IV*
- TZ31N-133-C14 Mshizii village, Shangai area, Lushoto District, 20-11-2010. Valleycut. Charcoal samples at 3 cm below boundary. *Possible palaeosol IV*
- TZ31N-155-C14 Mshizii village, Shangai area, Lushoto District, 20-11-2010. Valleycut. Charcoal sampled at same depth as OSL samples.
- TZ31N-170-C14 Mshizii village, Shangai area, Lushoto District, 30-10-2010. Valleycut. Charcoal sample of 170 cm. North-cut/left,
- TZ31S-200-C14 Mshizii village, Shangai area, Lushoto District, 30-10-2010. Valleycut. Charcoal sample of 200 cm, South-cut/right.

## 032-034

Shashui area, Mzungu village. Examination of the dark, blackish layer buried under 60 cm of Br colluvium, possible palaeosol, and its spatial distribution. 1 roadcut description and 2 corings in a hillslope with agricultural practice.

## 032

Exposure due to roadcut

0 cm Sandy clay, Br (10YR4/3), fz/mz ps a1, very sandy.

60 cm Sandy clay, BrBI (10YR2/2), fz/mz ps a1. *Possible palaeosol. OSL sample taken (TZ-02-60)*

70 cm Sandy clay, dBr (7.5YR3/4)

80 cm Sandy clay, BrR (5YR4/6), increase clay.

120 cm END

## 033

Coring 5m uphill in the direction of the slope from 032. In order to find the depth of the dark layer, suspected palaeosol.

0 cm Sandy clay, GrBr(7.5YR4/6), mixed with soil conglomerates of several cm, dR (5YR4/6).

50 cm Sandy clay, RBr (5YR4/6)

70 cm Sandy clay, dRB (5YR3/6)

90 cm Sandy clay, dRBr (5YR3/4), soil becoming moist, *could have influenced the colour.*

110 cm Sandy clay, rBr (5YR3/6)

120 cm Sandy clay, IRBr (5YR4/6), END  
No clear dark horizon found.

034

Coring 5 meter uphill in direction of the slope from 033.

0 cm Sandy clay, GeBr (7.5YR4/6)

20 cm Sandy clay, RBr (5YR3/6)&(5YR4/6), pieces of weathered bedrock. Quartz up to  
ggd: 5mm

100 cm END

Two corings uphill in agri-fields with cassava, coffee and maize. No sign of the dark, black layer. Blackish colour is present in mixed form at the top of the agricultural field in the loose material. In cut, like on the side of terraces, the boundaries of different fields and on the side of footpaths, the black layer is visible, covered with 40-60 cm Br colluvial material. On the agricultural field, the layer is not present in the subsoil and the colours of the material coincide with the material found under the black layer in the cut. The black layer is at the same level at some older trees, which are buried by the colluvial material as well. So, the buried, blackish A horizon is most likely the soil surface at the start of the agricultural practice in the area. At the down slope edges of the plots, the layer is buried by upslope eroded material, of which the top layer is eroded and mixed due to erosion and agricultural practice. Dating this layer would probably yield in the decadal scale, to give the onset of agricultural practise on the hillslope.

035

Coring 8m upslope large colluvium scarp. Steepness around 45 degrees, should be measured next time. Heavily degraded soil. But still used for (poor) agricultural practice of maize. Depth of underlying bedrock is the question. 'stepping stone' is expected. 1.50m deep.

0 cm Sandy clay, IOrBr

10 cm Sandy clay, IR

20 cm Sandy clay, Red. No changes until END

140 cm END

Very degraded soil, coinciding with the steepness of the slope. The depth of the bedrock must be between 150 and 200 cm, see 037. At the top of the colluvium scarp at the road, the soil profile is more developed than at this position. Why is it not eroded away as well? Might be to do with two things: 1) at the edge there are grasses and shrubs present. They are not removed here because it is unsuitable for agricultural practice. 2) the roadcut might be relatively new, so the topography might be different the time before, leaving the spot less exposed to erosion.

036

Coring 15 m upslope of the roadcut. Soil profile exist for 140 cm of homogeneous, BrR, Sandy Clay, containing quartz grains. Bedrock at 140 cm.

037

50m North of the roadcut, Colluvium is eroded away and underlying bedrock is exposed. Going up to 7-8m above roadlevel. It holds a soil cover of 150 cm, coinciding with the findings of coring 036. Not deeper than 150 cm. The bedrock is only few meters in horizontal distance behind the colluvium deposits that are exposed at the roadcut.

039

Lokozi village, valley 1 km south of Lokozi. 26-11-2010. Colluvium of 3 m thick at the end of ca 300 m slope (25-30%). Visible due to widening of the valleyfloor. 2 buried dark horizons, *possible palaeosols*. Due to problems with farmer, samples and description in next field, where cut is less clear. Description is done quickly, and samples are taken home for further description and colour sampling.

Exact boundaries in colour should be checked with picture taken. *Was necessary due to threatening of an aggressive and crazy farmer.* First palaeosol maybe artificially buried due to terracing. However, looks genuine. The second two dark horizon is situated on top of weathered bedrock. Possible formed in weathered bedrock, would explain the shallow horizon and extreme dark, black colour. Long term weathering and soil formation. *Three possible palaeosol horizons.* Only first 2 palaeosol sampled for dating. Last one did not contain datable material and to touch for OSL dating.'

0 cm Sandy clay, dRBR (5YR2/3) present day soil. Gradually from brown to yellowish.  
 30 cm Sandy clay, Fieldcolor: YeOr (7.5YR6/8); Homecolor: YeBr (10YR4/4), increase in sand. GZ vps a1 ggd: 5mm, quartz very abundant. Very touch.  
 80 cm Sandy clay, dBR (7.5YR3/3), GZ ps, less touch. *Possible palaeosol I.* OSL samples taken at 90 cm depth. Charcoal sample taken at 90 cm depth. *Might not be a palaeosol, or less developed.*  
 100 cm Sandy clay, BrBI (7.5YR4/2).  
 120 cm Sandy clay, BrBI (7.5YR2/2).GZ vps, touch, *Possible palaeosol II.* OSL sampled at 130 cm depth.

(From this point, the description has been made at desk, after sampling the profile at specific depths.)

140 cm S-clay, BrBI (7.5YR3/2)  
 150 cm S-clay, dRBr (5YR2/4). Touch  
 160 cm S-clay, dRBr (5YR3/3).  
 180 cm S-clay, dRBr (5YR3/2), increase in sand. GZ vps A1, GGD: 5 mm  
 210 cm S-clay, some parts BL (5YR1.7/1), very touch, high clay content. Some parts with increased sand content BrBI (5YR2/1). Small roots. *Possible palaeosol III.* No datable material collected. No charcoal present and OSL sampling physically impossible.  
 230 cm S-clay, increase in sand. Quartz grains GZ 850-1000 ps A1.  
 250 cm Clayey sand, BBr (7.5YR3/2) GZ 1000 vps A1 ggd: 5mm. Very touch. Probably weathered bedrock.  
 270 cm Clayey sand, yellowish Br (10YR4/4) with yellow particles and quartz grains. Little clay content and very tough. Weathered bedrock. END

OSL-samples:

TZ39A-90-I Lokozi village, Lushoto District, 26-11-2010  
 TZ39B-130-I Lokozi village, Lushoto District, 26-11-2010

C14-samples:

TZ39-90-C14 Lokozi village, Lushoto District, 26-11-2010.  
 10 cm in the palaeosol, same height as OSL samples.

## List of waypoints

Grid UTM  
Datum WGS 84

Header Name	Description	Type	Position	Altitude
Waypoint	001	24-SEP-10 02:49	User Waypoint 37 M 429751 9460649	1397 m
Waypoint	002	24-SEP-10 04:31	User Waypoint 37 M 430407 9459968	1485 m
Waypoint	003	24-SEP-10 04:43	User Waypoint 37 M 430364 9460245	1430 m
Waypoint	004	24-SEP-10 05:56	User Waypoint 37 M 429997 9463732	1219 m
Waypoint	005	25-SEP-10 07:16	User Waypoint 37 M 430047 9463776	1186 m
Waypoint	006	25-SEP-10 07:36	User Waypoint 37 M 430064 9463587	1197 m
Waypoint	007	25-SEP-10 07:42	User Waypoint 37 M 430044 9463315	1213 m
Waypoint	008	CUT VAN 5 METER	User Waypoint 37 M 429917 9463682	-
Waypoint	009	29-SEP-10 03:24	User Waypoint 37 M 430491 9459833	1503 m
Waypoint	010	29-SEP-10 05:05	User Waypoint 37 M 430573 9460246	1429 m
Waypoint	011	30-SEP-10 03:26	User Waypoint 37 M 430658 9460898	1350 m
Waypoint	012	30-SEP-10 06:07	User Waypoint 37 M 430370 9463250	1201 m
Waypoint	013	30-SEP-10 06:32	User Waypoint 37 M 430357 9463300	1208 m
Waypoint	014	01-OCT-10 04:37	User Waypoint 37 M 436739 9466483	1386 m
Waypoint	015	01-OCT-10 05:30	User Waypoint 37 M 437050 9466698	1342 m
Waypoint	016	04-OCT-10 03:11	User Waypoint 37 M 430364 9465128	1206 m
Waypoint	017	04-OCT-10 03:19	User Waypoint 37 M 430711 9465678	1233 m
Waypoint	018	04-OCT-10 03:26	User Waypoint 37 M 430732 9465771	1268 m
Waypoint	019	04-OCT-10 03:26	User Waypoint 37 M 430732 9465770	1267 m
Waypoint	020	04-OCT-10 03:40	User Waypoint 37 M 431218 9466691	1274 m
Waypoint	021	04-OCT-10 03:55	User Waypoint 37 M 430297 9467093	1246 m
Waypoint	022	04-OCT-10 04:08	User Waypoint 37 M 429091 9468070	1191 m
Waypoint	023	04-OCT-10 04:21	User Waypoint 37 M 428648 9467342	1183 m
Waypoint	024	04-OCT-10 04:28	User Waypoint 37 M 427977 9466721	1173 m
Waypoint	025	04-OCT-10 04:33	User Waypoint 37 M 427669 9466124	1168 m
Waypoint	026	04-OCT-10 04:39	User Waypoint 37 M 427386 9465738	1154 m
Waypoint	027	04-OCT-10 04:48	User Waypoint 37 M 427019 9465248	1176 m
Waypoint	028	05-OCT-10 02:11	User Waypoint 37 M 427270 9465483	1155 m
Waypoint	029	05-OCT-10 02:36	User Waypoint 37 M 427238 9465516	1189 m
Waypoint	030	05-OCT-10 02:52	User Waypoint 37 M 427310 9465583	1162 m
Waypoint	031	05-OCT-10 05:06	User Waypoint 37 M 427067 9465255	1127 m
Waypoint	032	06-OCT-10 04:11	User Waypoint 37 M 430406 9459978	1491 m
Waypoint	033	06-OCT-10 04:12	User Waypoint 37 M 430398 9459978	1490 m
Waypoint	034	06-OCT-10 04:12	User Waypoint 37 M 430389 9459975	1489 m
Waypoint	035	08-OCT-10 02:20	User Waypoint 37 M 427263 9465499	1171 m
Waypoint	036	08-OCT-10 03:32	User Waypoint 37 M 427266 9465526	1190 m
Waypoint	037	08-OCT-10 04:11	User Waypoint 37 M 427300 9465545	1170 m
Waypoint	038	02-NOV-10 00:19	User Waypoint 37 M 427300 9465542	-
Waypoint	039	26-NOV-10 05:52	User Waypoint 37 M 421719 9482415	1681 m
Waypoint	040	27-NOV-10 05:42	User Waypoint 37 M 427042 9465354	1177 m
Waypoint	041	27-NOV-10 05:53	User Waypoint 37 M 426971 9465142	1204 m
Waypoint	101	25-SEP-10 03:02	User Waypoint 37 M 430101 9462209	1204 m

## Appendix II: Site description and samples for dating

**Mzungu site Waypoint 002/032 Date: 24-SEP-10 04:31 Location: 37 M 430407 9459968**

Shashui area, Mzungu village. Examination of the dark, blackish layer buried under 60 cm of Br colluvium, possible palaeosol, and its spatial distribution. 1 roadcut description and 2 corings in a hillslope with agricultural practice.

Roadcut 002/032:

0 cm Sandy clay, Br (10YR4/3), fz/mz ps a1, very sandy.  
 60 cm Sandy clay, BrBl (10YR2/2), fz/mz ps a1. *Possible palaeosol. OSL sample taken (TZ-02-60)*  
 70 cm Sandy clay, dBr (7.5YR3/4)  
 80 cm Sandy clay, BrR (5YR4/6), increase clay.  
 120 cm END

033

Coring 5m uphill in the direction of the slope from 002. In order to find the depth of the dark layer, suspected palaeosol. *Not found!*

0 cm Sandy clay, GrBr(7.5YR4/6), mixed with soil conglomerates of several cm, dR (5YR4/6).  
 50 cm Sandy clay, RBr (5YR4/6)  
 70 cm Sandy clay, dRB (5YR3/6)  
 90 cm Sandy clay, dRBr (5YR3/4), soil becoming moist, *could have influenced the colour.*  
 110 cm Sandy clay, rBr (5YR3/6)  
 120 cm Sandy clay, IRBr (5YR4/6), END  
 No dark horizon found.

034

Coring 10 meter uphill in direction of the slope from 002.

0 cm Sandy clay, GeBr (7.5YR4/6)  
 20 cm Sandy clay, RBr (5YR3/6)&(5YR4/6), pieces of weathered bedrock. Quartz up to ggd:5mm  
 100 cm END

Two corings uphill in agri-fields with cassava & kofie, mais. No sign of the dark, black layer. Blackish colour is present in mixed form at the top of the agricultural field in the loose material. In cut, like on the side of terraces, the boundaries of different fields and on the side of footpaths, the black layer is visible, covered with 40-60 cm Br colluvial material. On the agricultural field, the layer is not present in the subsoil and the colours of the material coincide with the material found under the black layer in the cut. The black layer is at the same level at some older trees, which are buried by the colluvial material as well. So, the buried, blackish A horizon is most likely the soil surface at the start of the agricultural practise in the area. At the downslope edges of the plots, the layer is buried by upslope eroded material, of which the top layer is eroded and mixed due to erosion and agricultural practice. Dating this layer would probably yield in the decadal scale, to give the onset of agricultural practise on the hillslope.

OSL-samples:

TZ-02-60 Mzungu village, Lushoto District, 02-11-2010, PVC pipe  
 Expected age: 50-100 yrs BP. Erosion phase: III  
 Sample taken from A-horizon. Sample probably dates the deforestation of the hillslope and the start of agricultural practice and subsequent unstable hillslope period in which the colluvium on top of the palaeosol starts to form.  
 Aerial photograph of 1955 show a shrub covered hillslope, so deforested at 1955 but not yet used for agricultural practice.



**Waypoint 003****Date: 24-SEP-10 04:43****Location: 37 S 430364 9460245**

Mzungu village area. Small valley floor in a horseshoe shaped valley. Two buried, dark horizons. First possible palaeosol, at 100 cm, expected to be the onset of agriculture. Charcoal sample taken. Second possible palaeosol, at 230 depth, could represent an older phase, OSL sample taken. Uncertain whether second dark horizon represents old buried A-horizon.

- 0 cm Sandy clay, Br (10YR3/3), fz ps a2, quartz grains GGD:3 mm. Moderately clayey, high sand content. Rich of plant material and roots.
- 100 cm Sandy clay, DBrBI (7.5YR3/2), mz/gz vps, high sand content, charcoal, roots. Increase in clay content with depth. Sharp, 1-2 cm, transition with underlying horizon. *Possible buried horizon. Charcoal sampled at 110 cm. (TZ03-110-C14)*
- 120 cm Sandy clay, BrR (2.5YR3/3), mz, vps, roots.
- 150 cm Sandy clay, DRBr (5YR3/6), mz,vps, clay increase. *Charcoal sampled at 150 cm. (TZ03-150-C14)*
- 180 cm Sandy clay, RBr (5YR3/4), clay increase.
- 220 cm Sandy clay, DYeBr (7.5YR4/3), little sand. Black, dark spots. Gradual transition.
- 230 cm Sandy clay, BrBI (5YR3/2), mz, GGD 2 cm. Fe spots. Sharp transition with above layer (2cm). No charcoal. *Old palaeosol. OSL Sample taken, top at 230, bottom at 235. (TZ-03-230)*
- 245 cm Sandy clay, Br (5YR4/3).  
(start coring)
- 260 cm Sandy clay, OrBr (5YR5/8), little sand. Loamy. Pieces of weathered bedrock.
- 340 cm Weathered bedrock, END

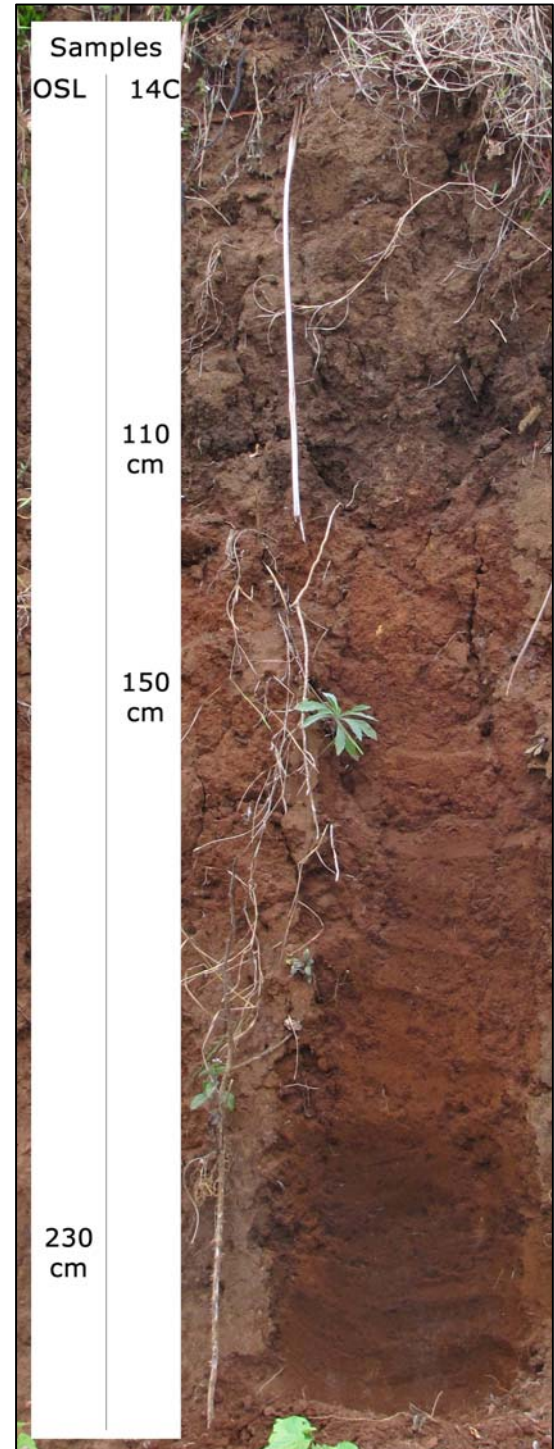
## OSL-sample:

- TZ-03-230 Mzungu village, Lushoto District, 02-11-2010  
Expected age: 300-4000 yrs BP. Erosion phase: I/II  
Sample taken from a possible A-horizon at 230 cm depth. Due to its depth, the age is difficult to estimate. Could be very old, or intermediate.

## C14-samples:

- TZ03-110-C14 Mzungu village, Lushoto District, 02-11-2010.  
Various charcoal pieces from a 'layer' at this depth.  
Expected age: 20-100 yrs BP. Erosion phase: III.  
Aerial photographs of 1955 show that the small hillslope uphill of the cut was probably still vegetated by some trees, unlike most of wide surroundings.  
Sample will probably date this buried A-horizon as near present. Charcoal could be the remnants of the burning of the field for agricultural practice.

- TZ03-150-C14 Mzungu village, Lushoto District, 02-11-2010. At the top of the DBrR layer.  
Expected age: 300-1000. Erosion phase: II.  
Sample will date the unstable period during which the last k-cycle builded up. There is no charcoal layer documented for this depth, so possible re-deposition of the sample (age overestimation).



**Waypoint 011****Date: 30-SEP-10 03:26****Location: 37 M 430658 9460898**

Valley near Mzungu village, dark, BrBl layer buried under 30 cm colluvium. Charcoal. On top of orange horizon, very touch, high clay content. Could be interesting spot for a coring.

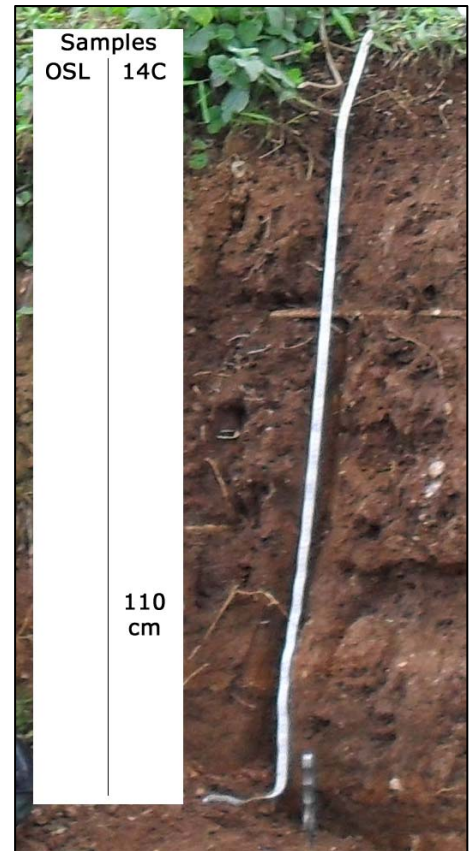
Valleycut, start of the cut is 1,5 m down of the road, 7m above valley floor, at the end of a 300 m long slope. Natural colluvium. Very rocky, large stones up to 10 cm.

- 0 cm Sandy clay, RBr (5YR4/4), charcoal. At 55 cm piece of cloth, human deposited. *Possibly deposited with roadconstruction.*
- 60 cm Sandy clay, IRBr (5YR3/4), iron spots, OrR rocks. Some areas more clayey than others.
- 85 cm Sand, Or, mz (210-300), ps.
- 90 cm Sandy clay, IRBr (5YR3/4), charcoal (large).
- 100 cm Sand, gz (1000-1400), vps. Sharp transition with underlying horizon.
- 105 cm Sandy clay, dRBr (5YR3/3), charcoal layer. Covered with coarse sand. *Charcoal sample taken at 110 cm.*
- 115 cm Sandy clay, ROrBr (2.5YR4/6), very coarse pieces of weathered bedrock, GGD 2 cm.
- 125 cm Sandy clay, dRBr (5YR3/3), very tough. At 130 charcoal pieces, at 140 red layer, at 145 dark brown layer.
- 150 cm (start coring) Sandy, loamy clay. dRBr (5YR3/4) charcoal pieces.
- 180 cm Sandy, loamy clay. IRBr (5YR4/6)
- 190 cm Sandy, loamy clay. RBr (5YR4/4). Charcoal
- 210 cm Sandy, loamy clay. BrR (5YR4/8)
- 240 cm Weathered yellow bedrock. END

**C14-sample:**

TZ11-110-C14 Mzungu village, Lushoto District. 110 cm depth from layer with abundant charcoal. Expected age: 15-55 yrs BP. Erosion phase: III.

Aerial photographs from 1955 show the uphill slopes totally covered with forest. In 1996 most of the slopes are deforested and used for agricultural practice (terraced fields). The charcoal layer of the sample is buried under very coarse sand. Probably buried between 1955 and 1996 due to deforestation and agricultural practice. Road construction could also have buried the horizon. (If this layer was the top layer, could have been older as well.)



**Waypoint 013****Date: 30-SEP-10 06:32****Location: 37 M 430357 9463300**

Location: Maweni area, Magila village, Lushoto district. Coring at 3 m distance downslope of a large boulder, best chance for nice hillslope deposition. Hopefully a thick deposition of colluvial material present. Conifer forest with fields used for agricultural practise of maize. Trees very abundant. gentle slopes.

Revisite 27-11-2010: The suspected palaeosol at around 150 cm depth is only slightly darker than the rest of the coring. Could mean a poorly developed palaeosol. Or the colour is given due to the black minerals that are spread out throughout the sample in lines due to coring. At least the palaeosol much less developed than present day soil profile. Charcoal found at 160 cm and 200 cm, samples taken. Charcoal not found in the rest of the coring except for top. The fact that it is present at 160 cm depth, strengthened the possible palaeosol. OSL sampling of possible palaeosol at 150 cm depth failed.

0 cm BBr (7.5YR3/2) charcoal present, probably from maize cultivation. Treeroot at 60 cm, 5 cm diameter.

70 cm Sandy, loamy clay. From BrBI (7.5YR4/3) changing to GrBr (10YR4/3). Fe, Mg accumulation and 'concreties'. Orange spots. Many different colour due to mineral accumulation. Very stiff and hard due to dryness.

110 cm Sandy, loamy clay. Br (10YR4/3). Fe spots. Quartz grains up to 1 cm diameter.

150 cm Clayey loam. BrBI (10YR3/2). *Possible palaeosol.*

160 cm Clayey loam. BrBI (10YR3/1) very loamy, very stiff. Quartz. Fe 'concreties'. Charcoal sampled at 160 cm. *Possible palaeosol.*

170 cm Sandy, loamy clay. dBrBI(10YR3/2). Increase in Fe. Weathered bedrock.

180 cm Sandy, loamy clay. GrBr (10YR4/2). Mix of many different colours and minerals.

190 cm Sandy, loamy clay. GeBr (10YR4/3). Purpleblack metal 'concreties'. Fe<sub>2</sub>

200 cm Sandy, loamy clay. GrBr (10YR4/1). Fe<sub>2</sub>. Mix with pieces of bedrock. Charcoal sampled at 200 cm, small piece.

240 cm Bedrock, gray. END



## C14-samples:

TZ13-160-C14 Maweni area, Magila Village, Lushoto District, 27-11-2010. 160 cm depth, in the possible palaeosol. Expected age: 500-5000 yrs BP. Erosion phase: I-II.

Would date probably within the stable period of the pedogenesis of the palaeosol. Aerial photographs (1955) show the same vegetational cover as present, low dense forest with some agricultural practice. Field has large, overgrown gullies.

TZ13-200-C14 Maweni area, Magila Village, Lushoto District, 27-11-2010. 200 cm depth, very small samples, probably not large enough for dating. Expected age: 2000-6000 yrs BP. Erosion phase: I. Will date the unstable phase before pedogenesis (150 cm).

**Waypoint 015****Date: 01-OCT-10 05:30****Location: 37 M 437050 9466698**

Housecut in Kwalei, close to the road and the mayor's office. 1.5m cut (no soil color chart, see pictures for color). The buried A-horizon looks different at the left and right side of the cut. Either topped or less developed on the right side, or two palaeosols on the left side on top of each other. The clay accumulation at 40 cm depth might mean that the soil has been buried for some time. At the left side the buried horizon is 20 cm deeper. Maybe a later filled up depression, with 2 A-horizons on top of each other.

## Description left side:

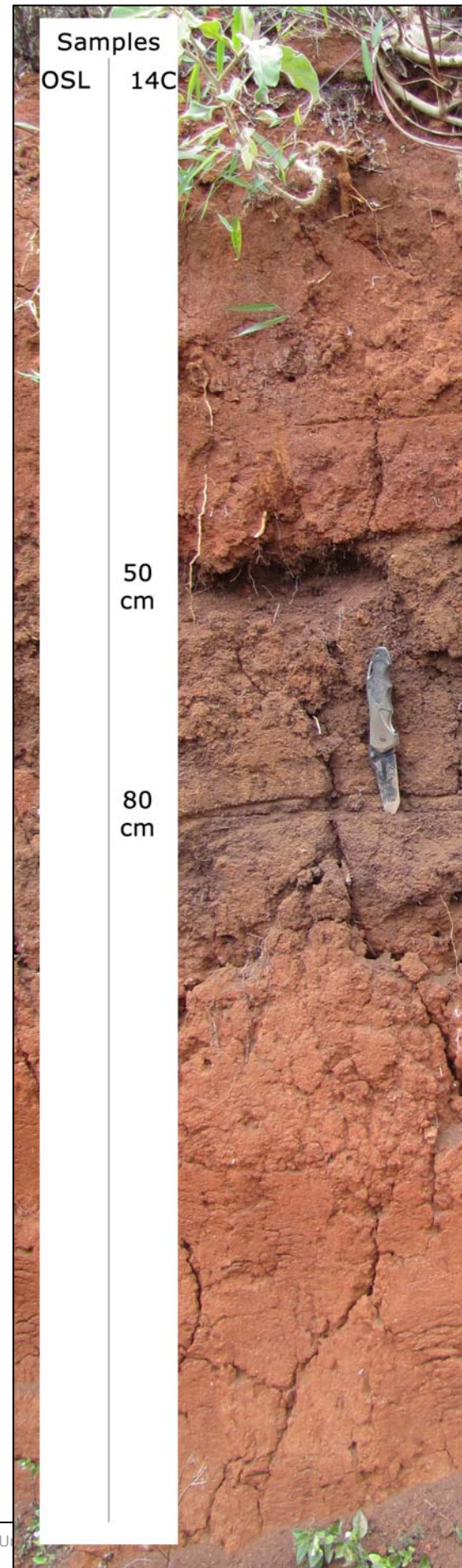
- 0 cm RBr top colluvium layer
- 40cm BrR, very clayey (accumulation) horizon. Tough.
- 50 cm Br horizon of a buried soil. Much less clay. Kwartz grains fz-gz vps. Very sharp boundary /1. Charcoal. *Sample of charcoals from the top 3 cm of the horizon. (TZ-C-15-50) charcoal not very abundant.*
- 80 cm BrBI horizon. Same texture. Charcoal very abundant in a line at the top of this horizon. Large pieces of burned wood. *Sample taken. (TZ-C-15-80)*
- 90 cm RBr B/C horizon up to the END

Right side of the cut: the BrBI layer is not present and the Br horizon is only 20 cm thick and less distinct and less dark.

- 0 cm RBr top colluvium layer
- 40cm BrR, very clayey (accumulation) horizon. Tough.
- 50 cm Br horizon of a buried soil. Much less clay. Kwartz grains fz-gz vps. Very sharp boundary /1.
- 70 cm RBr B/C horizon up to the END

## C14-samples:

- TZ15-50-C14 Kwalei Village, Lushoto District, 08-10-2010. Charcoal from the top 3 cm of the brown horizon, 50 cm depth. Charcoal not very abundant. Fresh colluvium on top of this layer is not of the mixed color of natural colluvium, possibly human deposited when created the road uphill. Not very suitable for dating, re-deposition from the charcoal layer at 80 cm possible.
- TZ15-80-C14 Kwalei Village, Lushoto District, 08-10-2010. From the top of the black layer at 80 cm depth. Charcoal (burned wood) very abundant. Waypoint 015. Expected age: 50-100 yrs. Erosion phase: III. Dates the age the buried palaeosol. The layer contains much burned wood, must be the result of a forest fire or a human controlled fire in order to prepare for agriculture.



**Waypoint 030****Date: 05-OCT-10 02:52****Location: 37 M 427310 9465583**

OSL Samples of 4 meter thick colluvium deposits. 55% slope of the the uphill of the colluvium. Middle part of the cut is 75 degrees.

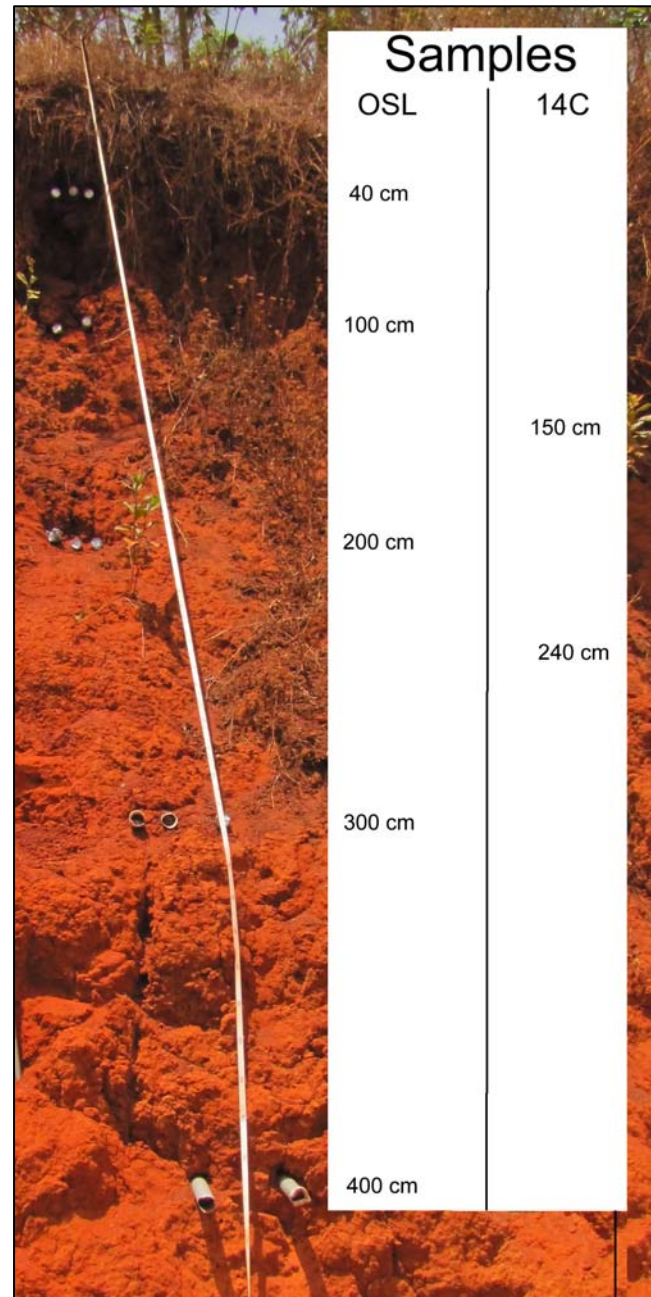
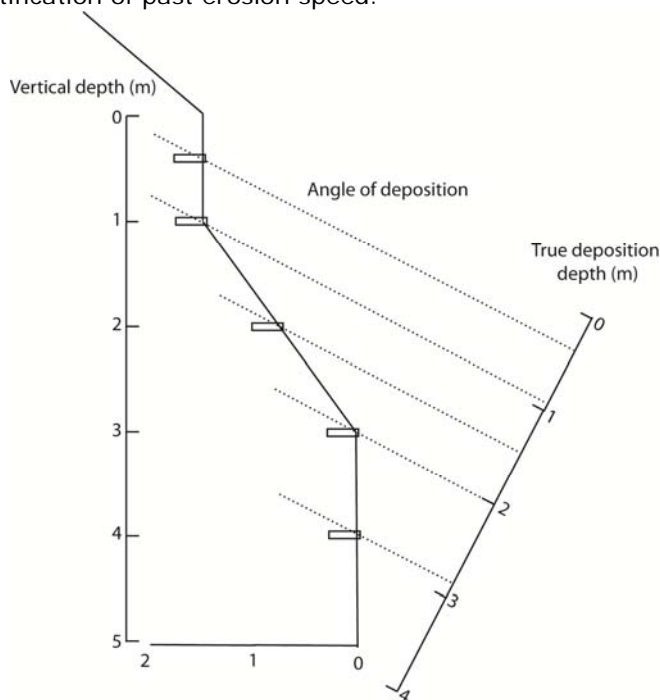
0 cm clayey-sand. Fz, ps. dRBr (5YR3/6). A poorly developed topsoil profile

55 cm clayey-sand. Increase in clay content. dBrR (2.5YR3/6). Further down, colour gets more reddish.

OSL-samples:

TZ30A-40 Mshizii village, Lushoto District, 03-11-2010,  
 TZ30B-100 Mshizii village, Lushoto District, 03-11-2010,  
 TZ30C-200 Mshizii village, Lushoto District, 03-11-2010,  
 TZ30D-300 Mshizii village, Lushoto District, 03-11-2010,  
 TZ30E-400 Mshizii village, Lushoto District, 03-11-2010,

Samples taken with continuous intervals with depth. If the sediment is deposited on a slope, the intervals are not continuous and the true depth between the samples will vary according to the angle of deposition (This is unknown). This phenomenon makes it unusefull for measuring the erosional speed. Dating one or more of these samples would give an indication on the situation, however not useful for exact quantification of past erosion speed.



C14-samples:

Charcoal pieces consist of singles, most likely re-deposited by erosion, prone to age-overestimation.

TZ30-150-C14 Mshizii village, Lushoto District, 03-11-2010. 150 cm depth. Sample taken 1,5 m left of the OSL sample line. For cross dating with OSL samples. Waypoint 030.

TZ30-240-C14 Mshizii village, Lushoto District, 03-11-2010. sampled at 240 cm. Sample taken 1,5 m left of the OSL sample line. For cross dating with OSL samples. Waypoint 030. (N.B. Some sand entered sample bag, could have caused contamination.)

Expected age: 100-3000 yrs BP. Nice to get an indication, but not accurate. Over estimation due to re-deposition possible/likely.

Mshizii site Waypoint 031

Date: 05-OCT-10 05:06

Location: 37 M 427067 9465255

Location: Mshizii village, Shangai area, Lushoto district;

In small valleyfloor, 2m cut at the outerbank of small meandering stream. 2 clear possible palaeosol horizons, 2 less clear, vaquer, possible palaeosols horizons. Material is very touch due to drought. Very resistant, OSL sumping only possible at two depths. Maybe at the downpart where the soil is soft, due to wetting of the stream, however no horizon there. Two clear cuts are visible, 5 meter apart from one another. The north cut exists of 2m wide profile, and the south cut of 1 m wide profile. Description is made incorporation both cuts. Where large differences arise between the two, this is noted. C14 sampling of palaeosols might be possible due to presence of charcoal, at least very abundant in second, dark horizon.

- 0 cm Sandy clay, RBr (5YR4/4), fz vps, colluvial top layer
- 35 cm Sandy clay, dRBr (5YR3/4), increased clay. mz vps, ggd:20mm. Charcoal very abundant in a layer on the top at the boundary. A crack at this boundary. Charcoal sampled (TZ31N-35-C14). *Could have been the top at the onset of agriculture, and charcoal layer is relic of burning for cultivation.*
- 40 cm Sand, dRBr (5YR3/4), pure sand, very little clay. Gz 420-1000 vps GGD: 5cm. Very sharp transition to next layer, /1. Thickness of sandy layer varies between 5 cm and 20 cm thickness. OSL sampled at 55 cm.
- 65 cm Sandy clay, Br (7.5YR4/3), charcoal, porous, very tough, clay accumulation, little sand. Thickness varies between 5 cm (N-cut) and 10 cm (S-cut). Charcoal sampled (TZ31N-65-C14-I and II). *Possible palaeosol I, only little developed.*
- 75 cm Clayey sand, RBr (5YR4/4), mz-gz vps a1
- 80 cm Sandy clay, BrBl (7.5YR3/2), fz ps a1 ggd:10mm, very tough. Charcoal sampled at 82 cm, 2 cm below /1 boundary. *Possible palaeosol II, clear, well developed.*
- 90 cm Sandy clay, Br (7.5YR4/3), vps a1, touch, less clayey.
- 100 cm Sandy clay, BrBl(7.5YR3/2), charcoal, very touch. Layer is covered by 1 cm layer of sand (mz), Br (7.5YR4/4). Charcoal very abundant in a layer. Less distinct than layer at 80 cm. *Possible palaeosol III, less developed.*
- 110 cm Sandy clay, dBr (7.5YR4/3)
- 130 cm Sandy clay, BrBl (7.5YR3/2). Charcoal in the upper part. Layer is covered by 1 cm thick sand layer, OrBr(7.5YR4/4), mz ps a1. Contains fe coating. *Possible palaeosol IV, clear, well developed.*
- 155 cm Clayey sand, Br (7.5YR4/3), fz ps. Large piece of charcoal at 170 cm. GW 190
- 200 cm Clayey sand, BrGr (7.5YR4/1), mz ps a1. Black spots, might be plant remains/soft charcoal. Wet, makes the layer soft. And might also cause a colour change. Charcoal sample taken.
- 230 cm END, level of the active stream.

Samples	OSL		<sup>14</sup> C	Near Present	Datings
	OSL	<sup>14</sup> C			
			35 cm		
	55 cm			Possible Palaeosol I	92 ± 45 yrs BP
			65 cm	Possible Palaeosol II	
			82 cm	Possible Palaeosol III	
			102 cm		
			125 cm	Possible Palaeosol IV	
			133 cm		
	155 cm	155 cm			253 ± 28 yrs BP
			170 cm		

## OSL-samples:

- TZ31A-55 Mshizii village, Lushoto District, 20-11-2010, PVC pipe  
Expected age: 50-500 yrs BP. Erosion phase II.  
The sample is in between two possible, little developed, buried A-horizons. Both horizons could be dated using charcoal. The OSL date would acknowledge or reject the outcome of the 14C dates and the expectation on the position of the near present palaeosol. It will date the instable period between the expected near present A-horizon and the first expected palaeosol.
- TZ31B-155 Mshizii village, Lushoto District, 20-11-2010, PVC pipe  
Expected age: 1000-5000 yrs BP. Erosion phase I.  
OSL sample taken from below the fourth possible palaeosol. Will date the unstable periode before the formation of this A-horizon. 14C date at the same depth, could be use as a check. For both samples, age-overestimation is possible. Good for a bottom age. Quality is expected to be more trustful than the 14C, less prone to age-overestimation.

## C14-samples:

- TZ31N-35-C14 Mshizii village, Shangai area, Lushoto District, 20-11-2010. Valleycut. Charcoal sample from layer at boundary at 35 cm, crack with above colluvium. *Possible pre-agricultural soil surface*. Expected age: 20-100 yrs BP. Erosion phase: III.
- TZ31N-65-C14-I Mshizii village, Shangai area, Lushoto District, 30-10-2010. Valleycut. Charcoal sample of 65-70 cm, North-cut. Very clayey layer. *Possible palaeosol I*
- TZ31N-65-C14-II Mshizii village, Shangai area, Lushoto District, 20-11-2010. Valleycut. Charcoal sample from inside the horizon. *Possible palaeosol I*  
Expected age: 50-200 yrs BP. Erosion phase: III/II.
- TZ31N-82-C14 Mshizii village, Shangai area, Lushoto District, 20-11-2010. Valleycut. Charcoal samples at 2 cm below boundary. *Possible palaeosol II*  
Expected age: 120-1000 yrs BP. Erosion phase: II.
- TZ31N-102-C14 Mshizii village, Shangai area, Lushoto District, 20-11-2010. Valleycut. Charcoal samples at 2 cm below boundary. *Possible palaeosol III*  
Expected age: 500-2000 yrs BP. Erosion phase: II.
- TZ31N-125-C14 Mshizii village, Shangai area, Lushoto District, 20-11-2010. Valleycut. Charcoal samples at 2 cm above boundary to *Possible palaeosol IV*
- TZ31N-130-C14 Mshizii village, Shangai area, Lushoto District, 30-10-2010. Valleycut. Charcoal sample of 130 cm, top of layer. North-cut/left. *Possible palaeosol IV*
- TZ31N-133-C14 Mshizii village, Shangai area, Lushoto District, 20-11-2010. Valleycut. Charcoal samples at 3 cm below boundary. *Possible palaeosol IV*  
Expected age: 1000-4000 yrs BP. Erosion phase: II/I.
- TZ31N-155-C14 Mshizii village, Shangai area, Lushoto District, 20-11-2010. Valleycut. Charcoal sampled at same depth as OSL samples.  
Expected age: 1000-4000 yrs BP. Erosion phase: II/I.  
Could be used to cross date the OSL samples. Single piece, could be re-deposited and age overestimation.
- TZ31N-170-C14 Mshizii village, Shangai area, Lushoto District, 30-10-2010. Valleycut. Charcoal sample of 170 cm. North-cut/left,  
Expected age: 1000-4000 yrs BP. Erosion phase: II/I.  
Could be used to cross date the OSL samples. Single piece, could be re-deposited and age overestimation.
- TZ31S-200-C14 Mshizii village, Shangai area, Lushoto District, 30-10-2010. Valleycut. Charcoal sample of 200 cm, South-cut/right.  
Expected age: 1000-4000 yrs BP. Erosion phase: II/I.  
Could be used to cross date the OSL samples. Single piece, could be re-deposited and age overestimation.

**Waypoint 039****Date: 26-NOV-10 05:52****Location: 37 M 421719 9482415**

Lokozi village, valley 1 km south of Lokozi. 26-11-2010. Colluvium of 3 m thick at the end of ca 300 m slope (25-30%). Visible due to widening of the valleyfloor. 2 buried dark horizons, *possible palaeosols*. Due to problems with farmer, samples and description in next field, where cut is less clear. Description is done quickly, and samples are taken home for further description and colour sampling.

Exact boundaries in colour should be checked with picture taken. *Was necessary due to threatening of an aggressive and crazy farmer*. First palaeosol maybe artificially buried due to terracing. However, looks genuine. The second two dark horizon is situated on top of weathered bedrock. Possible formed in weathered bedrock, would explain the shallow horizon and extreme dark, black colour. Long term weathering and soil formation. *Three possible palaeosol horizons*. Only first 2 palaeosol sampled for dating. Last one did not contain datable material and to touch for OSL dating.'

- 0 cm Sandy clay, dRBR (5YR2/3) present day soil. Gradually from brown to yellowish.
- 30 cm Sandy clay, Fieldcolor: YeOr (7.5YR6/8); Homecolor: YeBr (10YR4/4), increase in sand. GZ vps a1 ggd: 5mm, quartz very abundant. Very touch.
- 80 cm Sandy clay, dBR (7.5YR3/3), GZ ps, less touch. *Possible palaeosol I*. OSL samples taken at 90 cm depth. Charcoal sample taken at 90 cm depth. *Might not be a palaeosol, or less developed*.
- 100 cm Sandy clay, BrBI (7.5YR4/2).
- 120 cm Sandy clay, BrBI (7.5YR2/2). GZ vps, touch, *Possible palaeosol II*. OSL sampled at 130 cm depth.  
(From this point on, the description has been made at desk, after sampling the profile at specific depths.)
- 140 cm S-clay, BrBI (7.5YR3/2)
- 150 cm S-clay, dRBr (5YR2/4). Touch
- 160 cm S-clay, dRBr (5YR3/3).
- 180 cm S-clay, dRBr (5YR3/2), increase in sand. GZ vps A1, GGD: 5 mm
- 210 cm S-clay, some parts BL (5YR1.7/1), very touch, high clay content. Some parts with increased sand content BrBI (5YR2/1). Small roots. *Possible palaeosol III*. No datable material collected. No charcoal present and OSL sampling physically impossible.
- 230 cm S-clay, increase in sand. Quartz grains GZ 850-1000 ps A1.
- 250 cm Clayey sand, BBr (7.5YR3/2) GZ 1000 vps A1 ggd: 5mm. Very touch. Probably weathered bedrock.
- 270 cm Clayey sand, yellowish Br (10YR4/4) with yellow particles and quartz grains. Little clay content and very tough. Weathered bedrock. END

## OSL-samples:

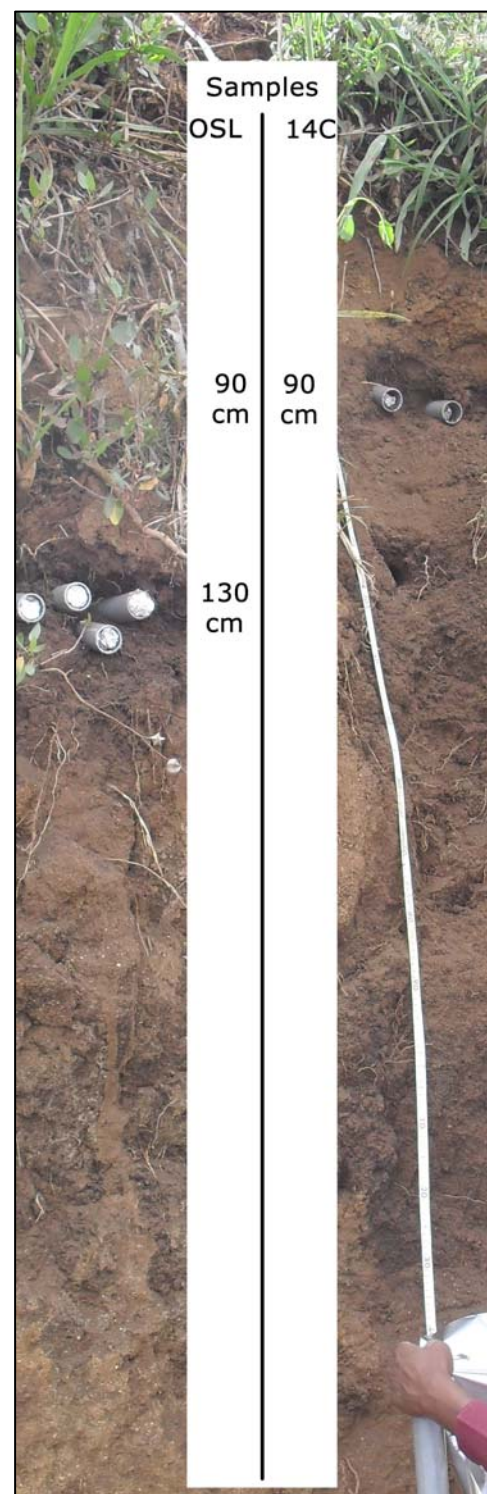
TZ39A-90 Lokozi village, Lushoto District, 26-11-2010, PVC pipe  
Expected age: present-100 yrs BP. Erosion phase III.  
Sample will date the near present A-horizon, not very well developed. Has probably been buried during the creation of the terraces up hill. Might not be very useful.

## TZ39B-130

Lokozi village, Lushoto District, 26-11-2010, PVC pipe  
Expected age: 100-1000 yrs BP. Erosion phase III/II.  
Sample taken in the A-horizon of the second palaeosol. Would date the stable period of this palaeosol. Could be near present, so the cover was created with deforestation and the upper part was deposited during the creation of the terrace. However could also be of older age, with one short K-cycle (less developed A-horizon) on top, before terracing took place.

## C14-samples:

TZ39-90-C14 Lokozi village, Lushoto District, 26-11-2010. 10 cm in the palaeosol, same height as OSL samples.  
Expected age: present-100 yrs BP. Erosion phase III.  
Sample will date the near present A-horizon, not very well developed. Has probably been buried during the creation of the terraces up hill. Could be used for cross-dating OSL.

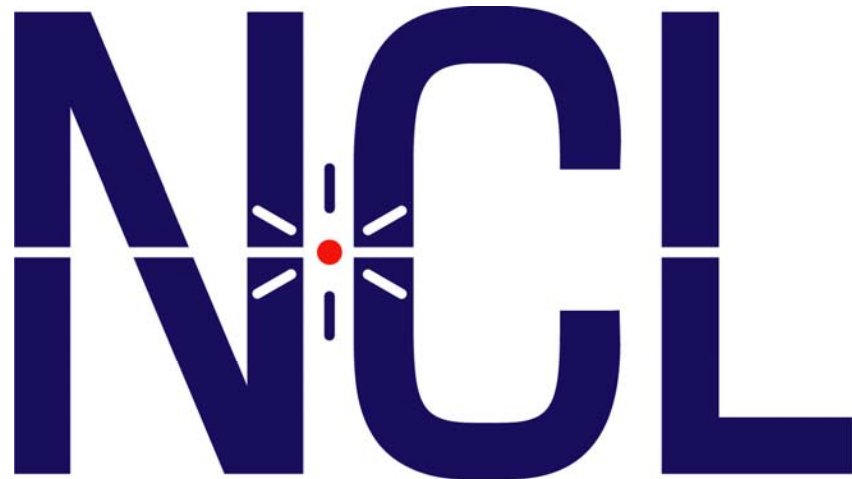


**List of OSL samples**

TZ-02-60-I	Mzungu village, Lushoto District, 02-11-2010, PVC pipe
TZ-02-60-II	Mzungu village, Lushoto District, 02-11-2010, PVC pipe
TZ-02-60-III	Mzungu village, Lushoto District, 02-11-2010, plastic bag
TZ-03-230-I	Mzungu village, Lushoto District, 02-11-2010, PVC pipe
TZ-03-230-II	Mzungu village, Lushoto District, 02-11-2010, PVC pipe
TZ-03-230-III	Mzungu village, Lushoto District, 02-11-2010, plastic bag
TZ30A-40-I	Mshizii village, Lushoto District, 03-11-2010, PVC pipe
TZ30A-40-II	Mshizii village, Lushoto District, 03-11-2010, PVC pipe
TZ30A-40-III	Mshizii village, Lushoto District, 03-11-2010, plastic bag
TZ30B-100-I	Mshizii village, Lushoto District, 03-11-2010, PVC pipe
TZ30B-100-II	Mshizii village, Lushoto District, 03-11-2010, PVC pipe
TZ30B-100-III	Mshizii village, Lushoto District, 03-11-2010, PVC pipe
TZ30C-200-I	Mshizii village, Lushoto District, 03-11-2010, PVC pipe
TZ30C-200-II	Mshizii village, Lushoto District, 03-11-2010, PVC pipe
TZ30C-200-III	Mshizii village, Lushoto District, 03-11-2010, PVC pipe
TZ30D-300-I	Mshizii village, Lushoto District, 03-11-2010, PVC pipe
TZ30D-300-II	Mshizii village, Lushoto District, 03-11-2010, PVC pipe
TZ30D-300-III	Mshizii village, Lushoto District, 03-11-2010, PVC pipe
TZ30E-400-I	Mshizii village, Lushoto District, 03-11-2010, PVC pipe
TZ30E-400-II	Mshizii village, Lushoto District, 03-11-2010, PVC pipe
TZ30E-400-III	Mshizii village, Lushoto District, 03-11-2010, PVC pipe
TZ30E-400-IV	Mshizii village, Lushoto District, 03-11-2010, Plastic bag
TZ31A-55-I	Mshizii village, Lushoto District, 20-11-2010, PVC pipe
TZ31A-55-II	Mshizii village, Lushoto District, 20-11-2010, PVC pipe
TZ31A-55-III	Mshizii village, Lushoto District, 20-11-2010, PVC pipe
TZ31A-55-IV	Mshizii village, Lushoto District, 20-11-2010, Plastic bag
TZ31B-155-I	Mshizii village, Lushoto District, 20-11-2010, PVC pipe
TZ31B-155-II	Mshizii village, Lushoto District, 20-11-2010, PVC pipe
TZ31B-155-III	Mshizii village, Lushoto District, 20-11-2010, PVC pipe
TZ31B-155-IV	Mshizii village, Lushoto District, 20-11-2010, PVC pipe
TZ39A-90-I	Lokozi village, Lushoto District, 26-11-2010, PVC pipe
TZ39A-90-II	Lokozi village, Lushoto District, 26-11-2010, PVC pipe
TZ39A-90-III	Lokozi village, Lushoto District, 26-11-2010, PVC pipe
TZ39A-90-IV	Lokozi village, Lushoto District, 26-11-2010, PVC pipe
TZ39B-130-I	Lokozi village, Lushoto District, 26-11-2010, PVC pipe
TZ39B-130-II	Lokozi village, Lushoto District, 26-11-2010, PVC pipe
TZ39B-130-III	Lokozi village, Lushoto District, 26-11-2010, PVC pipe
TZ39B-130-IV	Lokozi village, Lushoto District, 26-11-2010, PVC pipe

**List of charcoal samples**

TZ03-110-C14	Mzungu village, Lushoto District, 02-11-2010. Various charcoal pieces from a 'layer' at this depth.
TZ03-150-C14	Mzungu village, Lushoto District, 02-11-2010. At the top of the DBrR layer.
TZ11-110-C14	Mzungu village, Lushoto District. 110 cm depth from layer with abundant charcoal.
TZ13-160-C14	Maweni area, Magila Village, Lushoto District, 27-11-2010. 160 cm depth, in the possible palaeosol.
TZ13-200-C14	Maweni area, Magila Village, Lushoto District, 27-11-2010. 200 cm depth, very small samples, probably not large enough for dating.
TZ15-50-C14	Kwalei Village, Lushoto District, 08-10-2010. Charcoal from the top 3 cm of the brown horizon, 50 cm depth. Waypoint 015.
TZ15-80-C14	Kwalei Village, Lushoto District, 08-10-2010. From the top of the black layer at 80 cm depth. Charcoal (burned wood) very abundant. Waypoint 015.
TZ30-150-C14	Mshizii village, Lushoto District, 03-11-2010. 150 cm depth. Sample taken 1,5 m left of the OSL sample line. For cross dating with OSL samples. Waypoint 030.
TZ30-240-C14	Mshizii village, Lushoto District, 03-11-2010. sampled at 240 cm. Sample taken 1,5 m left of the OSL sample line. For cross dating with OSL samples. Waypoint 030. (N.B. Some sand entered sample bag, could have caused contamination.)
TZ31N-35-C14	Mshizii village, Shangai area, Lushoto District, 20-11-2010. Valleycut. Charcoal sample from layer at boundary at 35 cm, crack with above colluvium. <i>Possible pre-agricultural soil surface.</i>
TZ31N-65-C14-I	Mshizii village, Shangai area, Lushoto District, 30-10-2010. Valleycut. Charcoal sample of 65-70 cm, North-cut. Very clayey layer. <i>Possible palaeosol I</i>
TZ31N-65-C14-II	Mshizii village, Shangai area, Lushoto District, 20-11-2010. Valleycut. Charcoal sample from inside the horizon. <i>Possible palaeosol I</i>
TZ31N-82-C14	Mshizii village, Shangai area, Lushoto District, 20-11-2010. Valleycut. Charcoal samples at 2 cm below boundary. <i>Possible palaeosol II</i>
TZ31N-102-C14	Mshizii village, Shangai area, Lushoto District, 20-11-2010. Valleycut. Charcoal samples at 2 cm below boundary. <i>Possible palaeosol III</i>
TZ31N-125-C14	Mshizii village, Shangai area, Lushoto District, 20-11-2010. Valleycut. Charcoal samples at 2 cm above boundary to <i>Possible palaeosol IV</i>
TZ31N-130-C14	Mshizii village, Shangai area, Lushoto District, 30-10-2010. Valleycut. Charcoal sample of 130 cm, top of layer. North-cut/left. <i>Possible palaeosol IV</i>
TZ31N-133-C14	Mshizii village, Shangai area, Lushoto District, 20-11-2010. Valleycut. Charcoal samples at 3 cm below boundary. <i>Possible palaeosol IV</i>
TZ31N-155-C14	Mshizii village, Shangai area, Lushoto District, 20-11-2010. Valleycut. Charcoal sampled at same depth as OSL samples.
TZ31N-170-C14	Mshizii village, Shangai area, Lushoto District, 30-10-2010. Valleycut. Charcoal sample of 170 cm. North-cut/left,
TZ31S-200-C14	Mshizii village, Shangai area, Lushoto District, 30-10-2010. Valleycut. Charcoal sample of 200 cm, South-cut/right.
TZ39-90-C14	Lokozi village, Lushoto District, 26-11-2010. 10 cm in the palaeosol, same height as OSL samples.



# Netherlands Centre for Luminescence dating

Optical dating report

## Soil erosion history based on hillslope deposits in the Western Usambara Mountains of Tanzania

Philip S.J. Minderhoud

*Utrecht University*

*Department of Physical geography*

*Supervisors: Dr. J. Wallinga and A.C. Cummingham*

*Delft University of Technology*

*Faculty of applied sciences*



**Universiteit Utrecht**



## Table of content

1. Introduction .....	3
1.1 Optical Stimulated Luminescence dating.....	3
1.2 Origin of the samples .....	5
1.3 Sample preparation and instrumentation.....	5
1.3.1 Equivalent dose sample preparation .....	5
1.3.2 Equipment for equivalent dose determination .....	6
1.3.3 Dose rate sample preparation .....	7
1.3.4 Equipment for dose rate determination.....	7
1.4 Measurements.....	7
1.4.1 Scan.....	8
1.4.2 Thermal Transfer test .....	8
1.4.3 Pre-heat plateau test .....	8
1.4.4 Dose Recovery Test .....	9
1.4.5 Dose Response curve Test .....	9
1.4.6 Equivalent dose measurements .....	9
1.4.7 Dose rate determination.....	11
Results .....	12
2.1 Scan .....	12
2.2 Pre-heat plateau test.....	12
2.3 Thermal Transfer test.....	13
2.4 Dose Recovery test .....	13
2.5 Dose Response curve Test.....	14
2.6 Equivalent dose measurements.....	15
2.6.1 Single-aliquots.....	15
2.6.1 Single grains .....	16
2.7 Dose rate .....	17
3. Age determination of the samples.....	18
3.1 Central age model.....	18
3.2 Minimum age model .....	19
3.3 Truncation of the single grain data .....	20
3.4 Multi-grain aliquots versus single grains .....	23
3.4.1 Sample NCL-4211015 .....	23
3.4.2 Sample NCL-4211016 .....	25
3.4.3 Sample NCL-4211017 .....	27
3.5 The age of the samples.....	28
4. Discussion .....	30
Acknowledgements .....	31
References.....	32

## 1. Introduction

This is the report of the optical dating study that is carried out as a part of the graduation research '*Soil erosion history based on hillslope deposits in the West Usambara Mountains, Tanzania*' for the Master Physical Geography at Utrecht University. This research is an attempt to reconstruct the erosional history of the Usambara Mountains and to link this to the past environmental changes. The study focuses on the sedimentary record that is stored in colluvium and alluvium deposits. Age control is important for the interpretation of these records and optical dating is used to establish this. Initially three samples are selected for dating. The dating is carried out at the Netherlands Centre for Luminescence dating (NCL), which is part of the Reactor Institute Delft (Faculty of Applied Sciences, TU Delft, The Netherlands). The results from this laboratory research, together with the derived optical ages of the samples, are presented in this report. Details on the interpretation of the ages in combination with the sedimentary records are handled in the main thesis.

### **1.1 Optical Stimulated Luminescence dating**

Optical Stimulated Luminescence (OSL) dating (e.g. Aitken, 1998; Huntley et al, 1985; Lian & Roberts 2006; Wallinga, 2002) is a technique that uses the ability of natural crystalline materials, such as quartz and feldspar, to store energy over a long period of time. This energy is build up under ionizing radiation which causes electrons to be trapped in light-sensitive traps within the crystal lattice of the mineral. Exposure to sunlight, or an equivalent light source releases this energy, which can be measured in the form of a light signal, luminescence (Fig. 1). This signal, if stimulated by light, is called optical stimulated luminescence.

In a natural situation, when quartz or feldspar grains are exposed to sunlight, all the energy is released and the OSL signal is set to zero, so called 'bleaching'. When the grains become buried and remain unexposed to sunlight, they will slowly absorb energy by trapping electrons in their crystal lattice due to the flux of ionizing radiation from surrounding natural radioactivity and cosmic rays. The amount of energy storage within the lattice will be a function of time since last exposure to light. By measuring the total energy absorbed within the quartz or feldspar grains and dividing it by the radiation dose of the surrounding sediments, the age of last sunlight exposure, and thus age of deposition, can be determined.

This is described with the following equation:

$$\text{Age} = \text{Equivalent dose } (D_e) / \text{Dose rate } (D_r) \quad (1)$$

where equivalent dose ( $D_e$ ), also called paleodose, is the amount of radiation received by the mineral since burial (in Gy), and dose rate ( $D_r$ ) the amount of radiation received per year (in Gy).

OSL dating can successfully be applied up to 150 ka, due to saturation of the luminescence signal at this point. When samples are completely bleached, ideally, the lower limit of the method can be only a few years. However, dating young samples involves some extra implications, which are attributed later on. The accuracy of the OSL dating is around 5-10% of the age of the sample, with increasing uncertainty when the samples become very young (<1000 yrs) or old (>80 ka) (Murray & Olley, 2002). In this study we focus on OSL dating of quartz grains.

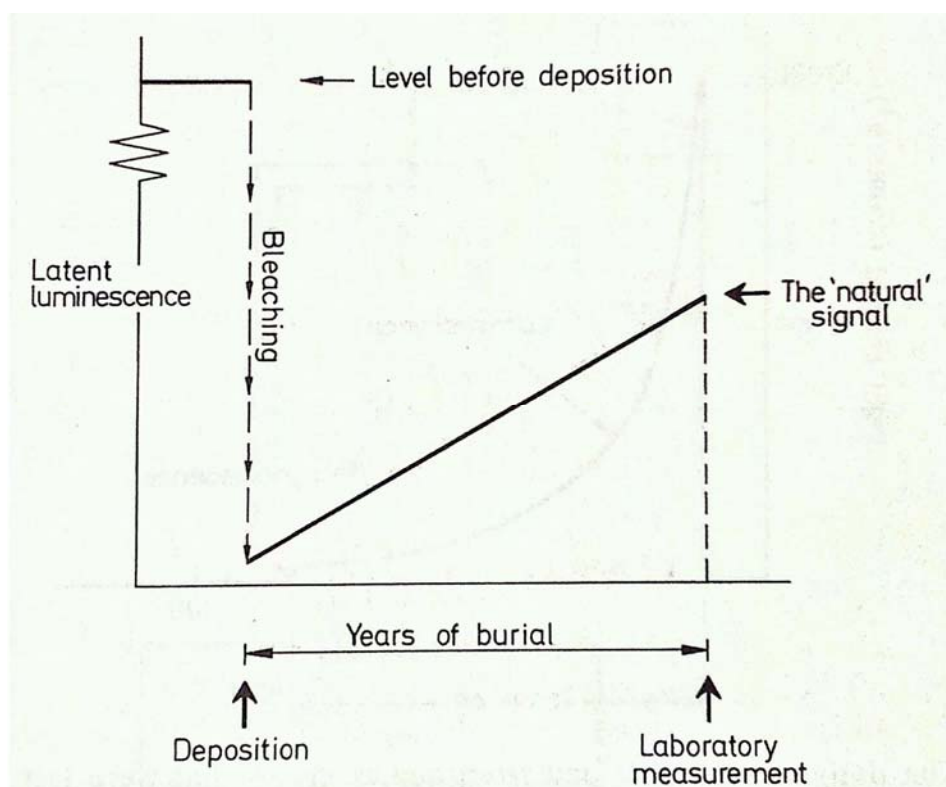


**Fig. 1.1** The latent luminescence signal of quartz. When exposed to sunlight, bleaching occurs, zeroing the luminescence signal. During the time of burial, the signal builds up. In the laboratory, the natural signal, also referred to as paleodose or equivalent dose, is measured. (Aitken, 1998)

## 1.2 Origin of the samples

The three samples that are examined in this study, were collected near the town of Soni, located in the Lushoto district in the West Usambara Mountains, NE Tanzania. The samples were gathered during a three month field study carried out at the end of 2010. Table 1.1 shows the names and the locations of the samples. For a more extensive description of the study area and the sample locations, see the main thesis.

Original sample name	NCL sample code	Latitude	Longitude	Surface elevation (m)	Depth below surface (m)
TZ-02-60	NCL-4211015	-45125.73	382226.5	1485	0.6
TZ31A-55	NCL-4211016	-45015.26	382032.1	1127	0.55
TZ31B-155	NCL-4211017	-45015.26	382032.1	1127	1.55

**Table 1.1** Sample names and their locations.

The samples were collected using 30 cm long PVC tubes (40 mm diameter) that were inserted horizontally in exposures that were cleaned on forehand to expose undisturbed sediment. In order to prevent light exposure through the tube, a piece of aluminum foil was put into the tube before hammering the tubes carefully into the soil. After inserting, the tubes were closed of from the light by aluminum foil and duct tape. Subsequently, the tubes were dug out of the exposure wall and the other side was closed the same way.

## 1.3 Sample preparation and instrumentation

The samples are taken out of the PVC-tube in the laboratory under subdued orange safelight in order to prevent bleaching. The samples are split in two, one part is used for equivalent dose determination and the other for dose rate assessment.

### 1.3.1 Equivalent dose sample preparation

The samples for equivalent dose ( $D_e$ ) determination are kept in the dark and only handled in the laboratory under subdued orange safelight conditions. The following steps are preformed to retrieve feldspar-free quartz from the samples:

- 1) The sample is wet-sieved using a Retsch AS200 Basic Analytical Sieve Shaker to divide the sample into the following fractions: <90  $\mu\text{m}$ , 90-180  $\mu\text{m}$ , 180-212  $\mu\text{m}$ , 212-250  $\mu\text{m}$  and >250  $\mu\text{m}$ .
- 2) The preferred grain size range, 180-212  $\mu\text{m}$ , is selected and treated with 10% hydrochloric acid (HCl) and 10% hydrogen peroxide ( $\text{H}_2\text{O}_2$ ) in order to remove carbonates and organic material from the sample.

- 3) Subsequently the sample is treated with 40% hydrofluoric acid (HF) to dissolve any feldspar in the sample and etch the quartz grains. The etching of the grains is important to get rid of the outer layer that was exposed to alpha radiation.
- 4) The sample is sieved once more, to get rid of severely etched quartz grains.

The samples are subsequently prepared for measurement. For single-aliquot measurements, the quartz grains (~80 grains of 180-212  $\mu\text{m}$  per discs) are mounted on 10 mm diameter stainless-steel discs in a 2 mm diameter mask in the middle of the discs. The grains are secured on the discs using silicone oil spray. For single grain measurements, one hundred individual quartz grains are mounted on aluminum discs. Each disc has 100 holes of 300  $\mu\text{m}$  diameter in a ten-by-ten grid drilled in them.

### **1.3.2 Equipment for equivalent dose determination**

For equivalent dose determination Risø TL-DA-15 TL/OSL readers are used (Bøtter-Jensen et al., 2003), equipped with a 7.5 mm Hoya U340 filter. Optical stimulation is done with blue diodes at 470 nm with a power of  $\sim 35\text{mW cm}^{-2}$ . Infrared stimulation is done with diodes at 875 nm, with a power of  $\sim 116\text{mW cm}^{-2}$ . The beta source used for irradiation is a  $^{90}\text{Sr}/^{90}\text{Y}$  beta source providing a dose rate of  $\sim 0.13\text{ Gy s}^{-1}$ .

For single grain measurements, a special attachment is used which is equipped with a Nd:YVO<sub>4</sub> diode-pumped laser with a wavelength of 532 nm and a maximum power of 50 W/cm<sup>2</sup>. A 2.5 mm Hoya U340 filter is used, in order to increase the light collection efficiency (Ballarini et al., 2005).

### 1.3.3 Dose rate sample preparation

The part of the samples that is used for dose rate ( $D_r$ ) estimation is handled by normal light. First of all, the water content of the sample is measured by weighting and drying the samples at 105 °C for 12 hours. Secondly, the sample is ashed at 500 °C for 24 hrs, combusting all organic material and yielding their weight percentage. Subsequently, the sample is ground in an Agate ball mill and mixed with molten wax. It is poured into mould to create a 9 cm disc with a thickness of 2 cm. The wax ensures to capture the radon gas which is part of the uranium-238 decay chain. In order to allow sufficient radon build-up, the disc is stored for two weeks, before it can be used for measurements.

### 1.3.4 Equipment for dose rate determination

For calculation of the natural dose rate of the sediments surrounding the samples, the radionuclide concentration is needed. This is measured by using high resolution gamma-ray spectroscopy on the waxed discs (Murray et al., 1987) using a Canberra broad energy HPGe gamma spectrometer (Venkataraman et al., 2003)

## 1.4 Measurements

In order to be able to correctly measure the equivalent dose, first the luminescence characteristic behaviors of the quartz samples need to be determined (Wintle & Murray, 2006). The tests for deriving these characterizations, all use modified versions of the single aliquot regenerative-dose (SAR) procedure (Murray and Wintle, 2000, 2003). Table 1.2 shows the generalized quartz SAR protocol.

Step	Treatment	Observe
1	Give dose, $D_i$	
2	Preheat (160-300 °C for 10 s)	
3	Optically stimulate for 40 s at 125 °C	$L_i$
4	Give test dose, $D_t$	
5	Heat of 160 °C (to <preheat in step 2)	
6	Optically stimulate for 40 s at 125 °C	$T_i$
7	Optically stimulate for 40 s at >preheat	
8	Return to 1	

**Table 1.2** Generalized SAR protocol. For the natural signal,  $i=0$  and  $D_0$  is the natural dose.  $L_i$  is the OSL response to regenerative dose and  $T_i$  the OSL signal from the test dose.  $L_i$  and  $T_i$  are derived from the measured stimulation curve. Typically the first 1-25 seconds minus the background signal measured from the last part. (Murray and Wintle, 2000, 2003).

### **1.4.1 Scan**

The scan is done to get a first impression of the sample and to determine whether the sample is contaminated with feldspar or other IR-sensitive minerals. These minerals can significantly affect the OSL signal, if unknown and/or treated wrongly (Wallinga et al., 2002) A simplified SAR procedure consisting of a few cycles is preformed:

- 1) The natural OSL dose is measured.
- 2) A test dose of 5 GY is given and the OSL signal is measured.
- 3) The sample is dosed again with 5 GY, then given a low temperature, infra-red "wash" and the OSL signal is measured again.

The OSL responses to the given dose before and after the IR wash can be compared to identify possible IR-sensitive minerals. Subsequently, by comparing the natural OSL dose with the OSL from the given dose, a very rough indication of the age of the sample can be given.

### **1.4.2 Thermal Transfer test**

Quartz crystals contain shallow traps that are temperature sensitive, but optically insensitive. When a sample is heated, it is possible that the trapped charge from these traps is released and recaptured in a deeper, OSL sensitive trap. If this is happening, it could result in a higher, artificial natural OSL signal, and thus in an overestimation of the original  $D_e$ . By performing a thermal transfer test the behavior of the quartz is monitored after heating (Wintle & Murray, 2006). The sample is first reset to zero by stimulating with blue light. Subsequently, the sample is heated at 140 °C and the OSL signal is measured, than this is repeated with increasing temperatures, with steps of 20 °C up to 280 °C. After every heating the OSL signal is measured. By plotting the OSL signal measured for each temperature, possible thermal transfer can be investigated.

### **1.4.3 Pre-heat plateau test**

A pre-heat plateau test (Aitken 1998) is preformed to investigate the dependency of the equivalent dose on the selected pre-heat temperature. Using an appropriate pre-heat temperature and, subsequently, cut-heat temperature, is important to empty the 110 °C TL peak and to remove any feldspar contribution in contaminated quartz samples and. The OSL signal of feldspar is less thermally stable, so it can be released at lower temperatures than the OSL quartz signal (Wallinga et al., 2002).

The standard SAR protocol (table 2) is performed with a range of pre-heat temperatures, from 180 °C up to 280 °C, with steps of 20 °C.

#### **1.4.4 Dose Recovery Test**

The luminescence sensitivity can change strongly when the sample is first heated. In order to check whether the first sensitivity measurement ( $T_0$ ) is correct to the previous natural signal ( $L_0$ ), a test is carried out on unheated portions that have been given a laboratory dose after bleaching the natural signal (Roberts et al., 1999; Wallinga et al., 2000). The SAR protocol that is chosen is a result of the above described tests and the appropriateness of this protocol is tested by performing a dose recovery test.

- 1) The natural OSL signal is reset by exposing it to blue light.
- 2) The aliquots are given a dose of 5 GY.
- 3) The aliquots are measured as being normal using the selected SAR procedure.

The results of the SAR measurements should be within a 10% error of the given dose to justify the considered SAR protocol.

#### **1.4.5 Dose Response curve Test**

The dose response curve test is performed to test the OSL response to high doses and to see the OSL signal saturation (Wintle & Murray, 2006). It can be used to see whether the sample can be dated with quartz. Young samples will plot in the linear region of the curve. Older samples might plot in the arch of the curve. The closer the natural signal is to saturation, the more problematic to date.

#### **1.4.6 Equivalent dose measurements**

The equivalent dose of a sample is determined by comparing the natural signal to the regeneration points for a known dose as is shown in figure 1.2.

The results of the above tests are used to determine the appropriate SAR protocol for measuring the equivalent dose. This resulted in a SAR protocol described in table 1.3. The multi-grain aliquots OSL signals are processed according to the recommendations of Cummingham and Wallinga (2010) by using the 'early-background' approach. This ensures a net signal that is most dominated by the 'fast' component, which yields the best results (the fast OSL component of quartz grains is most easily bleached by sunlight (Wintle & Murray, 2006)). The integral channels are

taken from 0-0.50 s for initial signal and 0.50-1.75 s for background subtraction (2.5 times longer).

For single-grain measurements, the 'early-background' approach is used as well. For the initial signal the first 0.17 s is used, and for background subtraction channels 0.17-0.60.

Step	Treatment	Conditions
1	Dose, $D_i$	N, 5, 0, 5, 5 (with IR wash prior to step 3) Gy
2	Preheat	240 °C for 10s
3	Measuring OSL (470 nm) ( $L_i$ )	125 °C for 40s
4	Test dose, $D_t$	5 Gy
5	Cutheat	220 °C
6	Measuring OSL (470 nm) ( $T_i$ )	125 °C for 40s
7	OSL bleach (470 nm)	250 °C for 40s
8	Repeat step 1-7	
Extra 1	LM-OSL measurement	Given dose of 10 Gy

**Table 1.3.** Adapted SAR procedure used in this study (modified after Murray and Wintle, 2003)

The  $D_e$  for each aliquot/grain is estimated using a linear fit to a single regenerative dose (Ballarini, 2006).

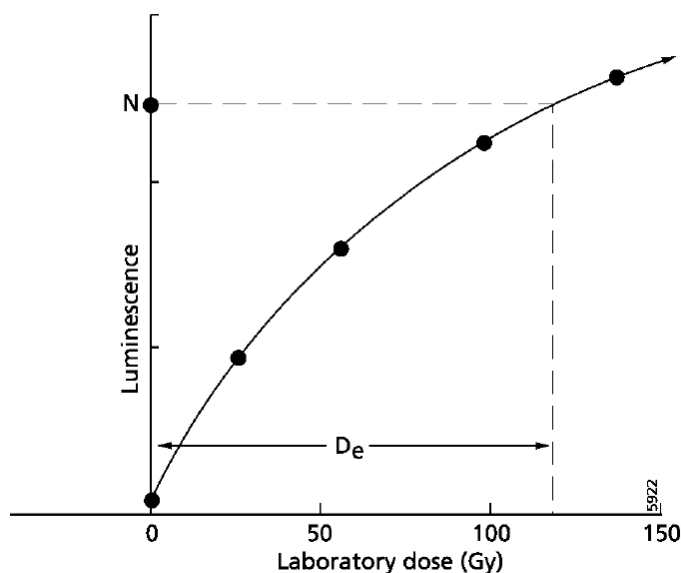


**Fig. 1.2** Equivalent dose determination using the SAR procedure (Table 1.2 & 1.3). The test-dose corrected OSL responses of the natural signal and the regeneration doses are plotted against the beta dose given in the laboratory. The equivalent dose is obtained by projecting the natural response on the reconstructed dose response curve (Wallinga, 2002; after Aitken, 1998).

The signals returned from the aliquots are given four tests before they are accepted.

1) Recycling test.

For this test the ratio of two sensitivity-corrected data points ( $L_i/T_i$ )/( $L_i/T_i$ ) is used (Wintle & Murray, 2006). The sample passes if the ratios are within 0.90 and 1.10 (10% variation).

2) IR-test

This test is done to measure any feldspar contribution to the OSL signal. This is done by performing a recycling test on the OSL response of the sample to a given dose with the response to the same given dose, after infrared stimulation (in order to deplete any feldspar OSL traps). The sample passes if the ratios are within 0.90 and 1.10 (10% variation).

3) Recuperation test.

After bleaching the sample, a measurement of a zero dose point, should give zero signal. But it is possible that some charge is transferred from deeper traps by the previous irradiation, optical stimulation and preheating. This causes the signal to be above zero, also called recuperation (Aitken, 1998). Samples are accepted if the recuperation is less than 10% of the given dose, in this case 0.5 GY.

4) LM-OSL test.

This test allows visualizing the dominance of the fast-OSL component, which is most suitable for dating (Murray and Wintle, 2006). It can also be used to check for the presents of the Ultra-fast component.

### **1.4.7 Dose rate determination**

The natural dose rate received by the sample is calculated from the radionuclide concentration of the surrounding sediment. Several radionuclides of the Uranium and Thorium series, together with K-40, are measured, to determine the radionuclide dose rate. The cosmic dose rate is determined by the location and altitude of the sample, the burial history of the sample and its depth below surface (Prescott & Hutton, 1994). The radionuclide dose rate and cosmic dose rate are corrected for the attenuation made on the dose rate by water and organic matter content of the sample. This results in the best estimate of the dose rate received by the sample in nature.

## 2. Results

### 2.1 Scan

The results from the scan test confirm the expectations that the sample are young and with a large differences in the measured equivalent dose (sign of poor bleaching). One of the samples shows some IR response, indicating some possible feldspar contamination. However this IR signal is not significant in proportion to the OSL signal, so no further laboratorial steps have been taken in order to remove this contamination. The SAR protocol incorporates an IR-test to filter out the samples that do respond significantly to infrared stimulation.

### 2.2 Pre-heat plateau test

Figure 2.1 shows the results of the preheat plateau test. Sample 15 shows a plateau in its equivalent dose (up to 220-240 °C), and a rise in signal for higher preheat temperatures. However sample 17 performs bad, with large variations in its  $D_e$  values, and no relation with temperature. This bad performance is possibly due to the dependency of pre-heat test to variations in the natural signal. For sample 17, the natural signal has very large variations in its natural OSL signal for the used data points. This preheat plateau test does not correct for this. The response of the samples to differences in preheat temperature can be investigated using a thermal transfer test.

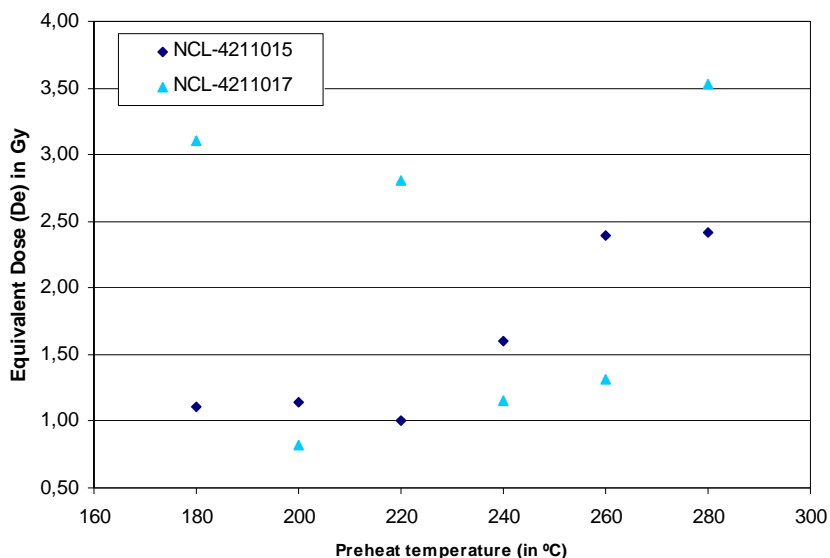


**Fig. 2.1** Preheat plateau test for samples 15 and 17.

### 2.3 Thermal Transfer test

The results from the thermal transfer test are shown in figure 2.2. The results show for all three samples in general no significant thermal transfer up to temperatures of 240 °C. Thermal transfer starts to occur slightly from 260 °C, but even on a preheat of 280 °C, the net change in the signal is only a few percent. Based on the thermal transfer results and the possible presence of an ultra-fast OSL component, the preheat and cutheat temperatures for the SAR protocol are chosen respectively 240 °C and 220 °C.

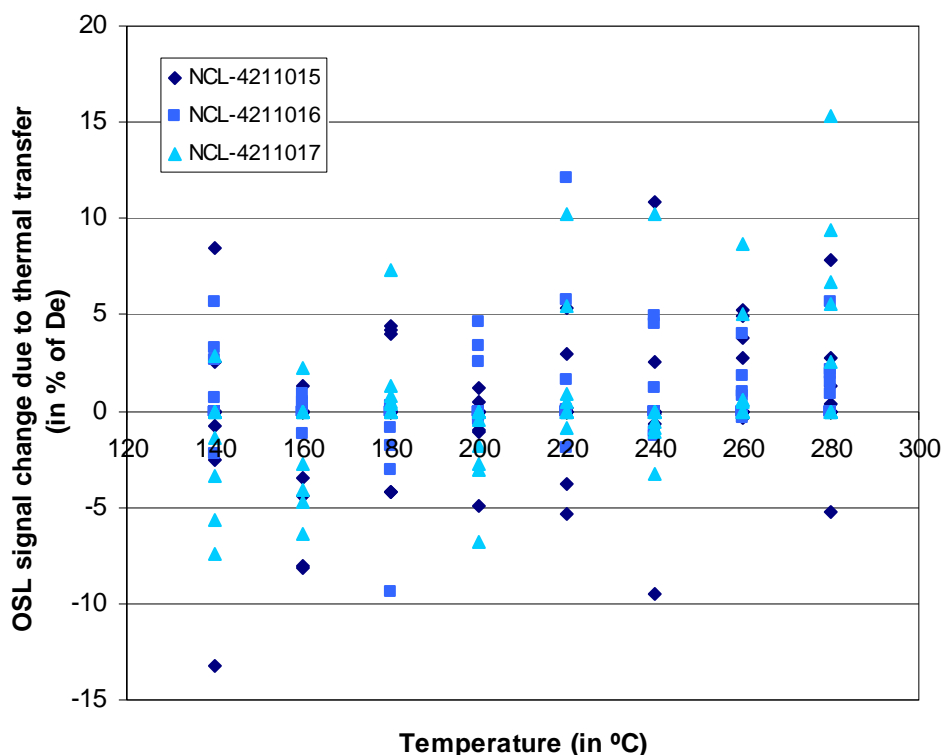


**Fig. 2.2** Results of the thermal transfer test.

### 2.4 Dose Recovery test

The results of the dose recovery test are satisfying (see figure 2.3). The given dose was perfectly recovered and the ratio between the two (given dose/measured dose) was  $0.99 \pm 0.02$ . All aliquot of each of the three samples plotted well within 10% test criterion. These results confirm that the chosen SAR protocol is correctly chosen and able to recover an artificially given dose very well.

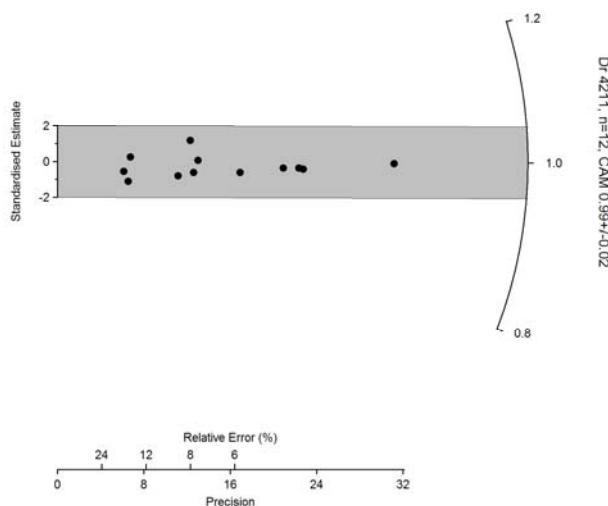


**Fig. 2.3** Radial plot showing the results of the dose recovery test. All points fall well within the range of two times the standard error. The axis on the right shows the ratio between given dose and measured dose and the bottom axis shows the precision of the data points.

### 2.5 Dose Response curve Test

The dose response curve, figure 2.4, shows the increasing saturation of the quartz grains. The natural signal plots almost at the origin of the graph, in the linear part of the curve. This means the  $D_e$  can be estimated using a linear fit to a single regenerative dose (Ballarini, 2006). The points of the repeated measurements all plot slightly higher than the original values. This might indicate that some small changes have occurred in the quartz during the measurements. The sensitivity check in the SAR protocol will account for this during the  $D_e$  measurements, might this influence the samples significantly.

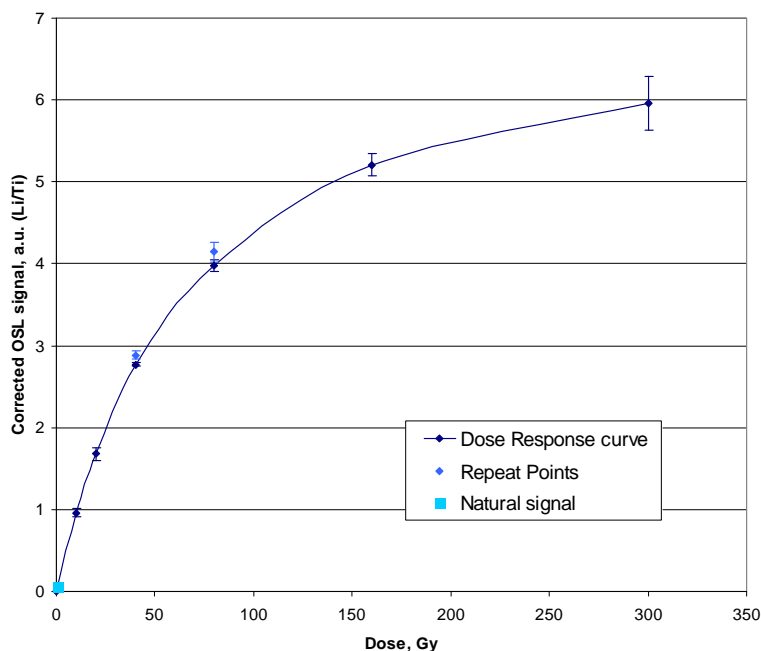


**Fig. 2.4** Dose response curve with error margins and repeated measurements points. The natural signal plots very close to the origin.

## 2.6 Equivalent dose measurements

A large number of  $D_e$  measurements on both multi-grains aliquots and single quartz grains are done. The aliquots and grains that passed the test criteria of the SAR protocol are shown, respectively, in figure 2.5 and 2.6. The results are not truncated, and also 'failing' grains that give a zero or negative  $D_e$  are shown.

### 2.6.1 Single-aliquots

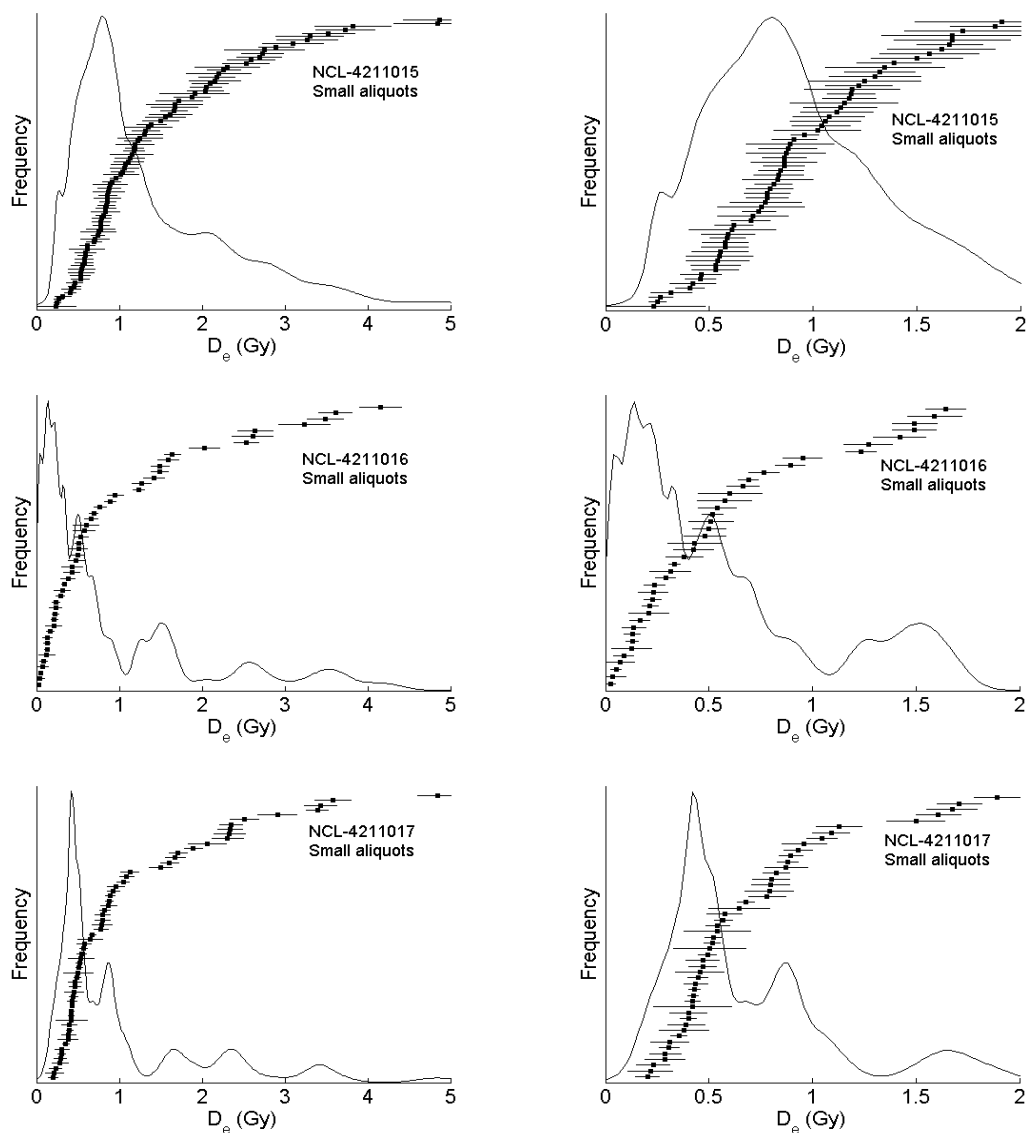


**Fig. 2.5** Frequency distribution of the equivalent dose ( $D_e$ ) measurements on the single-aliquots, plotted with the individual data points and their error. The right column gives the lower values in more detail.

### 2.6.1 Single grains

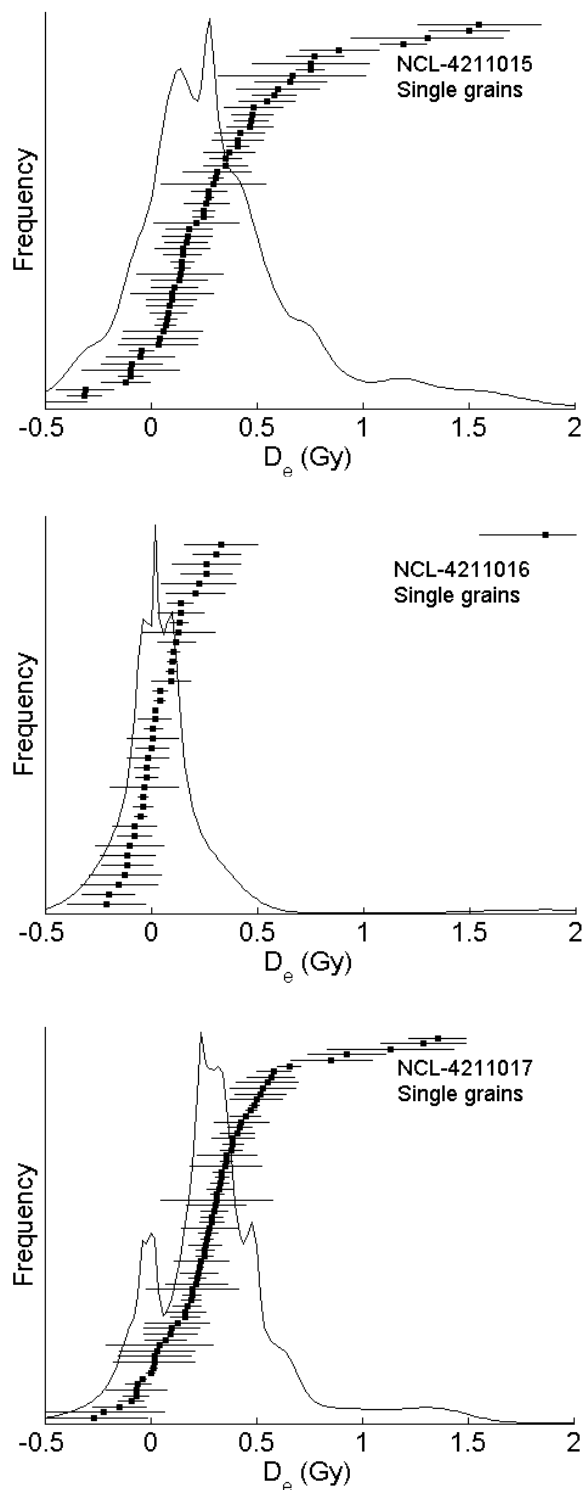


**Fig. 2.6** Frequency distribution of the equivalent dose measurements on single grains. The single data points are plotted with their error margin. Data points with values above 2 are not plotted in the graphs.

## 2.7 Dose rate

Table 2.1 shows the assumptions made for dose rate determination. For all three samples a gradual burial history is assumed. They are all three located in a colluvial/alluvial sedimentation system, where the overlying sediment is gradually deposited on top. The water and organic content matter are used as measured in the samples, except for sample 17. For this sample a wet saturation history is assumed due to its depth below surface and the nearby stream at the same height. These assumptions are used to correct the cosmic dose rate (in case of burial history) and the radionuclides (water and organic matter content) for attenuation occurred in nature.

Sample	NCL	Burial assumption	Grain size range		Water content				Organic content		
			lower ( $\mu\text{m}$ )	upper ( $\mu\text{m}$ )	Measured	Sat. hist.	Used		Measured	Used	
NCL-4211015		Gradual burial	180	212	16.79		16.79	± 5.54	16.08	16.08	± 1.61
NCL-4211016		Gradual burial	180	212	4.05		4.05	± 1.34	4.50	4.50	± 0.45
NCL-4211017		Gradual burial	180	212	15.44	wet	20.00	± 5.00	2.78	2.78	± 0.28

**Table 2.1** Dose rate assumptions.

The radionuclide concentrations of the samples are shown in table 2.2 together with the dose rate from each radiation type and the total dose rate received per sample. These are corrected for the assumptions made in table 2.1. As can be seen, sample NCL-4211017 has a higher total dose rate than overlying sample NCL-4211016, mainly due to a much higher K-40 concentration. Leaching of clay minerals and attached radionuclides, like K-40, to lower layers, could have created this difference. Such changes on the natural dose during the past are hard to track down and could lead in our case to a over- and underestimation of the 'true' paleodose.

Sample	Radionuclide concentrations (Bq/kg)															
	U			Th			K-40									
NCL-4211015	23,26	±	0,35	25,14	±	0,72	22	±	3							
NCL-4211016	8,05	±	0,16	10,55	±	0,30	94	±	3							
NCL-4211017	8,69	±	0,21	15,95	±	0,25	223	±	4							
Dose rates (Gy/ka)																
Internal			External			Cosmic			Total	Error	Error					
alpha			beta			gamma				(syst.)	(rand.)					
0,01	±	0,01	0,25	±	0,02	0,29	±	0,02	0,27	±	0,01	0,83	±	0,03	0,03	0,01
0,01	±	0,01	0,30	±	0,01	0,21	±	0,01	0,26	±	0,01	0,79	±	0,02	0,02	0,01
0,01	±	0,01	0,51	±	0,03	0,32	±	0,02	0,22	±	0,01	1,06	±	0,04	0,04	0,01

**Table 2.2** Radionuclide concentrations and dose rates for the three samples.

### 3. Age determination of the samples

Now that both the equivalent dose and the dose rate measurements are done, the age can be determined. However, determining the correct equivalent dose out of the various data points isn't as straightforward as it might look. Different methods and corresponding models are proposed for this purpose, like the central age model (CAM) and the minimum age model (MAM-3 and MAM-4, with 3 and 4 parameters) (Galbraith et al., 1999).

#### 3.1 Central age model

In an ideal situation, where all grains are well bleached before deposition, the variation in the  $D_e$  measurements is a product of in situ microdosimetry variations. This relative standard error in this dose rate distribution is referred to as 'overdispersion' ( $\sigma_b$ ) (Galbraith et al., 1999). When the scatter in a  $D_e$  dataset is solely determined by overdispersion, the CAM can be applied to deal with these variations, treating the dataset as a normal distribution. It will result in a mean equivalent dose and a corresponding standard error (fig. 3.1). For this study the CAM will not be appropriate since the spread in the  $D_e$  measurements is not only created by the overdispersion but also by poor bleached grains in the sediment (e.g. high outliers in  $D_e$  values). As shown in figure 8, applying the Central Age model will result in an overestimation of the natural dose due to incorporation of older grains and aliquots.

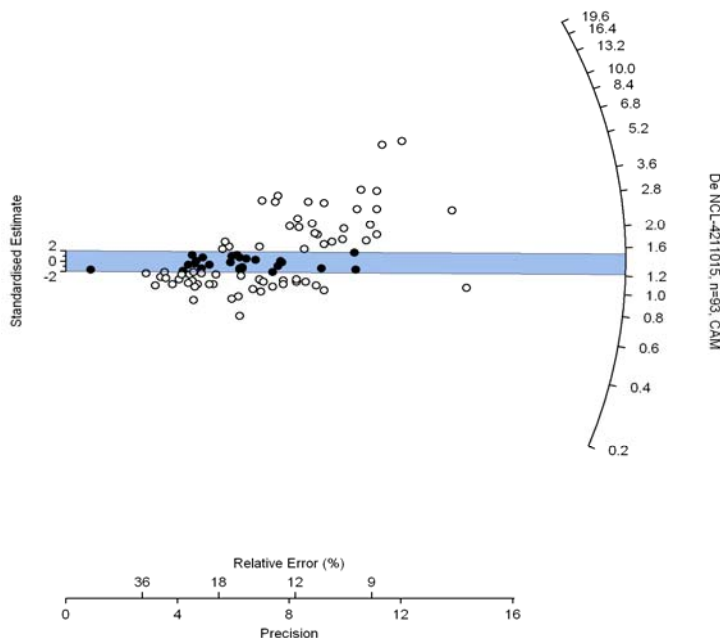


**Fig. 3.1** Radial plot with the data points of the multi-grain aliquot measurements of sample NCL-4211015. The blue band shows the outcome of the CAM, 1.344. Due to poor bleaching (points above the blue band) the CAM result gives an overestimate of the equivalent dose after last burial (The better bleached data points plot below the blue band).

### 3.2 Minimum age model

In order to deal with incorporated poor bleached grains a minimum age model, MAM, can be used (Galbraith et al., 1999). In our case we use the three parameter MAM-3. Its application is simpler and it is more suitable for application on multi-grain aliquots (Cunningham & Wallinga, submitted). There are two inputs that determine the outcome of the MAM-3, namely, the  $D_e$  dataset and the overdispersion ( $\sigma_b$ ). The outcome of the MAM-3 is very sensitive to these inputs and small changes in either the  $\sigma_b$  or the  $D_e$  dataset, will result in a different minimum age outcome.

In order to deal with this uncertainty, Cunningham & Wallinga (submitted) suggest to present OSL ages as probability distribution functions (PDF). These PDF's are created by bootstrap re-sampling of the  $D_e$  dataset and randomize the  $\sigma_b$  value. Bootstrapping is a method to determine the measures of accuracy of the MAM-3 model on the  $D_e$  dataset. The PDF of the minimum age of the sample is created by bootstrapping the  $D_e$  data, repeatedly constructing a new random  $D_e$  dataset within the variation of the original dataset. For each new synthetic dataset the minimum age is calculated by using a random, normal distributed  $\sigma_b$ , resulting in a unique minimum age value. After a large number of iteration (e.g. 1000), the distribution of the minimum ages is used to construct the PDF of the minimum age (figure 3.2). For a detailed explanation on the PDF of the MAM-3 via bootstrapping, see Cunningham & Wallinga (submitted).

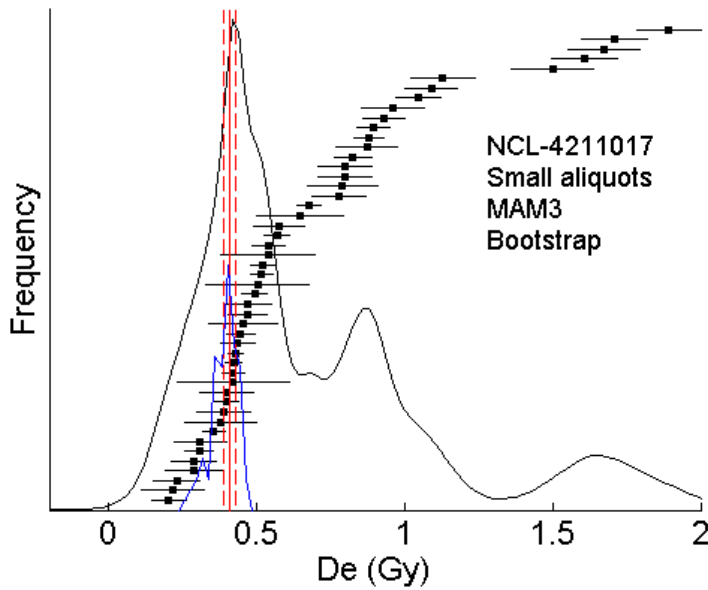


**Fig. 3.2** Multi-aliquot  $D_e$  dataset of sample NCL-4211017 with MAM-3 (with  $\sigma_b = 0.085$ ) outcome (red line, with error margin). The PDF of the MAM-3 for this dataset is plotted in blue Cunningham & Wallinga (submitted).

Selection of the correct  $\sigma_b$  value for a particular dataset is important and is dealt with by Cunningham et al. (submitted). Following the suggested approach, the correct  $\sigma_b$  values are determined, for single grain  $D_e$  datasets a  $\sigma_b$  of 0.2 and for the multi-grain aliquot datasets a  $\sigma_b$  of 0.085.

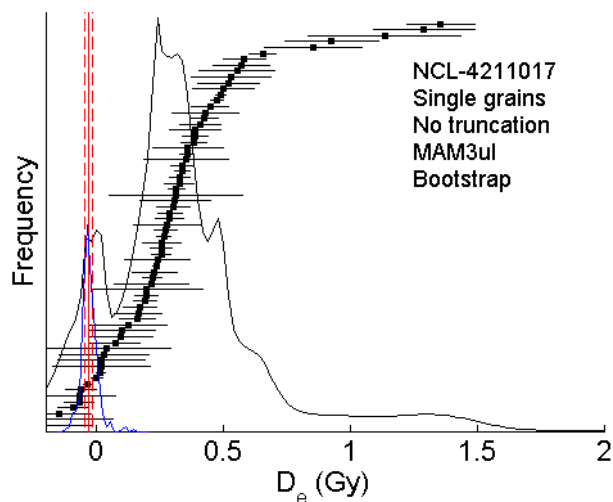
The MAM-3 is based on logarithmic functions and can therefore not deal with negative values. To deal with datasets with samples of zero or close to zero (with negative values within their probability range when bootstrapping) an unlogged version of the model, MAM-3<sub>ul</sub> is used. The unlogged MAM-3 approaches the original MAM-3 model, however in this study the unlogged MAM-3 sometimes produces structurally lower outcomes than the logged MAM-3. (see differences for sample NCL-4211015 between table 3.1 and 3.2).

When applying the minimum age model, it is important to keep in mind that what is recognized as natural dose, may instead be associated with grains that have experienced unusually low beta dose rates. Or with grains that have been deposited more recently and due to processes like bioturbation have intruded into deeper layers (Galbraith et al., 1999). Therefore one should be watchful on possible age underestimation.

### 3.3 Truncation of the single grain data

When the unlogged MAM-3 is applied on single grain datasets that incorporate zero or negative data points, the resulting minimum age will be close to zero or even in negative, futuristic values (fig. 3.3). Judging from the fact that the sample has already been sampled and thus deposition has already occurred, these outcomes can be firmly rejected. Therefore the  $D_e$  datasets needs some treatment before it can be successfully used by the unlogged MAM-3. Zero or negative data points, resulting from faulty measurements or 'failing' grains, should be removed from the dataset by truncation the data.

**Fig. 3.3** Example when the unlogged MAM-3 is used on an un-truncated single grain  $D_e$  dataset that incorporates negative data points. The unlogged MAM-3 produces a negative minimum age (red), also visible in the corresponding PDF (blue).



Removing data from the dataset could lead to the loss of 'true' signal, especially when dealing with (very) young samples, as it the case. The influence of the strength of the rejection criteria for truncation on the minimum age outcomes is shown in table 3.1 for the logged MAM-3 and table 3.2 for the MAM-3<sub>ul</sub>. The rejection criteria are in percentage of certainty that the data points are above zero.

Table 3.1 shows that the different rejection criteria do not affect the outcome of the unlogged version of the MAM-3, however truncation is needed to be able to run the model. For the unlogged MAM-3 version, table 3.2, the strength of the rejection criteria does matter significantly.

Rejection criteria	NCL-4211015	NCL-4211016	NCL-4211017
No truncation	0.2057	error	error
68% certain > 0	0.2425	0.1161	0.3109
95% certain > 0	0.2366	0.1173	0.3143
99% certain > 0	0.2551	0.1148	0.3181

**Tab. 3.1** Logged MAM-3 outcomes for different truncation criteria on single grain dataset ( $\sigma_b=0.2$ ).

Rejection criteria	NCL-4211015	NCL-4211016	NCL-4211017
No truncation	-0.0956	-0.0294	-0.0318
68% certain > 0	0.1168	0.0731	0.0341
95% certain > 0	0.1183	0.0772	0.2938
99% certain > 0	0.1686	0.1115	0.3018

**Tab. 3.2** Unlogged MAM-3 outcomes for different truncation criteria on single grain dataset ( $\sigma_b=0.2$ ).

The PDF's of the truncated datasets using the unlogged MAM-3 are shown in figure 3.4. With increasing rejection criteria, the minimum age approaches the value created by the logged MAM-3. This shows the unlogged MAM-3 tendency to produce a lower minimum age than the logged version on the same dataset when some data points are close to zero. Whenever this happens, the part of the dataset that is used by the MAM-3<sub>ul</sub> to produce the minimum age is much lower than for the logged MAM-3. As soon as the outcomes of both models approach each other (by increasing the rejection criteria) the amount of data points used becomes also similar. The shift in the MAM-3<sub>ul</sub> outcome for sample 15 and 16 between 95% and 99% could be the result to the removal of actual 'true' signal, since no significant increase is witnessed for the increase during 68% and 95%. This suggests using a truncation criterion of 95% for optimal results.

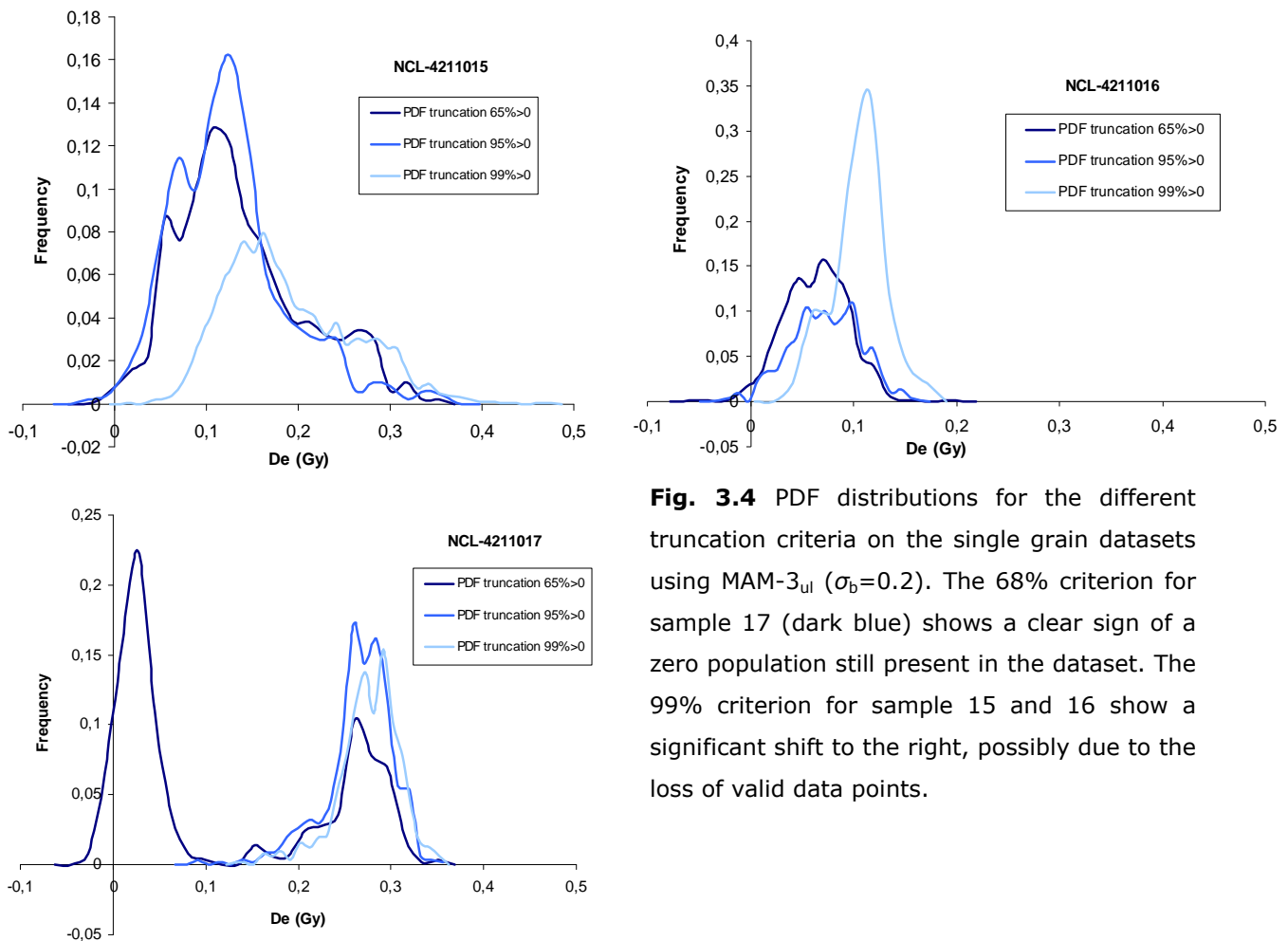


**Fig. 3.4** PDF distributions for the different truncation criteria on the single grain datasets using MAM-3<sub>ul</sub> ( $\sigma_b=0.2$ ). The 68% criterion for sample 17 (dark blue) shows a clear sign of a zero population still present in the dataset. The 99% criterion for sample 15 and 16 show a significant shift to the right, possibly due to the loss of valid data points.

### 3.4 Multi-grain aliquots versus single grains

Now that the correct truncation criterion for the single grain data is determined, the multi-grain and the single grain data can be compared. In general, when sufficient single grain data is available, it is superior to the multi-grain data since the signal of an individual grain is not influenced other, poor bleached grains and averaged out. Especially for young samples, of which the natural signals are very small, the signal of poor bleached grains can easily be several times higher, causing a much higher  $D_e$  to be measured for multi-grain aliquots. The results of both methods will be compared for each sample separately in order to determine the correct minimum age as precisely as possible. Following the suggestion of Cunningham & Wallinga (submitted) to treat OSL ages as PDF's rather than strict values, the PDF's of the minimum ages of both the multi-grain and single grain data are used. The age is calculated by dividing the  $D_e$  values by the dose rate (table 2.2) the sample received in nature according to equation 1.

#### 3.4.1 Sample NCL-4211015

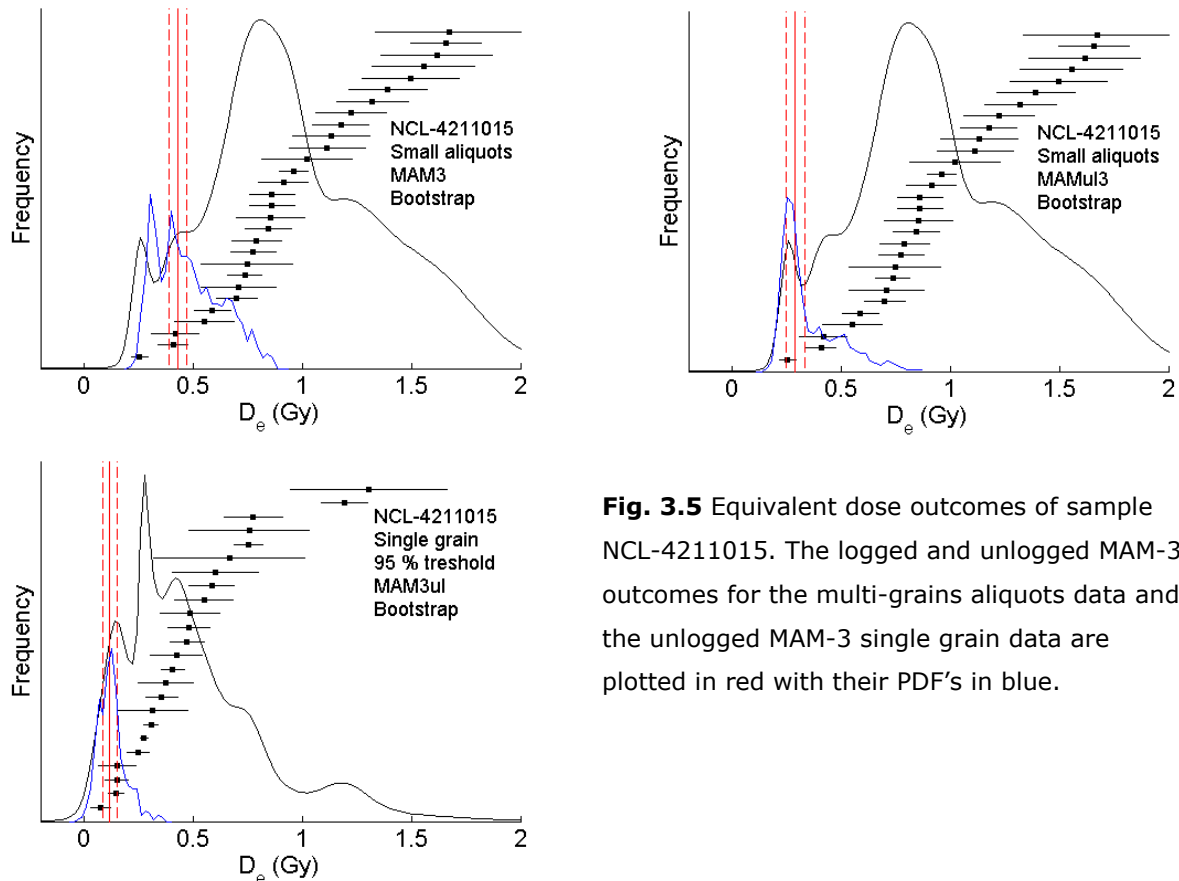


**Fig. 3.5** Equivalent dose outcomes of sample NCL-4211015. The logged and unlogged MAM-3 outcomes for the multi-grains aliquots data and the unlogged MAM-3 single grain data are plotted in red with their PDF's in blue.

In figure 3.5 the minimum ages for sample 15 are given together with their PDF's. For the multi-grain aliquots both the logged and unlogged model could be bootstrapped. For the single grain data this was only the case for the unlogged model. The single grain data is too close to zero for the logged model to be used for bootstrapping.

The PDF plots for sample 15 are plotted in figure 3.6. The first striking difference is the large difference between the single grain PDF with the multi-grain PDF's. As discussed before, when dealing with such young samples, the influence of the averaging that occurs when measuring multi-grain aliquots, can be quite significant. Especially with the large amount of poor bleached grains present in the sample. The difference between the two multi-grain PDF's can be an artifact of the poor performance of the logged MAM-3 on a young dataset. However, both highest peaks in probability of the minimum age according to the multi-grain measurements fall within reach of the single grain minimum age PDF. Therefore, the PDF of the MAM-3<sub>ul</sub> on the single grain data of sample NCL-4211015 is considered to be the best estimate for the true minimal age of the sample.

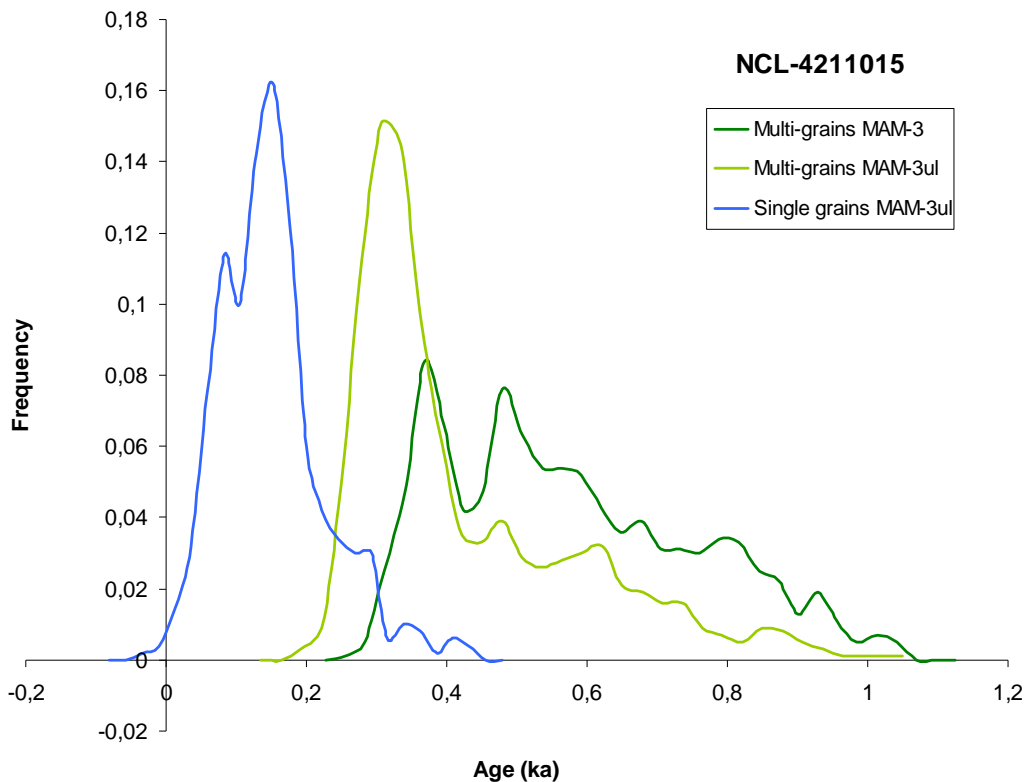


**Fig. 3.6** PDF's on the minimum age of sample NCL-4211015 for both single grains and multi-grains data.

### 3.4.2 Sample NCL-4211016

The datasets for sample 16 are shown in figure 3.7. Bootstrapping the logged MAM-3 for this dataset was impossible for both the multi-grains as the single grains datasets. A problem for this sample is the small dataset of the single grain  $D_e$  values that passed all test criteria ( $n=9$  for 95% truncation;  $n=7$  for 99% truncation). The single grain dataset with 99% truncation is included in this analysis, because it provides some extra insight on the sample. The PDF's of the minimum age are plotted together in figure 3.8.

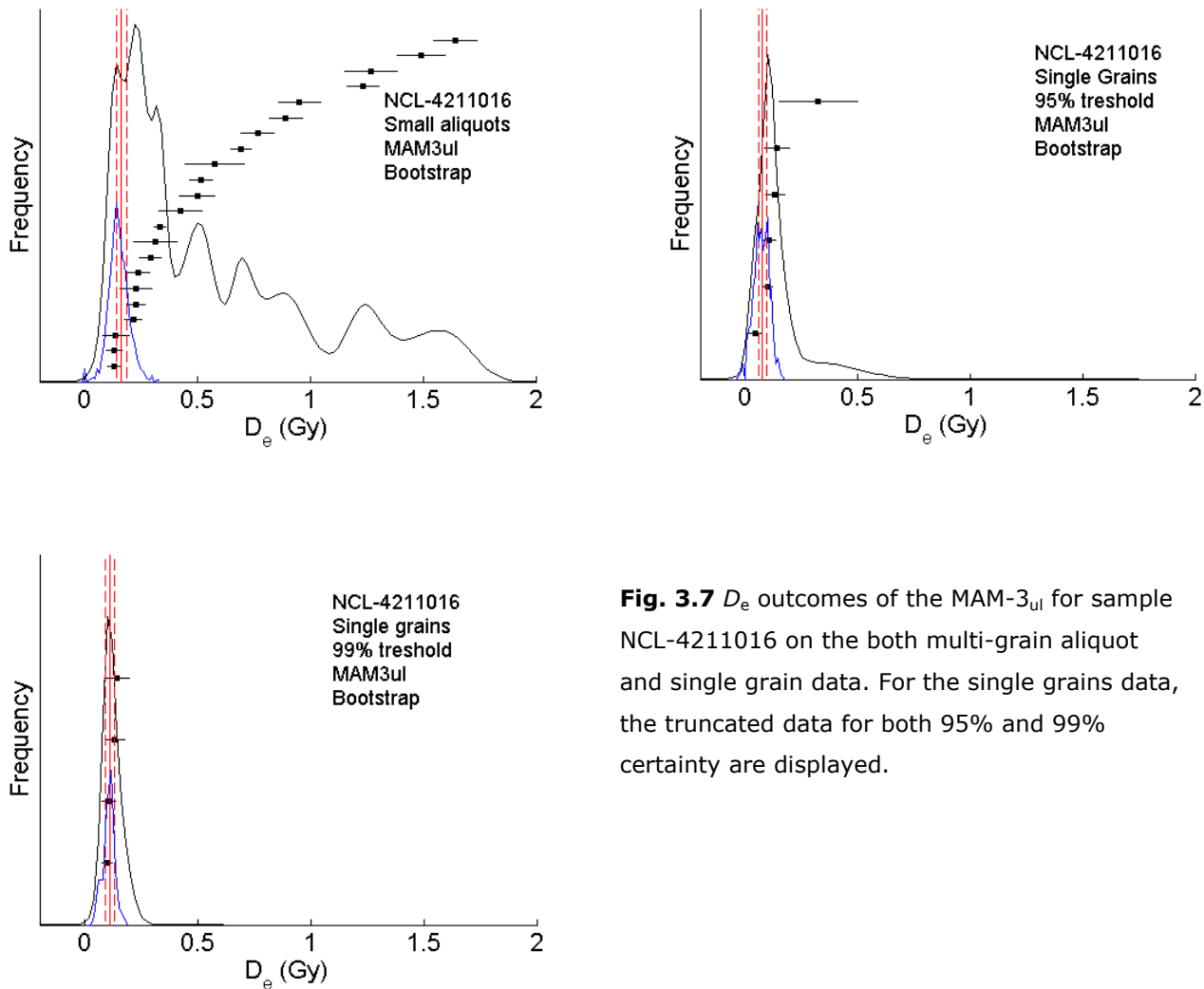


**Fig. 3.7**  $D_e$  outcomes of the MAM-3<sub>ul</sub> for sample NCL-4211016 on the both multi-grain aliquot and single grain data. For the single grains data, the truncated data for both 95% and 99% certainty are displayed.

The single grain  $D_e$  dataset loses two data points when the truncation criterion is increased from 95% to 99%. The minimum age outcome shifts significantly after this truncation, which is probably a result from the small dataset available. Although only 4 data points with a value below 2 Gy remain, the outcome is really consistent. The dataset is not large enough to be significant, but its performance is very well. It actually bridges the gap between the PDF's of the 95% truncated single grain data and the multi-grains data (fig.3.8). As we have seen before with sample 15, with the multi-grains data, the natural equivalent dose of the youngest grains is easily overruled by older, poorly bleached grains. This is probably also the case for sample 16, which would explain the very broad PDF of the minimum age of the multi-grain data. The minimum age of the multi-grain PDF on the right side of its optimum can therefore be considered as a result of incorporated, older grains, based on the single grain results. To be consistent with the other answers, the minimum age PDF of the 95% single grains data is chosen and since it covers the optimum in the multi-grain PDF, it is the again the best estimate for the true minimum age. However the accuracy of the 99% truncated single grain dataset should be kept in mind, it might point more precisely at the true minimum age of the sample.

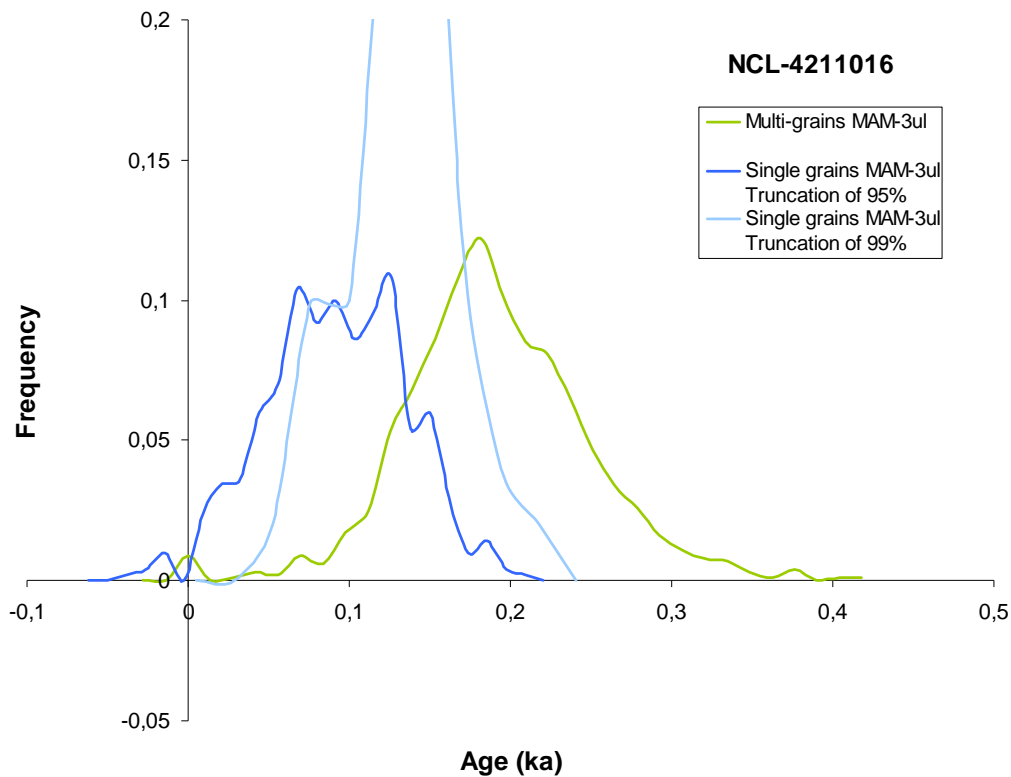


**Fig. 3.8** PDF's on the minimum age of sample NCL-4211016 for both single grains and multi-grains data. The single grains data is plotted for truncation of 95% and 99% certainty.

### 3.4.3 Sample NCL-4211017

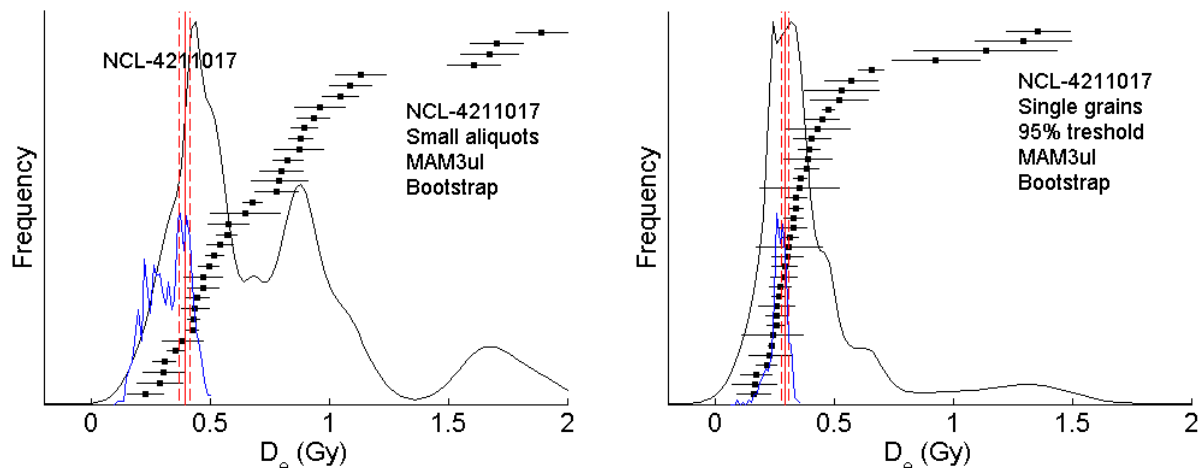


**Fig. 3.9**  $D_e$  outcomes of sample NCL-4211017. The unlogged MAM-3 outcomes for the multi-grains aliquots and single grain data are plotted in red with their PDF's in blue.

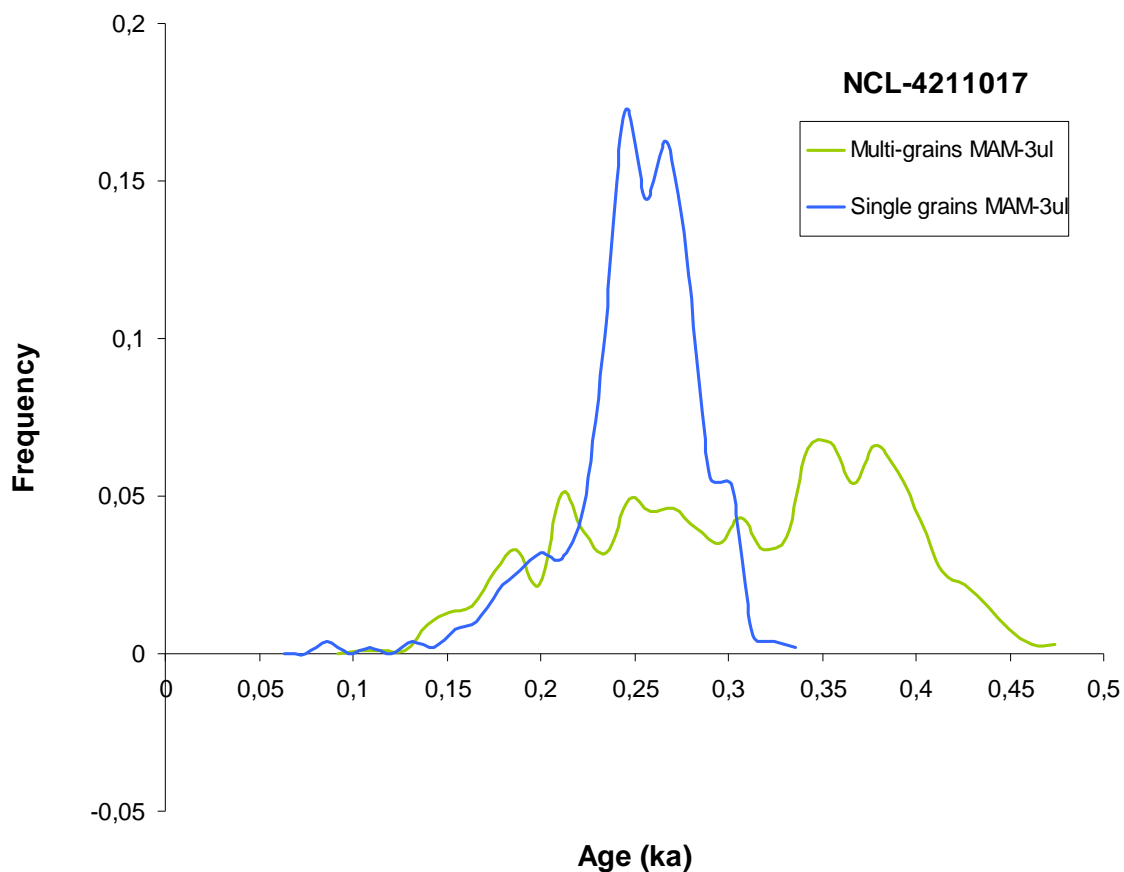


**Fig. 3.10** PDF's on the minimum age of sample NCL-4211017 for both single grains and multi-grains data.

The PDF's for sample 17 are a clear example of the accuracy of both methods. Where the single grain minimum age PDF is narrow and high, the multi-grain PDF is broad and low. So the multi-grain data is more sensible to small differences in the  $D_e$  dataset and the overdispersion, where the single grain data is more consistent. This could be caused by the large uncertainties belonging to the multi-grain data points in comparison of the single grain data points. The extent of the PDF to the higher values probably reflects the influence of poor bleached grains. For sample 17, the single grain minimum age PDF is clearly superior to the multi-grain PDF.

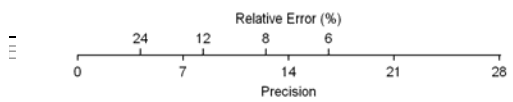
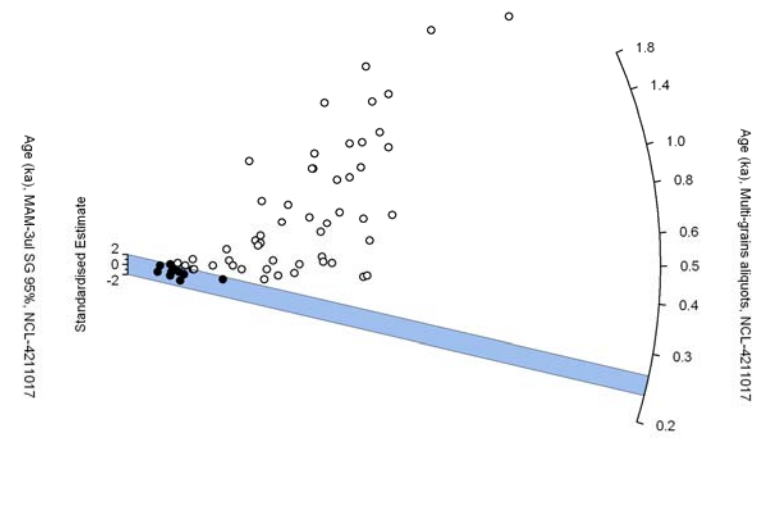
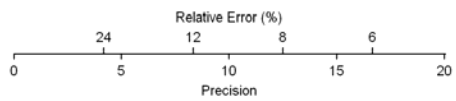
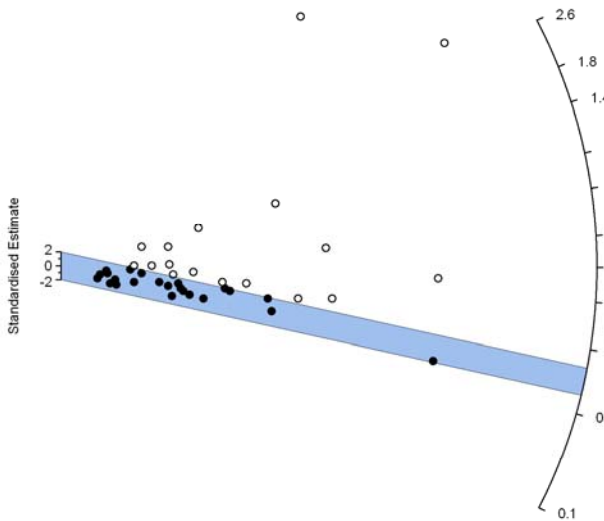
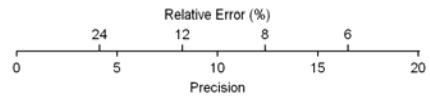
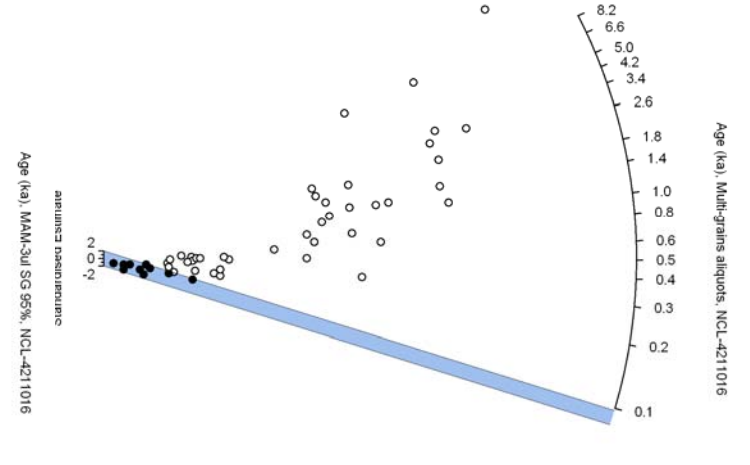
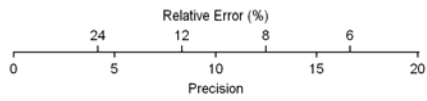
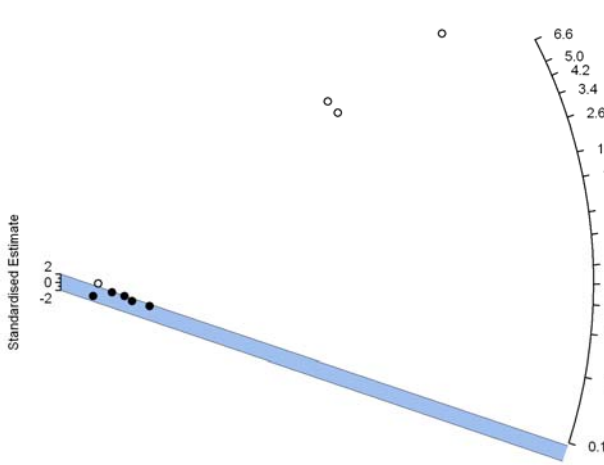
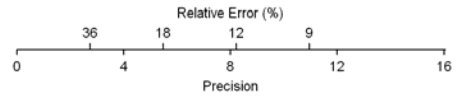
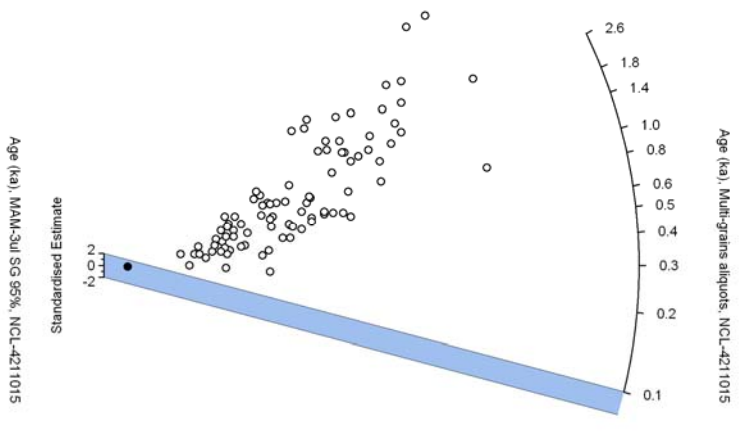
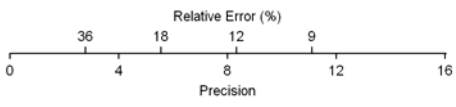
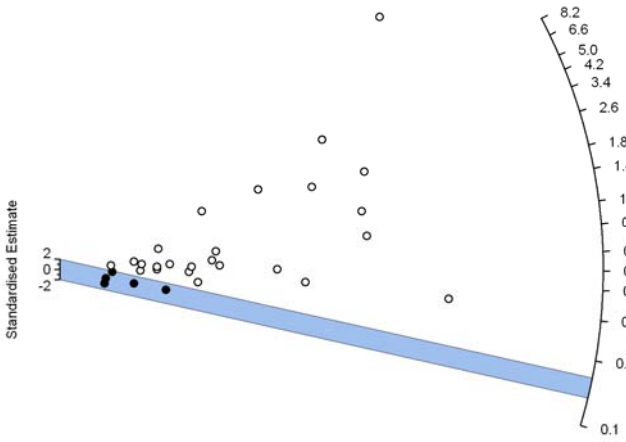
### 3.5 The age of the samples

The single grain data (95% truncation) proves to produce the optimal PDF for the 'true' minimum age of the samples. As Cunningham & Wallinga (submitted) describe, the PDF's can be used successfully to create robust OSL chronologies using Bayesian processing. However in order to be used as stand alone ages, the PDF's will have to be quantified in an age with error margin. This is done by taking the mean and the first or second  $\sigma$  range to describe the distribution. The PDF's can be used supplementary to visualize the distribution. For the three samples this will result in the minimum age shown in table 3.3. Figure 3.11 shows radial plots of these PDF's ages on the single grain and multi-grain data. Note that the error margin of the blue bar, is (much) smaller plotted than the real sigma 1 and 2 following from the minimum age PDF's (table 3.3). Therefore data might plot outside the blue region that is still included in the PDF distribution. For the total picture of the age, these plots should be interpreted together with the values from table 3.3 and the PDF distributions given in figures 3.6, 3.8 and 3.10.

	<b>NCL-4211015</b>	<b>NCL-4211016</b>	<b>NCL-4211017</b>
1 sigma (68% certainty)	154 +/- 70 BP	92 +/- 45 BP	253 +/- 28 BP
	1856 +/- 70 AD	1918 +/- 45 AD	1757 +/- 28 AD
2 sigma (95% certainty)	154 +/- 125 BP	92 +/- 85 BP	253 +/- 88 BP
	1856 +/- 125 AD	1918 +/- 85 AD	1757 +/- 88 AD

**Tab. 3.3** The minimum age in years BP derived from the minimum age PDF's using the quantiles of 1 and 2 sigma.

**Fig 3.11 (next page)** Radial plots for each sample with the mean outcome of the minimum age PDF of the single grain data (95% truncation), see table 3.3. On the left side the single grain dataset are shown and on the right side the multi-grain datasets. Age on the right side axis is in ka BP. Bottom axis shows the precision of the data.



## 4. Discussion

In this study the age of the young, poorly bleached samples is interpreted and analyzed as precise as possible by joined forces of both multi-grains and single grain measurements. It showed that multi-grains aliquots are prone to overestimate the age, due to the averaging of the natural signal with poorly bleached grains. Single grain measurements therefore performed better on these samples. By using the PDF's as the ages of the samples, the uncertainty of the age is larger than with the conventional methods, but the certainty that the 'true' age is captured in the dating is increased significantly.

The difference in performance of the logged and the unlogged MAM-3 when datasets approach zero is not well understood. The unlogged version is more tentative to produce lower ages that are based on a smaller portion of the data, than the logged version. The problems could be overcome for sample 16 and 17 by truncation of the dataset, but problems still occurred for sample 15. This could be caused by the large error terms of the data points in this dataset, however further analysis on the difference in behavior of the MAM-3 and the MAM-3<sub>ul</sub> is needed to determine the source of the anomaly.

The application of the minimum age model is based on the assumption that the youngest grains represent the last exposure to light of the soil horizon before it got (gradually) buried. The colluvial environments where the samples originate from are prone to have poor bleached sediments and indeed many poor bleached grains have been measured. When the minimum age of the sample is determined on the youngest of grains, a possibility arises that not the age of the last surfacing of the soil horizon is dated, but the age till when active (bio)turbation took place, transporting well bleached grains of quartz from younger, super positioned soil layers. This might cause an underestimation of the actual burial age of the soil horizon. Another uncertainty is caused by the dose rate. As the dose rate is measured at the present day situation, it does not include any past changes that could have altered the dose rate over time. For example, the two times higher K-40 concentration of sample 17 in comparison to sample 16, which is situated 1 meter higher at the same location. Leaching and subsequent deposition of K-40 from the higher layers to the lower could have significantly changed the dose rate received by both samples over time, rendering an age overestimation for sample 16 and an age underestimation for sample 17. Such uncertainties are difficult to solve with OSL dating alone.

Comparison with other, independent dating methods, like radiocarbon, could validate the accuracy of the datings. This is a future aim for this research.

## **Acknowledgements**

I wish to thank Dr. Jakob Wallinga for making this research possible at the NCL and as my main supervisor at TU Delft. Alastair Cunningham is thanked for introducing me in the mysteries of the single grain dating and for guiding me through his matlab mazes. Alice Versendaal is thanked for introducing me in the OSL laboratory and for teaching me the fundamentals of OSL dating and LARP. Romée Kars, Candice Johns, all the above mentioned and all other colleagues and students at the Reactor institute are thanked for making my stay a very pleasant one.

## References

- Aitken, M.J. 1998. An Introduction to Optical Dating. Oxford University Press, Oxford, 267 pp.
- Ballarini, M., 2006. Optical dating of quartz from young deposits. PhD thesis, Delft University of Technology.
- Bøtter-Jensen, L., Andersen, C.E., Duller, G.A.T., Murray A.S. 2003. Developments in radiation, stimulation and observation facilities in luminescence measurements. *Radiation Measurements* 37, 535-541.
- Cunningham, A.C. & Wallinga, J. 2010. Selection of integration time-intervals for quartz OSL decay curves, *Quaternary Geochronology* 5, 657-666.
- Cunningham, A.C., Wallinga, J., submitted. Realizing the potential of fluvial archives using robust OSL chronologies. Submitted to *Quaternary Geochronology*.
- Galbraith, R.F., Roberts, R.G., Laslett, G.M., Yoshida, H. & Olley, J.M., 1999. Optical dating of single and multiple grains of quartz from Jinmium rock shelter, northern Australia: Part I, experimental design and statistical models. *Archaeometry* 41: 339-364.
- Huntley, D.J., Godfrey-Smith, D.I., Thewalt, M.L.W., 1985. Optical dating of sediments. *Nature* 313, 105-107.
- Lian, O.B., Roberts, R.G. 2006. Dating the Quaternary: progress in luminescence dating of sediments. *Quaternary Science Reviews* 25, 2449-2468
- Murray, A.S., Olley, J.M. 2002. Precision and accuracy in the optically stimulated luminescence dating of sedimentary quartz: a status review. *Geochronometria* 21, 1-16.
- Murray, A.S., Wintle, A.G., 2000. Luminescence dating of quartz using an improved single-aliquot regenerative-dose protocol. *Radiation Measurements* 32, 57-73.
- Murray, A.S., Wintle, A.G., 2003. The single aliquot regenerative dose protocol: potential for improvements in reliability. *Radiation Measurements* 37, 377-381.
- Murray, A.S., Marten, R., Johnston, A., Marten, P., 1987. Analysis for naturally occurring radionuclides at environmental concentrations by gamma spectrometry. *Journal of Radioanalytical and Nuclear Chemistry* 115, 263-288.
- Prescott, J.R. and Hutton, J.T. 1994. Cosmic ray contributions to dose rates for luminescence and ESR dating: large depths and long-term time variations. *Radiation Measurements* 23, 497-500.
- Venkataraman, R., Bronson, F., Atrashkevich, V., Field, M., Young, B.M. 2003. Improved Detector Response Characterization Method in ISOCS and LabSOCS Methods and Applications of Radioanalytical Chemistry (MARC VI) conference, April 7-11, 2003, Kailua-Kona, Hawaii, USA
- Wallinga, J., 2002. Optically stimulated luminescence dating of fluvial deposits: a review. *Boreas* 31, 303-322.
- Wallinga, J., Murray, A.S. & Botter-Jensen, L., 2002. Measurement of the dose in quartz in the presence of feldspar contamination. *Radiation Protection Dosimetry* 101: 367-370.
- Wintle, A.G., Murray, A.S. 2006. A review of quartz optically stimulated luminescence characteristics and their relevance in single-aliquot regeneration dating protocols. *Radiation Measurements* 41, 369-391.